Nonequilibrium functional renormalization group with frequency-dependent vertex function: A study of the single-impurity Anderson model

Severin G. Jakobs, Mikhail Pletyukhov, and Herbert Schoeller
Institut für Theoretische Physik, RWTH Aachen University, and JARA-Fundamentals of Future Information Technology, D-52056 Aachen, Germany

(Received 1 December 2009; revised manuscript received 12 March 2010; published 12 May 2010)

We investigate nonequilibrium properties of the single-impurity Anderson model by means of the functional renormalization group (fRG) within Keldysh formalism. We present how the level broadening $\Gamma/2$ can be used as flow parameter for the fRG. This choice preserves important aspects of the Fermi-liquid behavior that the model exhibits in case of particle-hole symmetry. An approximation scheme for the Keldysh fRG is developed which accounts for the frequency dependence of the two-particle vertex in a way similar but not equivalent to a recently published approximation to the equilibrium Matsubara fRG. Our method turns out to be a flexible tool for the study of weak to intermediate on-site interactions $U \lesssim 3\Gamma$. In equilibrium we find excellent agreement with numerical RG results for the linear conductance at finite gate voltage, magnetic field, and temperature. In nonequilibrium, our results for the current agree well with time-dependent density-matrix RG. For the nonlinear conductance as function of the bias voltage, we propose reliable results at finite magnetic field and finite temperature. Furthermore, we demonstrate the exponentially small scale of the Kondo temperature to appear in the second-order derivative of the self-energy. We show that the approximation is, however, not able to reproduce the scaling of the effective mass at large interactions.

DOI: 10.1103/PhysRevB.81.195109 PACS number(s): 05.10.Cc, 72.10.Fk, 73.63.Kv

I. INTRODUCTION

Due to the enormous experimental progress in the investigation of nanoelectronic and molecular systems, one of the central issues of theoretical condensed-matter physics is the understanding of nonequilibrium phenomena in small strongly correlated quantum systems coupled to an environment. Traditionally such systems were investigated in the context of dissipative quantum mechanics, where energy exchange of a few-level system with a single bath of phonons was considered.[1] With the realization of various devices involving metallic islands,[2] quantum dots,[3] single molecules,[4] or quantum wires,[5,6] a tunneling coupling to leads was realized, which enabled the controlled study of local quantum systems coupled via particle exchange to the environment. Furthermore, in the presence of several leads, it became possible to study such systems in the presence of a finite bias voltage or temperature gradients (inhomogeneous boundary conditions), i.e., a nonequilibrium and current-carrying state can be realized in the stationary situation.

Whereas in equilibrium there are powerful numerical and analytical techniques to describe linear transport or spectral properties of mesoscopic systems, the available methods in nonequilibrium are quite restrictive and still under development in the nonperturbative regime. Exact solutions exist for some special cases.[7–9] Scattering Bethe-ansatz solutions have been applied to the interacting resonant level model[10] and the Anderson impurity model[11] but the full understanding of the stationary state in all regimes has not yet been reached. To describe the steady state in the presence of a finite bias voltage, numerical renormalization-group (NRG) methods using scattering waves,[12] time-dependent density-matrix renormalization group (TD-DMRG),[13] quantum Monte Carlo (QMC) with complex chemical potentials,[14] and an approach based on iterative summation of path integrals (ISPI) (Ref. 15) have been developed, but the efficiency of these methods is still not satisfactory in the regimes of strong Coulomb interaction and/or large bias voltage. To calculate the time evolution into the stationary state, numerical techniques such as TD-NRG,[16,17] TD-DMRG,[8,13,18] ISPI,[15] and QMC in nonequilibrium[19,20] have been used, as well as a Fock space formulation of the multilayer multiconfiguration time-dependent Hartree theory.[21] However, the description of finite bias or the long-time limit still remains difficult.

Perturbation expansions in the coupling between the local system and the reservoirs or in the Coulomb interaction on the local system cannot cover the most interesting regime of quantum fluctuations and strong correlations at very low temperatures. To improve them significantly, the most promising analytic approaches are perturbative RG methods for nonequilibrium systems. Several methods have been proposed, which differ significantly concerning the extent up to which nonequilibrium aspects are taken into account and how the perturbative expansion in the renormalized vertices is set up. One of the first formally exact nonequilibrium RG methods for zero-dimensional quantum systems (quantum dots) was developed in Refs. 22–24 and is called the real-time RG (RTRG) method. This technique is based on an expansion in the renormalized coupling between quantum system and reservoir, whereas the correlations on the local system are taken exactly into account. Later on, this method was formulated in pure frequency space (FS) and combined with a cutoff procedure on the imaginary frequency axis (introduced in Ref. 25), the so-called RTRG-FS method.[26] Within this technique it was possible to solve analytically the generic problem how RG flows are cut off by the physics of transport rates. Furthermore, it was demonstrated how all static and dynamic properties can be calculated analytically for the nonequilibrium Kondo model in weak coupling[27–29] and for the interacting resonant level model (IRLM) in the

scaling limit,[30] which are two fundamental models for the physics of spin and charge fluctuations, respectively. Another perturbative RG method in nonequilibrium (called PRG-NE), which also expands in the reservoir-system coupling, was developed in Refs. 31 and 32, where the slave particle approach was used in connection with Keldysh formalism and quantum Boltzmann equations. In these works it was investigated how the voltage and the magnetic field cuts off the RG flow for the Kondo model and how the frequency dependence of the vertices influences various logarithmic contributions for the susceptibility and the nonlinear conductance. A real-frequency cutoff was used and the RG was formulated purely on one part of the Keldysh-contour disregarding diagrams connecting the upper with the lower branch. This procedure turns out to be sufficient for the Kondo model to calculate logarithmic terms in leading order but the cutoff by relaxation and decoherence rates was included intuitively (recently an improved version of this method included parts of the spin relaxation and decoherence rates via self-energy insertions[33]). An alternative microscopic approach to RTRG-FS for combining relaxation and decoherence rates within a nonequilibrium RG method for the Kondo model was proposed in Ref. 34, where flow-equation methods[35] were generalized to the nonequilibrium situation. Within this method, it was shown for the Kondo model that the cutoff of the RG flow by spin relaxation/decoherence rates occurs due to a competition of one-loop and two-loop terms on the right-hand side of the RG equation for the vertex.

Whereas all of these perturbative RG methods are very successful, they have two important drawbacks. First, they expand all in the reservoir-system coupling and thus can only be used reliably in the regime of weak spin or orbital fluctuations (strong charge fluctuations seem to be covered by RTRG-FS as was demonstrated recently for the IRLM in Ref. 30). Second, the RTRG-FS and the PRG-NE scheme work in a basis of the many-particle eigenfunctions of the isolated local quantum system. As a consequence larger systems such as multilevel quantum dots, large molecules, or the crossover to the quantum wire case cannot be addressed due to an exponentially large number of relevant many-particle states. Therefore, another class of perturbative RG methods in nonequilibrium have been developed which are based on an expansion in the renormalized Coulomb interaction on the local quantum system by combining the Keldysh formalism with a quantum-field theoretical formulation of functional RG within the one-particle irreducible Wetterich scheme.[36] In the following we call this approach the functional renormalization group (fRG)-NE method. It has been proposed and applied to transport through quantum dots and quantum wires in Refs. 25, 30, and 37–39. Similar implementations of the method have been developed for the application to bulk systems, investigating, for instance, quantum criticality in nonequilibrium[40] or the long-time evolution of a Bose gas starting from a nonequilibrium state.[41] Since the method is nonperturbative in the reservoir-system coupling and is parametrized in terms of single-particle states, it has the advantage that the case of low voltage and temperature can be described and it can be applied to multilevel quantum dots and quantum wires, at least if Coulomb interactions are moderate.

So far, the fRG-NE scheme was used in approximation schemes with frequency-independent self-energy. This approach describes reliably the leading effects of weak interactions in an effective single-particle picture. At higher interactions the decay rates generated by inelastic effects of the interaction are no longer negligible and may drastically change the behavior of the system. These effects can only be described on the level of a frequency-dependent self-energy, which is the subject of the present paper. We will address the problem of enhancing the level of the truncation scheme used in fRG-NE, in order to enable it to describe interaction induced decay rates. The flow equations for the vertex functions are of such a structure that a frequency-dependent self-energy can only result from a frequency-dependent two-particle vertex. This is in turn a very complicated object, depending on four frequency, state, and Keldysh indices. Conservation laws for spin, momentum, and frequency, and the symmetry properties of the vertex function discussed in Ref. 42 can be used to reduce the complexity of the problem. Nevertheless, the two-particle vertex function remains so complicated that it seems preferable to develop the methodology first for a physical system with as few interacting degrees of freedom as possible. This restricts at least the dimensionality of the state dependence of the vertex function. Insight gained at this level can later be used to tackle larger systems.

We choose to investigate the single-impurity Anderson model[43] (SIAM) which is considered to be a generic model for strong local correlations[44] and is a minimal model to study the interplay of charge and spin fluctuations. It consists of a single-level quantum dot with two spin states and on-site Coulomb repulsion U, which is coupled to leads. Experimentally, it can be realized for small quantum dots or molecules. In the Coulomb-blockade regime, this model is equivalent to the Kondo model[45] and the unitarity limit of the Kondo effect has been measured.[46] The perturbation theory of this model in U is completely regular.[47–50] However, the low-energy behavior at large interaction U is governed by the so-called Kondo scale[44] which is exponentially small in U and hence cannot be described in any finite order perturbation theory. This makes the model an interesting object for RG studies. Since the model can be described in equilibrium very accurately by the NRG (Ref. 51) and even exact results for thermodynamic properties are available from Bethe ansatz[52] there is the possibility to benchmark our results at least in equilibrium.

In case of thermal equilibrium the Matsubara fRG has so far been applied to the SIAM in two distinct formulations. One of them is a recent study based on Hubbard-Stratonovich fields representing spin fluctuations.[53] The fRG-NE implementation presented in this paper does not pursue this idea but is based on a weak-coupling expansion analogously to the second class of equilibrium fRG studies of the SIAM.[54–57] These studies in turn have been done in two different truncation schemes. One of those schemes reduces the flow of the two-particle vertex to a renormalization of the static interaction strength and produces a frequency-independent self-energy. This approximation is able to reproduce a Kondo scale exponentially small in U which appears, e.g., in the pinning of the level to the chemical potential.[54,55]

It turned out to be a quite powerful tool for the description of static properties of diverse quantum-dot geometries even at fairly large interactions.[54] The approximation is however unable to describe finite frequency properties. Its restriction becomes manifest very clearly in the shape of the spectral function: the approximation of a static self-energy leads to a Lorentzian resonance peak. The sharp Kondo resonance, the side bands, the suppression of the Kondo resonance with temperature are features which cannot be described, in principle, by the static approximation.

The second more elaborate approximation scheme which has been used within the weak-coupling equilibrium fRG keeps the frequency dependence of the two-particle vertex function and neglects the three-particle vertex.[56,57] It yields quantitatively good results for small to intermediate interaction strengths. While finite frequencies properties are accessible to this frequency-dependent fRG approximation for not too large interactions, it has been observed that the large interaction asymptotics of this refined version are worse than the ones found in the static fRG; no Kondo scale exponentially small in U has been found.[57] Also a technical disadvantage related to the use of the Matsubara formalism becomes apparent: while the self-energy data are quite accurate on the imaginary frequency axis for small and intermediate U, the analytic continuation to the real axis was instable for nonzero temperatures, working only for certain parameter sets. Therefore only observables which are accessible from the imaginary frequency axis (without resorting to analytic continuation) can be systematically studied at finite temperature.[57] This finding is an additional motivation to study a frequency-dependent fRG within the Keldysh formalism, being formulated on the real-frequency axis from the outset.

Apart from the possibility to access real-frequency properties at finite temperature we envisage the opportunity to analyze the nonequilibrium behavior of the SIAM. This has been recently in the focus of diverse publications. Among them is also a nonequilibrium fRG study that is based on a real-frequency cutoff and a static approximation scheme;[38,39] results known from the Matsubara fRG could be partially reproduced by this method. It suffers however from the violation of causality related to the choice of the real-frequency cutoff. References 58 and 59 present perturbative studies that apply to moderate interactions and the special situation of particle-hole symmetry and vanishing magnetic field. The RTRG method was used in Ref. 22 to describe the mixed valence and empty-orbital regime of the SIAM at finite bias. The results seem to be reliable but it was not possible to study the Kondo regime since essential processes describing spin fluctuations were neglected. In Ref. 14 a time-independent description of nonequilibrium based on a density operator for the steady state is used to make the problem accessible to QMC. The main challenge of this method is the numerical analytic continuation of two imaginary quantities to the real axis. A recent improvement of nonequilibrium QMC applied to the SIAM at zero magnetic field and zero gate voltage[20] has given reliable results for $U<3-5\Gamma=6-10\Delta$ (in our notation $\Delta=\Gamma/2$ denotes the level broadening, i.e., Γ is the full width at half maximum of the noninteracting spectral density) for the dot occupation and the nonlinear current. The ISPI approach[15] provides an access to the current through the system for moderate U and not too low temperatures. A very promising tool is the recently introduced scattering states NRG.[12] Unfortunately the results for the conductance obtained by this method still bear a considerable numerical uncertainty. Spataru *et al.*[60]generalized the GW approximation to nonequilibrium and concentrate on the Coulomb-blockade regime of the model. The TD-DMRG technique[13] tries to access the steady-state transport features of the model from the transient regime. Data of the ISPI and the TD-DMRG methods for the current at moderate interactions have been found to agree very well with our fRG results.[61]

In contrast to many other methods, we propose in this paper a very flexible approach which provides reliable results for moderate interactions $U\lesssim 3\Gamma=6\Delta$. In equilibrium, we will show that the linear conductance agrees very well with NRG data at finite gate voltage, magnetic field, and temperature. In nonequilibrium at finite bias V, the nonlinear current $I(V)$ is found to agree very well with TD-DMRG data.[13] This provides the main evidence that our results can be trusted also for the nonlinear conductance $G(V)$ at finite magnetic field B and finite temperature T. In particular, at $T=B=0$, we find that our results for $G(V)$ do not show anomalous peaks as obtained within fourth-order perturbation theory.[59] Furthermore, we show that even the exponentially small scale of the Kondo temperature can be identified in the second-order derivative of the self-energy and the various Fermi-liquid relations are reproduced. However, the effective mass still does not contain an exponentially small scale leading to a too large broadening of the spectral density for interaction strengths $U>3\Gamma$, in line with the equilibrium Matsubara fRG.[57]

The paper is organized as follows. Section II introduces the model and its treatment within Keldysh formalism. In Sec. III we recapitulate the core elements of the fRG for irreducible vertex functions. A motivation and discussion of the choice of hybridization as flow parameter follow in Sec. IV. In Sec. V we describe the more basic frequency-independent approximation of the flow equations and show that in the case of equilibrium and zero temperature we reproduce exactly the flow equations known from the Matsubara fRG. Section VI is then devoted to the fRG in frequency-dependent approximation. There are three channels contributing to the flow of the two-particle vertex, and all three need to be taken into account. We describe an approximation scheme that simplifies the functional form in which the two-particle vertex depends on frequencies. In Sec. VII we demonstrate that the fRG approach in the chosen truncation and approximation scheme preserves the Fermi-liquid relations for the (imaginary part of the) self-energy; furthermore we determine the fRG estimate for the Fermi-liquid coefficients. Section VIII finally presents numerical results obtained from the fRG and compares them to other methods. A conclusion is given in Sec. IX. The appendices present some mainly technical considerations. In Appendix A we identify a set of independent components which completely determine the two-particle vertex function. The precise form of the flow equations in terms of these components is given in Appendices B and C. In Appendix D we recover within

the fRG approach the nonequilibrium Fermi-liquid relation known from Ref. 62.

II. SIAM AND KELDYSH FORMALISM

The single-impurity Anderson model[43] under consideration consists of a single electronic level with on-site repulsion, which is coupled to two noninteracting reservoirs addressed as left (L) and right (R). We denote the single-particle states of the impurity by $\sigma=\uparrow,\downarrow=+\frac{1}{2},-\frac{1}{2}$ according to the state of the electron spin. The matrix element of the on-site two-particle interaction is

$$\langle\sigma_1'\sigma_2'|v|\sigma_1\sigma_2\rangle=\begin{cases}U & \text{if } \sigma_1'=\sigma_1=\bar{\sigma}_2'=\bar{\sigma}_2,\\ 0 & \text{else}\end{cases} \tag{1}$$

with $U\geq 0$, where we used the notation $\bar{\sigma}=-\sigma$. In standard notation of second quantization the Hamiltonian is given by

$$H=H_{\mathrm{dot}}+H_{\mathrm{res}}+H_{\mathrm{coup}}, \tag{2a}$$

$$H_{\mathrm{dot}}=\sum_{\sigma}\left(eV_{\mathrm{g}}-\sigma B-\frac{U}{2}\right)d_{\sigma}^{\dagger}d_{\sigma}+Ud_{\uparrow}^{\dagger}d_{\uparrow}d_{\downarrow}^{\dagger}d_{\downarrow}, \tag{2b}$$

$$H_{\mathrm{res}}=\sum_{r=\mathrm{L,R}}H_{\mathrm{res}}^{(r)}=\sum_{r}\sum_{\sigma}\int dk_r\varepsilon_{k_r}c_{k_r\sigma}^{\dagger}c_{k_r\sigma}, \tag{2c}$$

$$H_{\mathrm{coup}}=\sum_{r}H_{\mathrm{coup}}^{(r)}=\sum_{r}\sum_{\sigma}\int dk_r(V_{k_r}d_{\sigma}^{\dagger}c_{k_r\sigma}+\mathrm{H.c.}), \tag{2d}$$

where the annihilators d_σ, $c_{k_r\sigma}$ and creators $d_\sigma^\dagger$, $c_{k_r\sigma}^\dagger$ obey the usual fermionic anticommutation rules. The single-particle energies of the dot

$$\varepsilon_\sigma=eV_{\mathrm{g}}-\sigma B-U/2 \tag{3}$$

depend on the gate voltage V_{g} and the magnetic field B and are shifted by $(-U/2)$ such that particle-hole symmetry is given when eV_{g} equals the chemical potential.

We are interested in the stationary state which emerges a long time after the system has been prepared in a product density matrix

$$\rho(t_0)=\rho_0=\rho_{\mathrm{L}}\otimes\rho_{\mathrm{dot}}\otimes\rho_{\mathrm{R}},\quad t_0\to-\infty. \tag{4}$$

Here, ρ_{L} and ρ_{R} describe each an individual grand-canonical equilibrium characterized by the Fermi function

$$f_r(\omega)=\frac{1}{e^{(\omega-\mu_r)/T}+1},\quad r=\mathrm{L,R}. \tag{5}$$

(We use units with $\hbar=1$ and $k_{\mathrm{B}}=1$ throughout this paper.) The temperature T is assumed to be equal in both reservoirs, whereas a possible difference between the two chemical potentials accounts for a finite bias voltage,

$$eV=\mu_{\mathrm{L}}-\mu_{\mathrm{R}}. \tag{6}$$

We measure single-particle energies relative to the mean chemical potential by setting

$$\mu_{\mathrm{L}}+\mu_{\mathrm{R}}=0. \tag{7}$$

We describe the system in the framework of Keldysh formalism,[63–66] where the single-particle propagator between two states q' and q has four components

$$G_{q|q'}^{-|-}(t|t')=G_{q|q'}^{\mathrm{c}}(t|t')=-i\ \mathrm{Tr}\ \rho_0\mathcal{T}a_q(t)a_{q'}^{\dagger}(t'), \tag{8a}$$

$$G_{q|q'}^{-|+}(t|t')=G_{q|q'}^{<}(t|t')=i\ \mathrm{Tr}\ \rho_0a_{q'}^{\dagger}(t')a_q(t), \tag{8b}$$

$$G_{q|q'}^{+|-}(t|t')=G_{q|q'}^{>}(t|t')=-i\ \mathrm{Tr}\ \rho_0a_q(t)a_{q'}^{\dagger}(t'), \tag{8c}$$

$$G_{q|q'}^{+|+}(t|t')=G_{q|q'}^{\tilde{c}}(t|t')=-i\ \mathrm{Tr}\ \rho_0\tilde{\mathcal{T}}a_q(t)a_{q'}^{\dagger}(t'), \tag{8d}$$

called chronologic, lesser, greater, and antichronologic, respectively. Here $\mathcal{T}$ ($\tilde{\mathcal{T}}$) denotes the time (antitime) ordering operator and $a_q(t)=d_\sigma(t)$ or $c_{k_r\sigma}(t)$ is in the Heisenberg picture at time t. In the time translational invariant stationary state $G(t|t')=G(t-t'|0)$ depends only on the difference of the two time arguments and we use the Fourier transform

$$G_{q|q'}^{j|j'}(\omega)=\int dte^{i\omega t}G_{q|q'}^{j|j'}(t|0),\quad j,j'=\mp. \tag{9}$$

Instead of the contour basis with indices $j=\mp$ we use the Keldysh basis[67] with indices $\alpha=1,2$. The transformation to this basis is given by

$$G^{\alpha|\alpha'}=\sum_{j,j'=\mp}(D^{-1})^{\alpha|j}G^{j|j'}D^{j'|\alpha'}, \tag{10}$$

where

$$D^{-|1}=D^{\mp|2}=(D^{-1})^{1|-}=(D^{-1})^{2|\mp}=\frac{1}{\sqrt{2}}, \tag{11a}$$

$$D^{+|1}=(D^{-1})^{1|+}=-\frac{1}{\sqrt{2}}. \tag{11b}$$

The resulting components of the single-particle Green's function

$$G^{1|1}=0,\quad G^{1|2}=G^{\mathrm{Av}},\quad G^{2|1}=G^{\mathrm{Ret}},\quad G^{2|2}=G^{\mathrm{K}} \tag{12}$$

are called advanced, retarded, and Keldysh, respectively. The self-energy is transformed correspondingly,

$$\Sigma^{\alpha'|\alpha}=\sum_{j',j=\mp}(D^{-1})^{\alpha'|j'}\Sigma^{j'|j}D^{j|\alpha}, \tag{13}$$

leading to

$$\Sigma^{1|1}=\Sigma^{\mathrm{K}},\quad \Sigma^{1|2}=\Sigma^{\mathrm{Ret}},\quad \Sigma^{2|1}=\Sigma^{\mathrm{Av}},\quad \Sigma^{2|2}=0. \tag{14}$$

The influence of the reservoirs on the dot Green's function can be described by reservoir self-energy contributions[68]

$$\Sigma_{\mathrm{res}_\sigma}^{(r)\alpha'|\alpha}(\omega)=\int dk_rV_{k_r}g_{k_r}^{\bar{\alpha}'|\bar{\alpha}}(\omega)V_{k_r}^{*} \tag{15}$$

with $\bar{1}=2$, $\bar{2}=1$, and g_{k_r} being the free propagator in the reservoir state k_r which is assumed to be spin independent. Explicitly, the individual Keldysh components are

$$\Sigma_{\mathrm{res}_\sigma}^{(r)\mathrm{Ret}}(\omega) = \frac{1}{2\pi}\int d\omega' \frac{\Gamma_r(\omega')}{\omega - \omega' + i\eta}, \tag{16a}$$

$$\Sigma_{\mathrm{res}_\sigma}^{(r)\mathrm{Av}}(\omega) = \Sigma_{\mathrm{res}_\sigma}^{(r)\mathrm{Ret}}(\omega)^*, \tag{16b}$$

$$\Sigma_{\mathrm{res}_\sigma}^{(r)\mathrm{K}}(\omega) = -i[1 - 2f_r(\omega)]\Gamma_r(\omega), \tag{16c}$$

where we made use of the hybridization function

$$\Gamma_r(\omega) = 2\pi \int dk_r |V_{k_r}|^2 \delta(\omega - \varepsilon_{k_r}). \tag{17}$$

As we are neither interested in the influence of the band structure of the reservoirs nor in the momentum dependence of the hopping elements, we linearize the reservoir dispersion, $\varepsilon_{k_r} = w_r k_r$ (with $w_r = d\varepsilon_{k_r}/dk_r$) being the inverse density of states at the Fermi level, $k_r = k_r^{\mathrm{F}}$) and set the hopping to momentum-independent constants, $V_{k_r = k_r^{\mathrm{F}}} \equiv V_r$. As a result, the hybridization functions are frequency-independent constants,

$$\Gamma_r(\omega) = \Gamma_r = 2\pi \frac{|V_r|^2}{w_r}. \tag{18}$$

The results presented later apply to the special case of symmetric coupling, $\Gamma_{\mathrm{L}} = \Gamma_{\mathrm{R}}$, which is technically easier for the implementation of our approximations.

Defining the total hybridization Γ via

$$\Gamma = \Gamma_{\mathrm{L}} + \Gamma_{\mathrm{R}}, \tag{19}$$

we find the reservoir-dressed noninteracting dot propagator

$$g_\sigma^{\mathrm{Ret}}(\omega) = \frac{1}{\omega - \varepsilon_\sigma + i\Gamma/2}, \tag{20a}$$

$$g_\sigma^{\mathrm{Av}}(\omega) = g_\sigma^{\mathrm{Ret}}(\omega)^*, \tag{20b}$$

$$g_\sigma^{\mathrm{K}}(\omega) = [1 - 2f_{\mathrm{eff}}(\omega)][g_\sigma^{\mathrm{Ret}}(\omega) - g_\sigma^{\mathrm{Av}}(\omega)], \tag{20c}$$

with the effective distribution function

$$f_{\mathrm{eff}}(\omega) = \sum_r \frac{\Gamma_r}{\Gamma} f_r(\omega). \tag{21}$$

A sketch of the model can be found in Fig. 1.

The current from the left reservoir through the dot to the right reservoir is given by[58,69]

$$I = e\frac{\Gamma_{\mathrm{L}}\Gamma_{\mathrm{R}}}{\Gamma}\int d\omega [f_{\mathrm{L}}(\omega) - f_{\mathrm{R}}(\omega)] \sum_\sigma \rho_\sigma(\omega), \tag{22}$$

where the spectral density can be obtained from the interacting single-particle dot Green's function as

$$\rho_\sigma(\omega) = -\frac{1}{\pi}\mathrm{Im}\, G_\sigma^{\mathrm{Ret}}(\omega). \tag{23}$$

In the case $\Gamma_{\mathrm{L}} = \Gamma_{\mathrm{R}}$, which we focus on later, the current is an odd function of the bias voltage: according to Eqs. (5)–(7), inverting the sign of V means interchanging f_{L} and f_{R}. As a consequence, the effective distribution function (21), the reservoir dressed propagator, Eq. (20), the interacting Green's function, and the spectral function (23) remain unchanged, while the sign of the current, Eq. (22), changes.

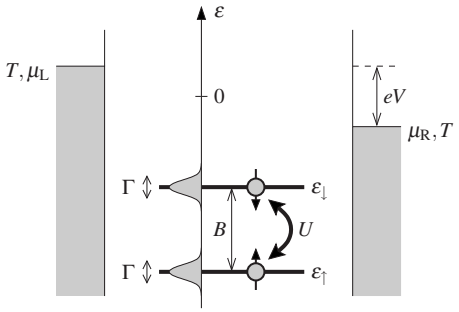

FIG. 1. Sketch of the model with single-particle energy in vertical direction.

We note that the Hamiltonian is of such a type that the dot Green's function in the spin basis exhibits the special behavior under time reversal described in Sec. 5.5 of Ref. 42. Therefore the Kubo-Martin-Schwinger (KMS) conditions which connect the components of the Green and vertex functions in thermal equilibrium and which we apply later on take the form of a generalized fluctuation dissipation theorem as stated in Sec. 5.6 of that reference.

III. VERTEX FUNCTIONS AND FUNCTIONAL RENORMALIZATION GROUP

A treatment of the problem within the fRG is set up by making the bare propagator g depend on a flow parameter λ. Most commonly λ is chosen to suppress low-energy degrees of freedom. Being functionals of the bare propagator, the interacting Green and vertex functions acquire a dependence on λ as well, which is described by an infinite hierarchy of coupled flow equations.[70] The flow parameter is introduced in such a way that two values of λ are of particular importance: at $\lambda = \lambda_{\mathrm{start}}$ the Green or vertex functions can be determined exactly or in reasonable approximation; at $\lambda = \lambda_{\mathrm{stop}}$ the free propagator takes its original value, $g(\lambda_{\mathrm{stop}}) = g$, and so do the interacting Green or vertex functions. Therefore the interacting Green or vertex functions can be found by (approximately) computing their flow from λ_{start} to λ_{stop}. In this paper we focus on the flow of the one-particle irreducible vertex functions[36,71] which has proven to provide a successful approach to the physics of diverse low-dimensional correlated electron problems.[72,73]

The one-particle irreducible vertex functions can be derived from generating functionals; details on this approach can be found for Matsubara formalism, e.g., in Ref. 74, and for Keldysh formalism in Ref. 38. Equivalently, the one-particle irreducible n-particle vertex function

$$\gamma_{q_1'\ldots q_n'|q_1\ldots q_n}^{\alpha_1'\ldots\alpha_n'|\alpha_1\ldots\alpha_n}(\omega_1', \ldots, \omega_n'|\omega_1, \ldots, \omega_n) \tag{24}$$

can be defined diagrammatically as the sum of all one-particle irreducible diagrams with n amputated incoming lines (having states $q_1, \ldots q_n$, Keldysh indices $\alpha_1, \ldots, \alpha_n$, and

frequencies $\omega_1,\ldots,\omega_n$) and n amputated outgoing lines (having states $q_1',\ldots,q_n'$, Keldysh indices $\alpha_1',\ldots,\alpha_n'$, and frequencies $\omega_1',\ldots,\omega_n'$). Due to frequency conservation only $(2n-1)$ of the $2n$ frequencies are independent. By the expression (24) we refer to a function depending only on $(2n-1)$ frequency arguments, the last one being redundant.

The vertex functions are antisymmetric under exchange of particles. In fact, the underlying diagrammatics is meant to be of the Hugenholtz type,[74] thus based on antisymmetrized interaction vertices

$$\bar{v}^{\alpha_1'\alpha_2'|\alpha_1\alpha_2}_{q_1'q_2'|q_1q_2} = \langle q_1'q_2'|v(|q_1q_2\rangle - |q_2q_1\rangle) \times \begin{cases} \frac{1}{2} & \text{if } \alpha_1+\alpha_2+\alpha_1'+\alpha_2' \text{ is odd,} \\ 0 & \text{else,} \end{cases} \tag{25}$$

where q, q_2 (q_1', q_2') are incoming (outgoing) single-particle states and α_1, α_2 (α_1', α_2') incoming (outgoing) Keldysh indices.

In order to evaluate a specific diagram contributing to a vertex function, one determines the symmetry factor S, the number n_{eq} of equivalent lines, the number n_{loop} of internal loops and the permutation P that describes which incoming index is connected to which outgoing one. The value of the diagram is then given by

$$\frac{(-1)^{n_{\mathrm{loop}}}(-1)^P}{2^{n_{\mathrm{eq}}}S}\left(\frac{2\pi}{i}\right)^{n-1}\left[\prod\frac{i}{2\pi}\bar{v}\right]\prod g, \tag{26}$$

where one has to sum over all internal state and Keldysh indices and to integrate over all independent internal frequencies. Details can be found in Ref. 42. Equation (26) defines the prefactor of the vertex functions in such a way, that they can be used themselves as vertices in diagrams with the identical prefactor rules applicable to bare n-particle interaction vertices. The self-energy is equal to the one-particle vertex, $\Sigma \equiv \gamma_{n=1}$.

A derivation of the flow equations for the vertex functions within the generating functional approach in Keldysh formalism is given in Ref. 38. Reference 25 describes an equivalent derivation of the flow equations based on diagrams and provides diagrammatic rules for their formulation. The resulting flow equations form an infinite coupled hierarchy where the flow of the n-particle vertex functions, $d\gamma_n^\lambda/d\lambda$, is a functional of $\Sigma^\lambda,\gamma_2^\lambda,\ldots,\gamma_{n+1}^\lambda$. For example, the flow equations for the one- and two-particle vertex function read

$$\frac{d}{d\lambda}\Sigma^\lambda_{1'|1} = -\frac{i}{2\pi}\gamma^\lambda_{1'2'|12}S^\lambda_{2|2'} \tag{27}$$

and

$$\frac{d}{d\lambda}\gamma^\lambda_{1'2'|12} = -\frac{i}{2\pi}\gamma^\lambda_{1'2'3'|123}S^\lambda_{3|3'} \tag{28a}$$

$$+\frac{i}{2\pi}\gamma^\lambda_{1'2'|34}S^\lambda_{3|3'}G^\lambda_{4|4'}\gamma^\lambda_{3'4'|12} \tag{28b}$$

$$+\frac{i}{2\pi}\gamma^\lambda_{1'4'|32}[S^\lambda_{3|3'}G^\lambda_{4|4'}+G^\lambda_{3|3'}S^\lambda_{4|4'}]\gamma^\lambda_{3'2'|14} \tag{28c}$$

$$-\frac{i}{2\pi}\gamma^\lambda_{1'3'|14}[S^\lambda_{3|3'}G^\lambda_{4|4'}+G^\lambda_{3|3'}S^\lambda_{4|4'}]\gamma^\lambda_{4'2'|32}. \tag{28d}$$

Here we use shorthand notation like

$$\gamma^\lambda_{1'2'|12} \equiv (\gamma_2^\lambda)^{\alpha_1'\alpha_2'|\alpha_1\alpha_2}_{q_1'q_2'|q_1q_2}(\omega_1'\omega_2'|\omega_1\omega_2) \tag{29}$$

and indices occurring twice in a product implicate summation over state and Keldysh indices and integration over independent frequencies. Furthermore,

$$S_\lambda = G_\lambda g_\lambda^{-1} s_\lambda g_\lambda^{-1} G_\lambda \tag{30}$$

with

$$s_\lambda = \frac{dg_\lambda}{d\lambda} \tag{31}$$

denotes the so-called single scale propagator. We call the contributions, Eqs. (28b)–(28d), to the flow of $\gamma^\lambda_{1'2'|12}$ particle-particle (PP), exchange particle-hole [PH(e)], and direct particle-hole [PH(d)] channel, respectively.

For practical computations the exact infinite set of flow equations is reduced to a closed finite set of approximated flow equations. Typical approximations are to neglect the flow of higher-order vertex functions by setting $d\gamma_n^\lambda/d\lambda \equiv 0$ for $n \geq n_0$ and to ascribe an effective parametrization to the remaining ones. In the present investigation of the SIAM we neglect the flow of γ_3^λ. Two different parametrizations of γ_2^λ will be discussed, a static (i.e., frequency-independent) and a dynamic (frequency-dependent) one.

IV. FLOW PARAMETER

In Ref. 42 it has been shown how the choice of the flow parameter determines whether certain exact properties of the vertex functions are conserved by an approximated fRG flow. For the study of the SIAM the conservation not only of causality but also of the KMS conditions characterizing thermal equilibrium is important. The correct description of thermal equilibrium is necessary in order to capture fundamental aspects of the low-energy properties of the model. Consider, for example, the expansion of the self-energy at $eV_g=\mu=0$, $B=0$ in leading order in frequency, temperature, and voltage,

$$\Sigma^{\mathrm{Ret}}_\sigma(\omega,T,V) \simeq \frac{U}{2} + \left(1-\frac{\tilde{\chi}_s+\tilde{\chi}_c}{2}\right)\omega - i\frac{(\tilde{\chi}_s-\tilde{\chi}_c)^2}{4\Gamma}\left[\omega^2+(\pi T)^2+\frac{3}{4}(eV)^2\right], \tag{32}$$

where $\tilde{\chi}_c$ and $\tilde{\chi}_s$ denote the reduced charge and spin susceptibility.[47,62] The Fermi-liquid behavior (32) determines

the proper shape of the spectral function, in particular, its height and width. The derivation of Eq. (32) is based on thermal equilibrium particle statistics and hence requires the validity of the KMS conditions for a treatment within Keldysh formalism.

Hybridization can be used as a flow parameter which conserves causality and the KMS conditions.[42] For that purpose the constants $\Gamma_{L,R}$ and Γ from Eqs. (18) and (19) are enhanced artificially by setting

$$\Gamma_\lambda = \Gamma + \lambda, \tag{33a}$$

$$\Gamma_\lambda^{(r)} = \Gamma_r + \frac{\Gamma_r}{\Gamma}\lambda, \quad r = \mathrm{L,R}, \tag{33b}$$

where λ flows from ∞ to 0. Via the hybridization, the components of the noninteracting reservoir dressed propagator acquire the λ dependence

$$(g_\lambda)_\sigma^{\mathrm{Ret}}(\omega) = \frac{1}{\omega - \varepsilon_\sigma + i(\Gamma+\lambda)/2}, \tag{34a}$$

$$(g_\lambda)_\sigma^{\mathrm{Av}}(\omega) = (g_\lambda)_\sigma^{\mathrm{Ret}}(\omega)^*, \tag{34b}$$

$$(g_\lambda)_\sigma^{\mathrm{K}}(\omega) = [1 - 2f_{\mathrm{eff}}(\omega)][(g_\lambda)_\sigma^{\mathrm{Ret}}(\omega) - (g_\lambda)_\sigma^{\mathrm{Av}}(\omega)], \tag{34c}$$

where $f_{\mathrm{eff}}^\lambda(\omega) \equiv f_{\mathrm{eff}}(\omega)$ does not depend on λ since $\Gamma_\lambda^{(r)}/\Gamma_\lambda = \Gamma_r/\Gamma$, compare Eq. (21). The components of the free single scale propagator $s_\lambda = dg_\lambda/d\lambda$ are given by

$$s_\lambda^{\mathrm{Ret}}(\omega) = -\frac{i}{2}[g_\lambda^{\mathrm{Ret}}(\omega)]^2, \tag{35a}$$

$$s_\lambda^{\mathrm{Av}}(\omega) = s_\lambda^{\mathrm{Ret}}(\omega)^\dagger, \tag{35b}$$

$$s_\lambda^{\mathrm{K}}(\omega) = [1 - 2f_{\mathrm{eff}}(\omega)][s_\lambda^{\mathrm{Ret}}(\omega) - s_\lambda^{\mathrm{Av}}(\omega)], \tag{35c}$$

and those of the full single scale propagator $S_\lambda = G_\lambda g_\lambda^{-1} s_\lambda g_\lambda^{-1} G_\lambda$ by

$$S_\lambda^{\mathrm{Ret}}(\omega) = -\frac{i}{2}[G_\lambda^{\mathrm{Ret}}(\omega)]^2, \tag{36a}$$

$$S_\lambda^{\mathrm{Av}}(\omega) = S_\lambda^{\mathrm{Ret}}(\omega)^\dagger, \tag{36b}$$

$$S_\lambda^{\mathrm{K}}(\omega) = -\frac{i}{2}G_\lambda^{\mathrm{Ret}}(\omega)G_\lambda^{\mathrm{K}}(\omega) + \frac{i}{2}G_\lambda^{\mathrm{K}}(\omega)G_\lambda^{\mathrm{Av}}(\omega) - i[1 - 2f_{\mathrm{eff}}(\omega)]G_\lambda^{\mathrm{Ret}}(\omega)G_\lambda^{\mathrm{Av}}(\omega). \tag{36c}$$

A special situation occurs when

$$G_\lambda^{\mathrm{K}}(\omega) = [1 - 2f_{\mathrm{eff}}(\omega)][G_\lambda^{\mathrm{Ret}}(\omega) - G_\lambda^{\mathrm{Av}}(\omega)]. \tag{37}$$

Then Eq. (36c) can be simplified to

$$S_\lambda^{\mathrm{K}}(\omega) = [1 - 2f_{\mathrm{eff}}(\omega)][S_\lambda^{\mathrm{Ret}}(\omega) - S_\lambda^{\mathrm{Av}}(\omega)]. \tag{38}$$

The condition (37) is fulfilled, for instance, due to the fluctuation dissipation theorem, in thermal equilibrium, when $\mu_{\mathrm{L}} = \mu_{\mathrm{R}}$ and $f_{\mathrm{L}}(\omega) = f_{\mathrm{R}}(\omega) = f(\omega) = f_{\mathrm{eff}}(\omega)$. In nonequilibrium inelastic interaction processes mediated by the two-particle interaction will in general break the relation (37): via contributions to Σ^{K} and to the anti-Hermitian part of Σ^{Ret} they tend to smoothen the effective distribution. Later we will feed back only the static part of the self-energy into the RG flow so that Eq. (37) is fulfilled automatically, see Sec. VI D.

The starting values of the vertex functions at $\lambda = \infty$ can be determined as follows. For $\lambda \to \infty$ the propagator $g_\lambda^{\alpha|\alpha'}$ vanishes as $1/\lambda$ whereas $\int d\omega g_\lambda^{\alpha|\alpha'}(\omega)$ approaches a finite constant. Hence all diagrams having more internal lines than integrations over independent frequencies vanish. For a diagram with m two-particle vertices which contributes to the n-particle vertex function γ_n the number of internal lines is $2m-n$ while the number of integrations over independent frequencies is $m-n+1$. Therefore only the first-order contributions to the vertex functions do not vanish for $\lambda \to \infty$. This can also be understood in terms of time-dependent diagrammatics: due to the diverging decay rate $\lambda \to \infty$ only diagrams which are completely local in time do not vanish. These are exactly the first-order diagrams, namely, the Hartree-Fock diagram for the self-energy Σ and the bare interaction vertex for γ_2,

$$\gamma_n(\lambda = \infty) = 0, \quad n \geq 3, \tag{39a}$$

$$\gamma_2(\lambda = \infty) = \bar{v}, \tag{39b}$$

$$\Sigma_\sigma^{\mathrm{Ret,Av}}(\lambda = \infty) = \lim_{\lambda\to\infty}\left[-\frac{i}{2\pi}\sum_{\sigma'}\bar{v}_{\sigma\sigma'|\sigma\sigma'}\int d\omega g_{\lambda\sigma'}^{<}(\omega)\right] = \frac{U}{2}, \tag{39c}$$

$$\Sigma^{\mathrm{K}}(\lambda = \infty) = 0. \tag{39d}$$

In Eq. (39b), $\bar{v}$ is given by

$$\bar{v}_{\sigma_1'\sigma_2'|\sigma_1\sigma_2}^{\alpha_1'\alpha_2'|\alpha_1\alpha_2} = \begin{cases} \frac{1}{2}\bar{v}_{\sigma_1'\sigma_2'|\sigma_1\sigma_2} & \text{if } \alpha_1' + \alpha_2' + \alpha_1 + \alpha_2 \text{ is odd,} \\ 0 & \text{else,} \end{cases} \tag{40}$$

with

$$\bar{v}_{\sigma_1'\sigma_2'|\sigma_1\sigma_2} = \begin{cases} U & \text{if } \sigma_1' = \sigma_1 = \bar{\sigma}_2' = \bar{\sigma}_2, \\ -U & \text{if } \sigma_1' = \bar{\sigma}_1 = \bar{\sigma}_2' = \sigma_2, \\ 0 & \text{else,} \end{cases} \tag{41}$$

compare Eqs. (1) and (25). The integral in Eq. (39c) has been evaluated by

$$-\frac{i}{2\pi}\int d\omega g_{\lambda\sigma'}^{<}(\omega) = \frac{1}{\pi}\int dx \frac{f_{\mathrm{eff}}(\varepsilon_{\sigma'} + x\Gamma_\lambda/2)}{x^2+1} \overset{\lambda\to\infty}{\to} \frac{1}{\pi}\int_{-\infty}^{0} dx \frac{1}{x^2+1} = \frac{1}{2}, \tag{42}$$

where $x = 2(\omega - \varepsilon_{\sigma'})/\Gamma_\lambda$. The physical interpretation of Eq. (42) is that the mean occupation of an infinitely broadened level is 1/2.

Hybridization as flow parameter has the advantage to conserve causality and the KMS conditions (the latter being violated, for example, by the imaginary frequency cutoff introduced in Ref. 25) and to be applicable to zero-dimensional systems (as opposed to the momentum cutoff). Since it changes the free propagator in a smooth way, S_λ is not restricted sharply to a single scale by a delta function, as it happens for step-function cutoffs, e.g., the momentum cutoff. Such a delta function simplifies the flow equations since it cancels one of the necessary integrations. The hybridization flow thus has the disadvantage of an extra integration in the flow equations compared to step function cutoffs.

V. FRG IN STATIC APPROXIMATION

Before discussing the more elaborate frequency-dependent truncation scheme, we describe a basic static approximation to the flow: the flow of the n-particle vertex functions for $n \geq 3$ is neglected and the flow of the two-particle vertex function is reduced to the flow of a frequency-independent effective interaction strength. As a consequence the self-energy remains frequency independent which means that the influence of the interaction on single-particle properties of the system is described by a mere shift of the single-particle levels. This approximation has been studied at $T=0$ within a fRG treatment based on Matsubara formalism using an imaginary frequency cutoff.[54,55] There it was shown to produce a Kondo scale exponentially small in U/Γ which occurs in the pinning of the renormalized level position to the chemical potential. Results for the dependence of the linear conductance on the gate voltage for different magnetic fields have been found to be in very good agreement with Bethe ansatz and numerical renormalization-group computations. It turns out that in thermal equilibrium at $T=0$ the hybridization flow produces the identical flow equations. Hence this Keldysh approach incorporates all features found in Ref. 55 for the Matsubara fRG.

Apart from its success in describing the linear conductance the applicability of the approximation in question is restricted. Given a frequency-independent self-energy, the spectral density $\rho_\sigma(\omega)$ is a Lorentzian that is centered at the renormalized level position $\tilde{\varepsilon}_\sigma$ and has fixed width and height,

$$\rho_\sigma(\omega) = \frac{1}{\pi} \frac{\Gamma/2}{(\omega - \tilde{\varepsilon}_\sigma)^2 + \Gamma^2/4}. \tag{43}$$

Therefore the approximation cannot describe any features connected to details of the spectral function such as the formation of a Kondo resonance with side bands and its dependence on temperature or voltage. That is why we do not elaborate in detail on this approximation but merely show that at zero temperature and in equilibrium the resulting flow equation are identical to those of Ref. 55.

Reducing the two-particle vertex function to a frequency-independent effective interaction means setting

$$(\gamma_2^\lambda)^{\alpha_1'\alpha_2'|\alpha_1\alpha_2}_{\sigma_1'\sigma_2'|\sigma_1\sigma_2}(\omega_1'\omega_2'|\omega_1\omega_2) = (\bar{v}_\lambda)^{\alpha_1'\alpha_2'|\alpha_1\alpha_2}_{\sigma_1'\sigma_2'|\sigma_1\sigma_2}, \tag{44}$$

where $\bar{v}_\lambda$ is obtained from $\bar{v}$ by replacing the bare interaction U by a renormalized one U_λ in Eq. (41). Here the effective interaction U_λ is a real number whose flow starts at

$$U_{\lambda=\infty} = U. \tag{45}$$

As a consequence of that approximation to the vertex function, the flowing self-energy remains frequency independent and real, so that we can speak of a flowing effective level position $\varepsilon_\sigma^\lambda = \varepsilon_\sigma + \Sigma^{\mathrm{Ret}}_{\lambda\sigma}$. The initial condition for the level position is according to Eqs. (3) and (39c),

$$\varepsilon_\sigma^{\lambda=\infty} = \varepsilon_\sigma + \Sigma_\sigma^{\mathrm{Ret}}(\lambda=\infty) = eV_g - \sigma B. \tag{46}$$

The starting values, Eqs. (45) and (46), are identical to those of Ref. 55. Note that in the framework used there the initial condition for the level position is the result of a first stage of flow from $\lambda=\infty$ to $\lambda=\lambda_0 \to \infty$, see, e.g., Ref. 54.

From Eq. (27) we derive the flow equation for the level position

$$\begin{aligned}\frac{d\varepsilon_\sigma^\lambda}{d\lambda} &= -\frac{i}{2\pi}\frac{U_\lambda}{2}\int d\omega S^{\mathrm{K}}_{\lambda\bar{\sigma}}(\omega) \\ &= -\frac{U_\lambda}{8\pi}\int d\omega\, \mathrm{sign}(\omega)\{[G^{\mathrm{Ret}}_{\lambda\bar{\sigma}}(\omega)]^2 + [G^{\mathrm{Av}}_{\lambda\bar{\sigma}}(\omega)]^2\},\end{aligned} \tag{47}$$

where we used Eq. (38) with

$$1 - 2f_{\mathrm{eff}}(\omega) = 1 - 2f(\omega) = \mathrm{sign}(\omega) \quad \text{for } T=0,\ \mu=0. \tag{48}$$

Inserting

$$G^{\mathrm{Ret}}_\lambda(\omega) = \frac{1}{\omega - \varepsilon^\lambda + i(\Gamma+\lambda)/2} = G^{\mathrm{Av}}_\lambda(\omega)^\dagger \tag{49}$$

we can evaluate the integral in Eq. (47) and obtain

$$\frac{d\varepsilon_\sigma^\lambda}{d\lambda} = \frac{U_\lambda}{2\pi}\frac{\varepsilon^\lambda_{\bar{\sigma}}}{\varepsilon^{\lambda 2}_{\bar{\sigma}} + (\Gamma+\lambda)^2/4}. \tag{50}$$

The flow Eq. (28) for γ_2 generates a frequency-dependent vertex function which has a richer structure in terms of Keldysh and spin indices than indicated in Eq. (44). It can be shown that after neglecting the contribution from the three-particle vertex function (28a) this structure can be reduced to the simple form given in Eq. (44) by setting all outer frequency arguments equal to the chemical potential μ. We note that this projection onto the Fermi surface is the core idea of the static approximation. The resulting flow equation acquires the form

$$\begin{aligned}\frac{dU_\lambda}{d\lambda} = \frac{U_\lambda^2}{2}[&(I^{\mathrm{pp}}_\lambda)^{22|12}_{\uparrow\downarrow}(0) + (I^{\mathrm{pp}}_\lambda)^{22|21}_{\uparrow\downarrow}(0) \\ &+ (I^{\mathrm{ph}}_\lambda)^{21|22}_{\uparrow\downarrow}(0) + (I^{\mathrm{ph}}_\lambda)^{22|12}_{\uparrow\downarrow}(0)],\end{aligned} \tag{51}$$

where we abbreviated frequency integrals appearing in the particle-particle and particle-hole channel by

$$(I_\lambda^{\mathrm{pp}})_{\sigma_1\sigma_2}^{\alpha_1\alpha_2|\alpha_1'\alpha_2'}(\omega)=\frac{i}{2\pi}\int d\omega'\left[G_{\lambda\sigma_1}^{\alpha_1|\alpha_1'}\left(\frac{\omega}{2}+\omega'\right)S_{\lambda\sigma_2}^{\alpha_2|\alpha_2'}\left(\frac{\omega}{2}-\omega'\right)+S_{\lambda\sigma_1}^{\alpha_1|\alpha_1'}\left(\frac{\omega}{2}+\omega'\right)G_{\lambda\sigma_2}^{\alpha_2|\alpha_2'}\left(\frac{\omega}{2}-\omega'\right)\right], \tag{52a}$$

$$(I_\lambda^{\mathrm{ph}})_{\sigma_1\sigma_2}^{\alpha_1\alpha_2|\alpha_1'\alpha_2'}(\omega)=\frac{i}{2\pi}\int d\omega'\left[G_{\lambda\sigma_1}^{\alpha_1|\alpha_1'}\left(\omega'-\frac{\omega}{2}\right)S_{\lambda\sigma_2}^{\alpha_2|\alpha_2'}\left(\omega'+\frac{\omega}{2}\right)+S_{\lambda\sigma_1}^{\alpha_1|\alpha_1'}\left(\omega'-\frac{\omega}{2}\right)G_{\lambda\sigma_2}^{\alpha_2|\alpha_2'}\left(\omega'+\frac{\omega}{2}\right)\right]. \tag{52b}$$

Making use of Eqs. (36a), (36b), (37), (38), (48), and (49) we evaluate the integrals and obtain

$$\frac{dU_\lambda}{d\lambda}=\frac{U_\lambda^2}{\pi}\frac{\varepsilon_\uparrow^\lambda}{\varepsilon_\uparrow^{\lambda 2}+(\Gamma+\lambda)^2/4}\frac{\varepsilon_\downarrow^\lambda}{\varepsilon_\downarrow^{\lambda^2}+(\Gamma+\lambda)^2/4}. \tag{53}$$

The substitution $\lambda\to 2\lambda$ maps the flow Eqs. (50) and (53) onto those of Ref. 55. We note in passing, that the static approximation scheme can be carried out as well with the imaginary frequency cutoff from Ref. 25 instead of the hybridization flow parameter; the special advantage of the hybridization flow to conserve the KMS relations becomes relevant only in the dynamic approximation scheme introduced in Sec. VI. The flow equations of the static scheme based on the imaginary frequency cutoff are again identical to Eqs. (50) and (53) and to the flow equations of Ref. 55. The real-frequency cutoff used in Ref. 38, on the other hand, produces different flow equations which nevertheless lead again to the same final solution.[38]

It is easy to generalize the static approximation scheme to nonequilibrium. Since the Keldysh component of the self-energy is not renormalized we merely need to replace Eq. (48) by

$$1-2f_{\mathrm{eff}}(\omega)=\sum_r\frac{\Gamma^{(r)}}{\Gamma}\mathrm{sign}(\omega-\mu_r), \tag{54}$$

which leads to a superposition of the flow equations found for thermal equilibrium in the form

$$\frac{d\varepsilon_\sigma^\lambda}{d\lambda}=\frac{U_\lambda}{2\pi}\sum_r\frac{\Gamma_r}{\Gamma}\frac{\varepsilon_{\bar\sigma}^\lambda-\mu_r}{(\varepsilon_{\bar\sigma}^\lambda-\mu_r)^2+(\Gamma+\lambda)^2/4}, \tag{55a}$$

$$\frac{dU_\lambda}{d\lambda}=\frac{U_\lambda^2}{\pi}\sum_r\frac{\Gamma_r}{\Gamma}\frac{(\varepsilon_\uparrow^\lambda-\mu_r)}{(\varepsilon_\uparrow^\lambda-\mu_r)^2+(\Gamma+\lambda)^2/4}\times\frac{(\varepsilon_\downarrow^\lambda-\mu_r)}{(\varepsilon_\downarrow^\lambda-\mu_r)^2+(\Gamma+\lambda)^2/4}. \tag{55b}$$

This approach, however, does not provide a reliable description of the influence of bias voltage, since it restricts the spectral function by construction to a single Lorentzian peak; a splitting or damping of the peak is principally impossible.

VI. FRG IN DYNAMIC APPROXIMATION

In order to overcome the restrictions of the approximation described in Sec. V, a frequency-dependent self-energy is required. The flow Eq. (27) produces a frequency-dependent self-energy only if the two-particle vertex function is frequency dependent. Therefore our aim is to extend the scheme described in Sec. V in a way that a frequency-dependent two-particle vertex function is generated. We seek for an extension which is as basic as possible; in particular, we neglect the influence of the three-particle vertex function further on, such that the flow of the two-particle vertex function is induced by the three contributions, Eqs. (28b)–(28d).

A. Ladder approximations

Recent investigations of the SIAM by diagrammatic techniques have revealed the importance of the exchange particle-hole ladder [random phase approximation (RPA) series] for the emergence of Kondo physics.[75,76] Let us therefore in a first step neglect all contributions to the flow of the two-particle vertex function except for the exchange particle-hole channel, Eq. (28c). If we suppress additionally the feedback of the self-energy into the propagators except for the initial Hartree term, Eq. (39c), then the flow equation for the two-particle vertex functions reads

$$\begin{aligned}\frac{d}{d\lambda}(\gamma_\lambda^{\mathrm{x}})_{1'2'|12}&=\frac{i}{2\pi}(\gamma_\lambda^{\mathrm{x}})_{1'4'|32}[s_{3|3'}^\lambda g_{4|4'}^\lambda+g_{3|3'}^\lambda s_{4|4'}^\lambda]\times(\gamma_\lambda^{\mathrm{x}})_{3'2'|14}\\&=\frac{i}{2\pi}(\gamma_\lambda^{\mathrm{x}})_{1'4'|32}\frac{dg_{3|3'}^\lambda g_{4|4'}^\lambda}{d\lambda}(\gamma_\lambda^{\mathrm{x}})_{3'2'|14},\end{aligned} \tag{56}$$

where g^λ is obtained from Eq. (34) by replacing ε_σ with $\varepsilon_\sigma+U/2$. We denoted the vertex function in this approximation with a superscript "x" which refers to "exchange." The solution of the flow Eq. (56) with the initial condition $\gamma_{\lambda=\infty}^{\mathrm{x}}=\bar v$ is given by the exchange particle-hole ladder (RPA series)

$$\begin{aligned}(\gamma_\lambda^{\mathrm{x}})_{1'2'|12}&=\bar v_{1'2'|12}+\frac{i}{2\pi}\bar v_{1'4'|32}g_{3|3'}^\lambda g_{4|4'}^\lambda\bar v_{3'2'|14}+\cdots\\&=\bar v_{1'2'|12}+\frac{i}{2\pi}\bar v_{1'4'|32}g_{3|3'}^\lambda g_{4|4'}^\lambda(\gamma_\lambda^{\mathrm{x}})_{3'2'|14}.\end{aligned} \tag{57}$$

Due to frequency conservation at each interaction vertex, the frequency dependence of the ladder is reduced to a single bosonic combination of the external frequencies,

$$\gamma_\lambda^{\mathrm{x}}(\omega_1',\omega_2'|\omega_1,\omega_2)=(\gamma_\lambda^{\mathrm{x}})(X), \tag{58}$$

with

$$X = \omega_2' - \omega_1 = \omega_2 - \omega_1'. \tag{59}$$

We evaluate the RPA series and obtain

$$(\gamma_\lambda^{\mathrm{x}})^{12|22}_{\sigma\bar{\sigma}|\sigma\bar{\sigma}}(X) = \frac{U}{2} + \frac{U^2}{4}\frac{(B_\lambda^{\mathrm{x}})_{\sigma\bar{\sigma}}(X)}{1 - \frac{U}{2}(B_\lambda^{\mathrm{x}})_{\sigma\bar{\sigma}}(X)}, \tag{60}$$

where

$$(B_\lambda^{\mathrm{x}})_{\sigma\bar{\sigma}}(X) = \frac{i}{2\pi}\int d\omega \left[g^{\mathrm{Ret}}_{\lambda\sigma}\left(\omega - \frac{X}{2}\right) g^{\mathrm{K}}_{\lambda\bar{\sigma}}\left(\omega + \frac{X}{2}\right) + g^{\mathrm{K}}_{\lambda\sigma}\left(\omega - \frac{X}{2}\right) g^{\mathrm{Av}}_{\lambda\bar{\sigma}}\left(\omega + \frac{X}{2}\right)\right] \tag{61}$$

denotes the particle-hole polarization operator. In the special case $T=0$, $B=0$, $V=0$, $eV_g=\mu=0$ we find

$$(B_\lambda^{\mathrm{x}})_{\sigma\bar{\sigma}}(X) = -\frac{2}{\pi}\frac{\Gamma_\lambda}{X(X - i\Gamma_\lambda)}\ln\left(1 + i\frac{X}{\Gamma_\lambda/2}\right). \tag{62}$$

Expanding $1/(B_\lambda^{\mathrm{x}})_{\sigma\bar{\sigma}}(X)$ in powers of X/Γ_λ results in

$$(\gamma_\lambda^{\mathrm{x}})^{12|22}_{\sigma\bar{\sigma}|\sigma\bar{\sigma}}(X) \simeq \frac{U}{2} - \frac{i}{2\pi}\frac{U^2}{X - i(\Gamma_\lambda/2 - U/\pi)}, \quad X \ll \Gamma_\lambda, \tag{63}$$

which features a singularity when λ reaches the value

$$\lambda = \lambda_c = 2U/\pi - \Gamma. \tag{64}$$

Additionally, for $\lambda < \lambda_c$ the function $(\gamma_\lambda^{\mathrm{x}})^{12|22}_{\sigma\bar{\sigma}|\sigma\bar{\sigma}}(X)$ exhibits the wrong analytic behavior, being analytic in the upper half plane of X instead of the lower one as required by causality.[42] Therefore the flow $\lambda \to 0$ can only be finished if

$$U < U_c = \pi\Gamma/2. \tag{65}$$

This limitation is not even overcome when the full self-energy is fed back into the flow, replacing s and g in Eq. (56) by S and G.

Hence we also have to take into account the other two channels, Eqs. (28b) and (28d). A parquet summation based procedure mixing the exchange particle-hole and the particle-particle channel has been set up in Ref. 75, in which the authors study the SIAM within Matsubara formalism. Essentially the particle-particle channel serves them to renormalize the interaction U which enters the exchange channel to an effective value U_{eff} which is always lesser than U_c. The difference $U_c - U_{\mathrm{eff}}$ is then used as a measure for the Kondo scale.

We aim to implement a similar proceeding within the framework of the functional RG. We consider it appropriate to include also contributions from the direct particle-hole channel because this channel bears the same singularity as the exchange channel. In order to see this let us define the particle-particle and the direct particle-hole ladder on the analogy of Eq. (56) by the flow equations

$$\frac{d}{d\lambda}(\gamma_\lambda^{\mathrm{p}})_{1'2'|12} = \frac{i}{4\pi}(\gamma_\lambda^{\mathrm{p}})_{1'2'|34}\frac{dg^\lambda_{3|3'}g^\lambda_{4|4'}}{d\lambda}(\gamma_\lambda^{\mathrm{p}})_{3'4'|12}, \tag{66a}$$

$$\frac{d}{d\lambda}(\gamma_\lambda^{\mathrm{d}})_{1'2'|12} = -\frac{i}{2\pi}(\gamma_\lambda^{\mathrm{d}})_{1'3'|14}\frac{dg^\lambda_{3|3'}g^\lambda_{4|4'}}{d\lambda}(\gamma_\lambda^{\mathrm{d}})_{4'2'|32}. \tag{66b}$$

In correspondence with Eq. (57) the solutions of these flow equations satisfy

$$(\gamma_\lambda^{\mathrm{p}})_{1'2'|12} = \bar{v}_{1'2'|12} + \frac{i}{4\pi}\bar{v}_{1'2'|34}g_{3|3'}g_{4|4'}(\gamma_\lambda^{\mathrm{p}})_{3'4'|12}, \tag{67a}$$

$$(\gamma_\lambda^{\mathrm{d}})_{1'2'|12} = \bar{v}_{1'2'|12} - \frac{i}{2\pi}\bar{v}_{1'3'|14}g_{3|3'}g_{4|4'}(\gamma_\lambda^{\mathrm{d}})_{4'2'|32}. \tag{67b}$$

Their frequency dependence takes the form

$$(\gamma_\lambda^{\mathrm{p}})(\omega_1', \omega_2'|\omega_1, \omega_2) = (\gamma_\lambda^{\mathrm{p}})(\Pi), \tag{68a}$$

$$(\gamma_\lambda^{\mathrm{d}})(\omega_1', \omega_2'|\omega_1, \omega_2) = (\gamma_\lambda^{\mathrm{d}})(\Delta), \tag{68b}$$

with

$$\Pi = \omega_1 + \omega_2 = \omega_1' + \omega_2', \tag{69a}$$

$$\Delta = \omega_1' - \omega_1 = \omega_2 - \omega_2'. \tag{69b}$$

Evaluating Eq. (67a) one finds

$$(\gamma_\lambda^{\mathrm{p}})^{12|22}_{\sigma\bar{\sigma}|\sigma\bar{\sigma}}(\Pi) = \frac{U}{2} + \frac{U^2}{4}\frac{(B_\lambda^{\mathrm{p}})_{\sigma\bar{\sigma}}(\Pi)}{1 - \frac{U}{2}(B_\lambda^{\mathrm{p}})_{\sigma\bar{\sigma}}(\Pi)}, \tag{70}$$

where at $T=0$, $B=0$, $V=0$, $eV_g=\mu=0$ the particle-particle polarization operator B_λ^{p} takes the form

$$(B_\lambda^{\mathrm{p}})_{\sigma\bar{\sigma}}(\Pi) = \frac{2}{\pi}\frac{\Gamma_\lambda}{\Pi(\Pi + i\Gamma_\lambda)}\ln\left(1 - i\frac{\Pi}{\Gamma_\lambda/2}\right), \tag{71}$$

such that $\gamma_\lambda{}^{\mathrm{p}}$ is a regular function on the real Π axis for all values of U. In contrast, $(\gamma_\lambda^{\mathrm{d}})^{12|22}$ satisfies

$$(\gamma^{\mathrm{d}})^{12|22}_{\sigma\bar{\sigma}|\sigma\bar{\sigma}}(\Delta) = \frac{1}{2}[(\gamma^{\mathrm{p}})^{12|22}_{\sigma\bar{\sigma}|\sigma\bar{\sigma}}(\Delta) + (\gamma^{\mathrm{x}})^{12|22}_{\sigma\bar{\sigma}|\sigma\bar{\sigma}}(\Delta)^*], \tag{72}$$

$$(\gamma^{\mathrm{d}})^{12|22}_{\sigma\bar{\sigma}|\sigma\sigma}(\Delta) = \frac{1}{2}[(\gamma^{\mathrm{p}})^{12|22}_{\sigma\bar{\sigma}|\sigma\bar{\sigma}}(\Delta) - (\gamma^{\mathrm{x}})^{12|22}_{\sigma\bar{\sigma}|\sigma\bar{\sigma}}(\Delta)^*], \tag{73}$$

and thus possesses the same singularity as the exchange particle-hole channel.

B. Approximated mixing of the channels

In an approximation taking into account all three channels, Eqs. (28b)–(28d), the two-particle vertex function will

depend on all three frequencies, $\gamma(\Pi,X,\Delta)$. Due to frequency conservation these three ones are indeed sufficient to express the general frequency dependence. In the following the three bosonic frequency arguments of the vertex function will always be indicated in the order (Π,X,Δ). When all three contributions, Eqs. (28b)–(28d), to the flow are taken into account simultaneously, then the dependence on Π,X,Δ is mixed through the feedback of the vertex function on the right-hand side of the flow equation that reads

$$\frac{d}{d\lambda}\gamma^{\lambda}_{1'2'|12}(\Pi,X,\Delta) = \frac{i}{2\pi}\int d\omega \Bigg\{ \gamma^{\lambda}_{1'2'|34}\left(\Pi,\omega+\frac{X-\Delta}{2},\omega-\frac{X-\Delta}{2}\right) S^{\lambda}_{3|3'}\left(\frac{\Pi}{2}-\omega\right) G^{\lambda}_{4|4'}\left(\frac{\Pi}{2}+\omega\right)$$
$$\times \gamma^{\lambda}_{3'4'|12}\left(\Pi,\frac{X+\Delta}{2}+\omega,\frac{X+\Delta}{2}-\omega\right) \tag{74a}$$
$$+ \gamma^{\lambda}_{1'4'|32}\left(\frac{\Pi+\Delta}{2}+\omega,X,\frac{\Pi+\Delta}{2}-\omega\right)\left[S^{\lambda}_{3|3'}\left(\omega-\frac{X}{2}\right) G^{\lambda}_{4|4'}\left(\omega+\frac{X}{2}\right) + G^{\lambda}_{3|3'}\left(\omega-\frac{X}{2}\right) S^{\lambda}_{4|4'}\left(\omega+\frac{X}{2}\right)\right]$$
$$\times \gamma^{\lambda}_{3'2'|14}\left(\omega+\frac{\Pi-\Delta}{2},X,\omega-\frac{\Pi-\Delta}{2}\right) \tag{74b}$$
$$- \gamma^{\lambda}_{1'3'|14}\left(\omega+\frac{\Pi-X}{2},\omega-\frac{\Pi-X}{2},\Delta\right)\left[S^{\lambda}_{3|3'}\left(\omega-\frac{\Delta}{2}\right) G^{\lambda}_{4|4'}\left(\omega+\frac{\Delta}{2}\right) + G^{\lambda}_{3|3'}\left(\omega-\frac{\Delta}{2}\right) S^{\lambda}_{4|4'}\left(\omega+\frac{\Delta}{2}\right)\right]$$
$$\times \gamma^{\lambda}_{4'2'|32}\left(\frac{\Pi+X}{2}+\omega,\frac{\Pi+X}{2}-\omega,\Delta\right)\Bigg\}. \tag{74c}$$

Here we use shorthand notation like

$$\gamma^{\lambda}_{1'2'|12} \equiv (\gamma^{\lambda}_{2})^{\alpha'_1\alpha'_2|\alpha_1\alpha_2}_{\sigma'_1\sigma'_2|\sigma_1\sigma_2} \tag{75}$$

and indices occurring twice in a product implicate summation over state and Keldysh indices. The flow Eq. (74) leads to a complicated dependence of the vertex function on the three frequencies (Π,X,Δ). As a consequence a numerical solution of the flow equation requires a sampling of three-dimensional frequency space which constitutes a high computational effort. The structure of the flow equation suggests to approximate the frequency dependence of the two-particle vertex function by

$$\gamma_{\lambda}(\Pi,X,\Delta) \simeq \bar{v} + \varphi^{\mathrm{p}}_{\lambda}(\Pi) + \varphi^{\mathrm{x}}_{\lambda}(X) + \varphi^{\mathrm{d}}_{\lambda}(\Delta), \tag{76}$$

where the bare interaction vertex $\bar{v}$ is the initial value at the beginning of the flow, $\bar{v}=\gamma_{\lambda=\infty}$, and where $\varphi^{\mathrm{p}}_{\lambda}(\Pi)$, $\varphi^{\mathrm{x}}_{\lambda}(X)$, $\varphi^{\mathrm{d}}_{\lambda}(\Delta)$ are approximations to the parts of γ produced by the three channels, Eqs. (74a)–(74c), respectively. An analogous approximation has been investigated in studies of the SIAM based on the equilibrium Matsubara fRG.[57] The results achieved with and without this approximation were of the same quality. Reliable results were obtained for small and intermediate U/Γ. The limiting effect for large U/Γ seems to stem from omitting the three-particle vertex function. For small U/Γ the system can be described by second-order perturbation theory which also produces a two-particle vertex function of the form (76). Our fRG treatment will fully comprise the diagrams of second-order perturbation theory for the self-energy and for the vertex function. Therefore, for $U\to 0$ the fRG results asymptotically approach those of second-order perturbation theory.

In order to achieve the form (76) where the frequency dependence is split up into three functions we have to eliminate X and Δ from Eq. (74a), Π and Δ from Eq. (74b), and Π and X from Eq. (74c). It is obvious that any manipulation of this type can only yield convincing results if the frequency dependence of the vertex functions is not very pronounced. This limits the range of applicability of the approximation to small and intermediate interaction strengths. Kondo physics emerging for large U/Γ cannot be described in general: we expect $\gamma(\Pi,X,\Delta)$ to exhibit a sharp resonance as function of X in this regime (cf. Ref. 75 and Sec. VI A); furthermore omitting the three-particle vertex is not justified for large U/Γ.

Different approaches in order to get rid of the frequency mixing on the right-hand side of Eq. (74) are conceivable. The variety of reasonable replacements is however restricted by the necessity that the components of the vertex function maintain their fundamental features concerning exchange of particles, causality, and the KMS conditions as described in Ref. 42. We have tested different possibilities. Here we present only that one which provided the most convincing results. It is based on a procedure to assign a static vertex to the functions $\varphi^{\mathrm{p,x,d}}_{\lambda}$,

$$\varphi^{\mathrm{p}}_{\lambda}(\Pi) \to \Phi^{\mathrm{p}}_{\lambda}, \tag{77a}$$

$$\varphi_\lambda^{\mathrm{x}}(X) \to \Phi_\lambda^{\mathrm{x}}, \tag{77b}$$

$$\varphi_\lambda^{\mathrm{d}}(\Delta) \to \Phi_\lambda^{\mathrm{d}}. \tag{77c}$$

The $\Phi_\lambda^{\mathrm{p,x,d}}$ are frequency independent and represent effective static interactions between particles of either opposite or identical spin state. Since permutations of the incoming indices map the exchange particle-hole channel onto the direct particle-hole channel and vice versa, the $\Phi^{\mathrm{x,d}}$ have to satisfy

$$(\Phi_\lambda^{\mathrm{x}})_{\sigma\bar{\sigma}\bar{\sigma}\sigma}^{\alpha_1'\alpha_2'|\alpha_2\alpha_1} = -(\Phi_\lambda^{\mathrm{d}})_{\sigma\bar{\sigma}|\bar{\sigma}\sigma}^{\alpha_1'\alpha_2'|\alpha_1\alpha_2}, \tag{78a}$$

$$(\Phi_\lambda^{\mathrm{x}})_{\sigma\bar{\sigma}\bar{\sigma}\sigma}^{\alpha_1'\alpha_2'|\alpha_1\alpha_2} = -(\Phi_\lambda^{\mathrm{d}})_{\sigma\bar{\sigma}|\sigma\bar{\sigma}}^{\alpha_1'\alpha_2'|\alpha_2\alpha_1}, \tag{78b}$$

$$(\Phi_\lambda^{\mathrm{x}})_{\sigma\sigma\sigma\sigma}^{\alpha_1'\alpha_2'|\alpha_1\alpha_2} = -(\Phi_\lambda^{\mathrm{d}})_{\sigma\sigma|\sigma\sigma}^{\alpha_1'\alpha_2'|\alpha_2\alpha_1}. \tag{78c}$$

This is achieved in the parametrization

$$(\Phi_\lambda^{\mathrm{p}})_{\sigma_1'\sigma_2'|\sigma_1\sigma_2} = \begin{cases} U_\lambda^{\mathrm{p}} & \text{if } \sigma_1' = \sigma_1 = \bar{\sigma}_2' = \bar{\sigma}_2, \\ -U_\lambda^{\mathrm{p}} & \text{if } \sigma_1' = \bar{\sigma}_1 = \bar{\sigma}_2' = \sigma_2, \\ 0 & \text{else}, \end{cases} \tag{79a}$$

$$(\Phi_\lambda^{\mathrm{x}})_{\sigma_1'\sigma_2'|\sigma_1\sigma_2} = \begin{cases} U_\lambda^{\mathrm{x}} & \text{if } \sigma_1' = \sigma_1 = \bar{\sigma}_2' = \bar{\sigma}_2, \\ -U_\lambda^{\mathrm{d}} & \text{if } \sigma_1' = \bar{\sigma}_1 = \bar{\sigma}_2' = \sigma_2, \\ -W_{\lambda\sigma_1}^{\mathrm{d}} & \text{if } \sigma_1' = \sigma_1 = \sigma_2' = \sigma_2, \\ 0 & \text{else}, \end{cases} \tag{79b}$$

$$(\Phi_\lambda^{\mathrm{d}})_{\sigma_1'\sigma_2'|\sigma_1\sigma_2} = \begin{cases} U_\lambda^{\mathrm{d}} & \text{if } \sigma_1' = \sigma_1 = \bar{\sigma}_2' = \bar{\sigma}_2, \\ -U_\lambda^{\mathrm{x}} & \text{if } \sigma_1' = \bar{\sigma}_1 = \bar{\sigma}_2' = \sigma_2, \\ W_{\lambda\sigma_1}^{\mathrm{d}} & \text{if } \sigma_1' = \sigma_1 = \sigma_2' = \sigma_2, \\ 0 & \text{else}, \end{cases} \tag{79c}$$

and

$$(\Phi_\lambda^{\mathrm{p,x,d}})_{\sigma_1'\sigma_2'|\sigma_1\sigma_2}^{\alpha_1'\alpha_2'|\alpha_1\alpha_2} = \begin{cases} \frac{1}{2}(\Phi_\lambda^{\mathrm{p,x,d}})_{\sigma_1'\sigma_2'|\sigma_1\sigma_2} \\ \text{if } \alpha_1' + \alpha_2' + \alpha_1 + \alpha_2 \text{ is odd} \\ 0 \text{ else}, \end{cases} \tag{80}$$

with $U_\lambda^{\mathrm{p,x,d}}$ and $W_{\lambda\sigma}^{\mathrm{d}}$ being real numbers, compare Eqs. (40) and (41). The detailed procedure to determine appropriate constants $U_\lambda^{\mathrm{p,x,d}}$, $W_{\lambda\sigma}^{\mathrm{d}}$ has to be consistent with the flow equations and is discussed below in Sec. VI C. In Eq. (79a) we exclude the possibility that an effective interaction between two particles of identical spin state could result from the particle-particle channel. The reason is that a static interaction vertex between particles of identical spin state vanishes when being antisymmetrized since the direct and exchange terms cancel each other. This is consistent with the fact that such a contribution is not generated by the flow Eq. (81a) below since $\bar{v}+\Phi_\lambda^{\mathrm{x}}+\Phi_\lambda^{\mathrm{d}}$ allows only interactions of particles in opposite spin states. Also the fact that $U_\lambda^{\mathrm{p,x,d}}$ are independent of the spin (while $W_{\lambda\sigma}^{\mathrm{d}}$ is not) is consistent with the structure of an effective interaction vertex, compare Eq. (41), and will be reproduced by the flow equations below.

When inserting now the form (76) on the right-hand side of the flow equation (74), the sum structure is reproduced by the flow if we replace $\varphi_\lambda^{\mathrm{x}}(X)$ and $\varphi_\lambda^{\mathrm{d}}(\Delta)$ in the particle-particle channel, Eq. (74a), by the constant vertices $\Phi_\lambda^{\mathrm{x}}$, $\Phi_\lambda^{\mathrm{d}}$ and proceed analogously for the other channels: in the flow of any channel the other two channels are reduced to constant vertices. The flow equations for $\varphi_\lambda^{\mathrm{p,x,d}}$ are then given by

$$\frac{d}{d\lambda}(\varphi_\lambda^{\mathrm{p}})_{1'2'|12}(\Pi) = \frac{1}{2}[\bar{v} + \varphi_\lambda^{\mathrm{p}}(\Pi) + \Phi_\lambda^{\mathrm{x}} + \Phi_\lambda^{\mathrm{d}}]_{1'2'|34} \times (I_\lambda^{\mathrm{pp}})_{34|3'4'}(\Pi)[\bar{v} + \varphi_\lambda^{\mathrm{p}}(\Pi) + \Phi_\lambda^{\mathrm{x}} + \Phi_\lambda^{\mathrm{d}}]_{3'4'|12}, \tag{81a}$$

$$\frac{d}{d\lambda}(\varphi_\lambda^{\mathrm{x}})_{1'2'|12}(X) = [\bar{v} + \Phi_\lambda^{\mathrm{p}} + \varphi_\lambda^{\mathrm{x}}(X) + \Phi_\lambda^{\mathrm{d}}]_{1'4'|32} \times (I_\lambda^{\mathrm{ph}})_{34|3'4'}(X)[\bar{v} + \Phi_\lambda^{\mathrm{p}} + \varphi_\lambda^{\mathrm{x}}(X) + \Phi_\lambda^{\mathrm{d}}]_{3'2'|14}, \tag{81b}$$

$$\frac{d}{d\lambda}(\varphi_\lambda^{\mathrm{d}})_{1'2'|12}(\Delta) = -[\bar{v} + \Phi_\lambda^{\mathrm{p}} + \Phi_\lambda^{\mathrm{x}} + \varphi_\lambda^{\mathrm{d}}(\Delta)]_{1'3'|14} \times (I_\lambda^{\mathrm{ph}})_{34|3'4'}(\Delta)[\bar{v} + \Phi_\lambda^{\mathrm{p}} + \Phi_\lambda^{\mathrm{x}} + \varphi_\lambda^{\mathrm{d}}(\Delta)]_{4'2'|32}, \tag{81c}$$

where we used a summation convention for index numbers representing the state σ and the Keldysh index α, and

$$(I_\lambda^{\mathrm{pp,ph}})_{34|3'4'} = \delta_{\sigma_3\sigma_3'}\delta_{\sigma_4\sigma_4'}(I_\lambda^{\mathrm{pp,ph}})_{\sigma_3\sigma_4}^{\alpha_3\alpha_4|\alpha_3'\alpha_4'} \tag{82}$$

refers to Eq. (52).

The different spin and Keldysh components of the functions $\varphi^{\mathrm{p,x,d}}$ are not completely independent of each other: there exist identities connecting them which stem from the invariance under exchange of particles and complex conjugation.[42] Further identities follow from spin conservation and from the special structure of the flow Eq. (81). In Appendix A we determine a set of independent spin and Keldysh components of the functions $\varphi^{\mathrm{p,x,d}}$ from which all other components can be derived. It is then sufficient to compute the RG flow of these independent components; the corresponding flow equations are presented in Appendices B and C.

C. How to determine $U_\lambda^{\mathrm{p,x,d}}$ and $W_{\lambda\sigma}^{\mathrm{d}}$

The approximation scheme described above requires a procedure which assigns effective constant interaction vertices $\Phi_\lambda^{\mathrm{p,x,d}}$ to the functions $\varphi_\lambda^{\mathrm{p}}(\Pi)$, $\varphi_\lambda^{\mathrm{x}}(X)$, $\varphi_\lambda^{\mathrm{d}}(\Delta)$. Hence it is a central question how to determine appropriate real numbers $U_\lambda^{\mathrm{p,x,d}}$, $W_{\lambda\sigma}^{\mathrm{d}}$ which characterize the vertices $\Phi_\lambda^{\mathrm{p,x,d}}$ in Eq. (79). We propose a very simple scheme for the case of thermal equilibrium. In order to generalize this approach to nonequilibrium however we will need to formulate additional constraints.

Let us first assume thermal equilibrium. Then we can show that

$$\Phi_\lambda^{\mathrm{P}} = \varphi_\lambda^{\mathrm{p}}(\Pi = 0), \tag{83a}$$

$$\Phi_\lambda^{\mathrm{x}} = \varphi_\lambda^{\mathrm{x}}(X = 0), \tag{83b}$$

$$\Phi_\lambda^{\mathrm{d}} = \varphi_\lambda^{\mathrm{d}}(\Delta = 0) \tag{83c}$$

have exactly the structure given in Eqs. (79) and (80). For the proof we make use of the special spin and Keldysh structure of $\varphi^{\mathrm{p,x,d}}$ that is described in Appendix A.

We first discuss the particle-hole channel. From Eqs. (A15a) and (A18a) we infer that $(a_\lambda^{\mathrm{d}})_{\sigma\bar{\sigma}}(0)$ and $(a_\lambda^{\mathrm{d}})_{\sigma\sigma}(0)$ are real numbers. Using the KMS conditions (A19) combined with Eq. (C8) we conclude further that $(b_\lambda^{\mathrm{d}})_{\sigma\bar{\sigma}}(0)=0$ and $(b_\lambda^{\mathrm{d}})_{\sigma\sigma}(0)=0$. In thermal equilibrium we can use the fluctuation dissipation theorem

$$G_\lambda^{\mathrm{K}}(\omega) = [1 - 2f(\omega)][G_\lambda^{\mathrm{Ret}}(\omega) - G_\lambda^{\mathrm{Av}}(\omega)], \tag{84a}$$

$$S_\lambda^{\mathrm{K}}(\omega) = [1 - 2f(\omega)][S_\lambda^{\mathrm{Ret}}(\omega) - S_\lambda^{\mathrm{Av}}(\omega)], \tag{84b}$$

to show that

$$(I_\lambda^{\mathrm{ph}})_{\sigma\bar{\sigma}}^{21|22}(0) + (I_\lambda^{\mathrm{ph}})_{\sigma\bar{\sigma}}^{22|12}(0) = -2\,\mathrm{Re}\left\{\frac{i}{2\pi}\int d\omega[G_\sigma^{\mathrm{Av}}(\omega)S_{\bar{\sigma}}^{\mathrm{Av}}(\omega) + S_\sigma^{\mathrm{Av}}(\omega)G_{\bar{\sigma}}^{\mathrm{Av}}(\omega)][1 - 2f(\omega)]\right\} \tag{85}$$

is a real number. From the flow Eq. (C6a) it follows that $(a_\lambda^{\mathrm{x}})_{\sigma\bar{\sigma}}(0)$ is real. The KMS condition (A13) then entails that $(b_\lambda^{\mathrm{x}})_{\sigma\bar{\sigma}}(0)=0$. In total this means that we can set

$$\Phi_\lambda^{\mathrm{d}} = \varphi_\lambda^{\mathrm{d}}(0) \quad \text{and} \quad \Phi_\lambda^{\mathrm{x}} = \varphi_\lambda^{\mathrm{x}}(0), \tag{86}$$

with

$$U_\lambda^{\mathrm{x}} = 2(a_\lambda^{\mathrm{x}})_{\sigma\bar{\sigma}}(0), \tag{87a}$$

$$U_\lambda^{\mathrm{d}} = 2(a_\lambda^{\mathrm{d}})_{\sigma\bar{\sigma}}(0), \tag{87b}$$

$$W_{\lambda\sigma}^{\mathrm{d}} = 2(a_\lambda^{\mathrm{d}})_{\sigma\sigma}(0). \tag{87c}$$

When we insert Eq. (87c) into Eq. (C7a) this yields, in particular, $d(a_\lambda^{\mathrm{d}})_{\sigma\bar{\sigma}}/d\lambda=0$. Combining this with the initial condition $(a_{\lambda=\infty}^{\mathrm{d}})_{\sigma\bar{\sigma}}=0$ we conclude from Eq. (87b) that

$$U_\lambda^{\mathrm{d}} \equiv 0. \tag{88}$$

For the particle-particle channel we combine the fluctuation dissipation theorem, Eq. (84), with

$$1 - 2f(\omega) = -[1 - 2f(-\omega)] \tag{89}$$

(mind the convention $\mu=0$) to find that

$$(I_\lambda^{\mathrm{pp}})_{\sigma\bar{\sigma}}^{22|12}(0) + (I_\lambda^{\mathrm{pp}})_{\sigma\bar{\sigma}}^{22|21}(0) = 2\,\mathrm{Re}\left\{\frac{i}{2\pi}\int d\omega[G_\sigma^{\mathrm{Ret}}(\omega)S_{\bar{\sigma}}^{\mathrm{Av}}(-\omega) + S_\sigma^{\mathrm{Ret}}(\omega)G_{\bar{\sigma}}^{\mathrm{Av}}(-\omega)]\times[1 - 2f(\omega)]\right\} \tag{90}$$

is a real number. Hence it follows from the flow Eq. (C3a) that $(a_\lambda^{\mathrm{p}})_{\sigma\bar{\sigma}}(0)$ is real. The KMS condition (A10) then demands that $(b_\lambda^{\mathrm{p}})_{\sigma\bar{\sigma}}(0)=0$. Therefore we can set

$$\Phi_\lambda^{\mathrm{p}} = \varphi_\lambda^{\mathrm{p}}(0) \tag{91}$$

with

$$U_\lambda^{\mathrm{p}} = 2(a_\lambda^{\mathrm{p}})_{\sigma\bar{\sigma}}(0). \tag{92}$$

(Note that $(\bar{v} + \Phi_\lambda^{\mathrm{p}} + \Phi_\lambda^{\mathrm{x}} + \Phi_\lambda^{\mathrm{d}}) = \bar{v}_\lambda$ is exactly the flowing effective interaction vertex used in the static approximation scheme in Sec. V.)

In the case of nonequilibrium with $\mu_{\mathrm{L}} + \mu_{\mathrm{R}} = 0$ we will also use Eqs. (87) and (92). While U_λ^{d} and W_λ^{d} are then again guaranteed to be real valued by Eqs. (A15a) and (A18a), additional assumptions are necessary to ensure this for U_λ^{x} and U_λ^{p}. If the propagator which we feed back into the flow of the two-particle vertex satisfies Eq. (37), then Eq. (85) is still valid in nonequilibrium, with $f_{\mathrm{eff}}(\omega)$ replacing $f(\omega)$; this warrants that U_λ^{x} is real. Under the additional assumptions

$$\Gamma_{\mathrm{L}} = \Gamma_{\mathrm{R}} \quad \text{and} \quad T_{\mathrm{L}} = T_{\mathrm{R}} \tag{93}$$

also Eq. (90) can be maintained; in that case also U_λ^{p} is real.

D. Self-energy feedback

The propagators S, G appearing in the flow equation for the self-energy and for the vertex function are full propagators, which means that they are dressed with the current value of the self-energy $\Sigma^\lambda(\omega)$. In this way the self-energy feeds back into its own flow and into the flow of the vertex function. In the preceding section we described that our flow scheme requires the validity of the fluctuation dissipation theorem such as Eq. (37), or, equivalently,

$$\Sigma_\lambda^{\mathrm{K}}(\omega) = [1 - 2f_{\mathrm{eff}}(\omega)][\Sigma_\lambda^{\mathrm{Ret}}(\omega) - \Sigma_\lambda^{\mathrm{Av}}(\omega)]. \tag{94}$$

While this identity is guaranteed in equilibrium by the KMS conditions, it constitutes an approximation in nonequilibrium; interaction effects that lead to a redistribution of particle statistics are neglected.

The results discussed in Sec. VIII below show that the feedback of the full frequency-dependent self-energy into the flow leads to an artificial smoothening of spectral features. The Kondo resonance at $\omega=0$, for instance, acquires a much broader shape than expected. Better results are achieved with a different feedback scheme for the self-energy which reduces its backcoupling into the flow to a simple shift of the single-particle levels. In analogy to the way of determining an effective static interaction vertex from the vertex function in Sec. VI C, we assign a real and static level shift E to the self-energy by setting

$$E_\sigma^{\mathrm{Ret}\,\lambda} = E_\sigma^{\mathrm{Av}\,\lambda} = \mathrm{Re}\,\Sigma_\sigma^{\mathrm{Ret}\,\lambda}(\omega = 0), \tag{95a}$$

$$E_\sigma^{\mathrm{K}\lambda} = 0. \tag{95b}$$

Only this static renormalization enters the propagators on the right-hand side of the flow equations for Σ^λ and γ^λ. Due to the missing Keldysh component of E_σ^λ the condition (37) is then readily fulfilled.

It turns out that this static self-energy feedback produces results distinctly better than in case of the full frequency-dependent self-energy feedback. We also studied mixed schemes, for instance, to feed the static self-energy into the flow of γ^Λ while the full self-energy is used for the flow of Σ^Λ, or vice versa. However, static feedback into both flow equations performed better. Hence all results shown in Sec. VIII are computed with this scheme. The fact that static feedback performs best highlights the difference between the Keldysh fRG and its Matsubara counterpart, where the full self-energy feedback is used.[57] Note that in frequency-dependent approximations the two methods are not equivalent (in equilibrium), even if the same feedback scheme is used. We suspect that the feedback of the full self-energy into the flow becomes favorable in a truncation scheme taking into account contributions from the flow of the three-particle vertex. Such a scheme, allowing for a renormalization of the static part of the two-particle vertex, might lead to an enhanced effective interaction strength, higher values of the effective mass, and a sharpening of spectral features—following the tendency expected from the Ward identities.[47–49]

VII. APPROXIMATE SOLUTION IN THE PARTICLE-HOLE SYMMETRIC POINT

In this section we discuss the special case of vanishing magnetic field, $B=0$, and particle-hole symmetry; the latter is given for $eV_g=(\mu_L+\mu_R)/2=0$. Note that we already introduced before the restriction $\Gamma_L=\Gamma_R$. In that symmetric situation the RG flow does not generate any contribution to $\mathrm{Re}\,\Sigma^{\mathrm{Ret}}_\Lambda(\omega=0)$ which hence remains at its initial value $U/2$ given in Eq. (39c). The renormalized effective level position is then given by

$$\varepsilon^\Lambda_\sigma = \varepsilon_\sigma + \mathrm{Re}\,\Sigma^{\mathrm{Ret}}_{\Lambda\sigma}(\omega=0) = 0, \tag{96}$$

compare Eqs. (3) and (95a). Hence the effective single-particle levels for the two spin states are degenerate and fixed in the middle of the two chemical potentials throughout the flow.

This section is organized as follows. At first, we discuss the structure of the vertex functions in the particle-particle (PP) and exchange particle-hole [PH(e)] channels. At second, we focus on the vertex functions in the direct particle-hole [PH(d)] channel. We distinguish this case from the other two channels because of a bit more involved spin structure. At third, we formulate a simplified version of the flow Eq. (27) for the self-energy. On its basis we recover the Fermi-liquid relations[47,62] for the (imaginary part of) self-energy providing an analytical fRG estimate for a characteristic energy scale of the quasiparticle resonance at zero frequency.

A. Particle-particle and exchange particle-hole channels

Let us first discuss the structure of the vertex functions in the particle-particle and exchange particle-hole channels characterized by energy exchange frequencies Π and X, respectively.

From Eqs. (87b) and (88) we establish the property

$$(a^{\mathrm{d}}_\Lambda)_{\sigma\bar\sigma}(0) \equiv U^{\mathrm{d}}_\Lambda/2 = 0, \tag{97}$$

which leads, as we will show below, to decoupling of PP and PH(e) channels from PH(d) channel.

Taking into account Eq. (97) we introduce for convenience the following shorthand notations [cf. Eqs. (79), (A9), and (A12)],

$$a_1(\Pi) = (a^{\mathrm{p}}_\Lambda)_{\sigma\bar\sigma}(\Pi) + \frac{U+U^{\mathrm{x}}_\Lambda}{2}, \tag{98}$$

$$F_1(\Pi) = (I^{\mathrm{pp}}_\Lambda)^{22|12}_{\sigma\bar\sigma}(\Pi) + (I^{\mathrm{pp}}_\Lambda)^{22|21}_{\sigma\bar\sigma}(\Pi), \tag{99}$$

$$b_1(\Pi) = (b^{\mathrm{p}}_\Lambda)_{\sigma\bar\sigma}(\Pi), \tag{100}$$

$$H_1(\Pi) = 2i\,\mathrm{Im}\left[(I^{\mathrm{pp}}_\Lambda)^{22|11}_{\sigma\bar\sigma}(\Pi) + \frac{1}{2}(I^{\mathrm{pp}}_\Lambda)^{22|22}_{\sigma\bar\sigma}(\Pi)\right], \tag{101}$$

and

$$a_3(X) = \frac{U+U^{\mathrm{p}}_\Lambda}{2} + (a^{\mathrm{x}}_\Lambda)_{\sigma\bar\sigma}(X), \tag{102}$$

$$F_3(X) = (I^{\mathrm{ph}}_\Lambda)^{21|22}_{\sigma\bar\sigma}(X) + (I^{\mathrm{ph}}_\Lambda)^{22|12}_{\sigma\bar\sigma}(X), \tag{103}$$

$$b_3(X) = (b^{\mathrm{x}}_\Lambda)_{\sigma\bar\sigma}(X), \tag{104}$$

$$H_3(X) = 2i\,\mathrm{Im}\left[(I^{\mathrm{ph}}_\Lambda)^{12|21}_{\sigma\bar\sigma}(X) + \frac{1}{2}(I^{\mathrm{ph}}_\Lambda)^{22|22}_{\sigma\bar\sigma}(X)\right], \tag{105}$$

where the functions (98) and (102) are specifically defined to fulfill $a_1(0)=a_3(0)$. The flow Eqs. (C3a) and (C6a) can be then transformed into

$$\frac{da_1(\Pi)}{d\Lambda} = [a_1(\Pi)]^2 F_1(\Pi) + \left(\frac{\tilde U_\Lambda}{2}\right)^2 F_3(0), \tag{106}$$

$$\frac{da_3(X)}{d\Lambda} = \left(\frac{\tilde U_\Lambda}{2}\right)^2 F_1(0) + [a_3(X)]^2 F_3(X), \tag{107}$$

where the static part

$$\tilde U_\Lambda = U + U^{\mathrm{p}}_\Lambda + U^{\mathrm{x}}_\Lambda = 2a_1(0) = 2a_3(0) \tag{108}$$

obeys the equation

$$\frac{d\tilde U_\Lambda}{d\Lambda} = \frac{\tilde U^2_\Lambda}{2}[F_1(0) + F_3(0)]. \tag{109}$$

In case of particle-hole symmetry and zero magnetic field the following property holds

$$F_3(X) = -F_1(-X), \tag{110}$$

which, in particular, implies $F_1(0)+F_3(0)=0$. Therefore the static component $\tilde U_\Lambda \equiv U$ does not flow within the approximation introduced in Sec. VI B.

The flow Eqs. (C3b) and (C6b) for the functions (100) and (104) read in the new notations

$$\frac{db_1(\Pi)}{d\lambda} = |a_1(\Pi)|^2 H_1(\Pi) + 2i\ \mathrm{Im}\{a_1(\Pi)b_1(\Pi)F_1(\Pi)\}, \tag{111}$$

$$\frac{\partial b_3(X)}{\partial\lambda} = |a_3(X)|^2 H_3(X) + 2i\ \mathrm{Im}\{a_3(X)b_3(X)F_3(X)\}. \tag{112}$$

The functions $F_{1,3}$ and $H_{1,3}$ are given by

$$F_1(\Pi) = \frac{i}{2\pi}\frac{\partial}{\partial\lambda}\int d\omega' \left[G_\sigma^{\mathrm{Ret}}\left(\frac{\Pi}{2}+\omega'\right) G_{\bar\sigma}^{\mathrm{K}}\left(\frac{\Pi}{2}-\omega'\right) + G_\sigma^{\mathrm{K}}\left(\frac{\Pi}{2}+\omega'\right) G_{\bar\sigma}^{\mathrm{Ret}}\left(\frac{\Pi}{2}-\omega'\right)\right], \tag{113}$$

$$F_3(X) = \frac{i}{2\pi}\frac{\partial}{\partial\lambda}\int d\omega' \left[G_\sigma^{\mathrm{Ret}}\left(\omega'-\frac{X}{2}\right) G_{\bar\sigma}^{\mathrm{K}}\left(\omega'+\frac{X}{2}\right) + G_\sigma^{\mathrm{K}}\left(\omega'-\frac{X}{2}\right) G_{\bar\sigma}^{\mathrm{Av}}\left(\omega'+\frac{X}{2}\right)\right] \tag{114}$$

and

$$H_1(\Pi) = \frac{i}{2\pi}\frac{\partial}{\partial\lambda}\int d\omega' [G_\sigma^{\mathrm{Ret}} G_{\bar\sigma}^{\mathrm{Ret}} + G_\sigma^{\mathrm{Av}} G_{\bar\sigma}^{\mathrm{Av}} + G_\sigma^{\mathrm{K}} G_{\bar\sigma}^{\mathrm{K}}], \tag{115}$$

$$H_3(X) = \frac{i}{2\pi}\frac{\partial}{\partial\lambda}\int d\omega' [G_\sigma^{\mathrm{Ret}} G_{\bar\sigma}^{\mathrm{Av}} + G_\sigma^{\mathrm{Av}} G_{\bar\sigma}^{\mathrm{Ret}} + G_\sigma^{\mathrm{K}} G_{\bar\sigma}^{\mathrm{K}}], \tag{116}$$

where the partial derivative $\partial/\partial\lambda$ is supposed to act only on explicitly λ-dependent term within G's, and the arguments of Green's functions in Eqs. (115) and (116) correspond to those in Eqs. (113) and (114), respectively. (For brevity we also denote $G_\lambda \equiv G$.) By a straightforward evaluation one can check that in equilibrium the following identities hold

$$H_1(\Pi) = \coth\left(\frac{\Pi}{2T}\right)[F_1(\Pi) - F_1^*(\Pi)], \tag{117}$$

$$H_3(X) = -\coth\left(\frac{X}{2T}\right)[F_3(X) - F_3^*(X)]. \tag{118}$$

With their help we can establish that the combinations

$$c_1(\Pi) = b_1(\Pi) - \coth\left(\frac{\Pi}{2T}\right)[a_1(\Pi) - a_1^*(\Pi)], \tag{119}$$

$$c_3(X) = b_3(X) + \coth\left(\frac{X}{2T}\right)[a_3(X) - a_3^*(X)] \tag{120}$$

obey the equations

$$\frac{dc_1}{d\lambda} = 2\ \mathrm{Re}\{a_1 F_1\} c_1, \tag{121}$$

$$\frac{dc_3}{d\lambda} = 2\ \mathrm{Re}\{a_3 F_3\} c_3, \tag{122}$$

respectively. Since initially $c_1(\Pi) = c_3(X) \equiv 0$, they also remain zero during the flow, accordingly to Eqs. (121) and (122). This proves that the KMS relations (A10) and (A13) inherent to the equilibrium state are exactly preserved under the fRG flow in the chosen approximation.

The derivative of the function F_3 at zero temperature reads

$$\left.\frac{\partial F_3(X)}{\partial X}\right|_{X=0} \equiv F_3'(0) = -\frac{1}{\pi}\frac{\partial}{\partial\lambda}\int d\omega' \Bigg\{ 2\delta(\omega')[G_\sigma^{\mathrm{Ret}}(\omega')\mathrm{Im}\, G_{\bar\sigma}^{R}(\omega') - \mathrm{Im}\, G_\sigma^{\mathrm{Ret}}(\omega') G_{\bar\sigma}^{\mathrm{Av}}(\omega')] + h_F(\omega')\Bigg[G_\sigma^{\mathrm{Ret}}(\omega')\mathrm{Im}\frac{\partial G_{\bar\sigma}^{\mathrm{Ret}}(\omega')}{\partial\omega'} - \mathrm{Im}\frac{\partial G_\sigma^{\mathrm{Ret}}(\omega')}{\partial\omega'} G_{\bar\sigma}^{\mathrm{Av}}(\omega')\Bigg]\Bigg\}, \tag{123}$$

where $h_F(\omega) \equiv 1 - 2f(\omega) \overset{T\to 0}{=} \mathrm{sign}(\omega)$. Under constraints adopted in this section the formula (123) simplifies to

$$F_3'(0) = -\frac{i}{\pi}\frac{\partial}{\partial\lambda}\int d\omega' \Bigg\{ 4\delta(\omega')[\mathrm{Im}\, G_\sigma^{\mathrm{Ret}}(\omega')]^2 + h_F(\omega')\frac{\partial}{\partial\omega'}[\mathrm{Im}\, G_\sigma^{\mathrm{Ret}}(\omega')]^2\Bigg\} = -\frac{2i}{\pi}\frac{\partial}{\partial\lambda}[\mathrm{Im}\, G_\sigma^{\mathrm{Ret}}(0)]^2 = \frac{16i}{\pi\Gamma_\lambda^3}. \tag{124}$$

In the approximation achieved by neglecting the self-energy feedback $G_\lambda \to g_\lambda$ we can replace in Eq. (114) the partial derivative $\partial/\partial\lambda$ by the full one $d/d\lambda$. Then we find that

$$F_3(X) = \frac{d}{d\lambda}\left[-\frac{2}{\pi}\frac{\Gamma_\lambda}{X(X-i\Gamma_\lambda)}\ln\left(1 + i\frac{X}{\Gamma_\lambda/2}\right)\right] \tag{125}$$

is given by the full λ derivative of the particle-hole polarization operator (62). In particular, we obtain $F_3(0) = -4/(\pi\Gamma_\lambda^2)$, and at small $X \le \Gamma_\lambda$ we approximately have

$$F_3(X) \approx \frac{4}{\pi(2X - i\Gamma_\lambda)^2}. \tag{126}$$

This leads to an approximate solution of the Eq. (107),

$$a_3(X) \approx -\frac{U}{2}\frac{X + iB(U,\lambda)}{X - iB(U,\lambda)}, \tag{127}$$

where the width of the Lorentzian is given by

$$B(U,\lambda) = \frac{4U}{\pi} e^{-4U/\pi\Gamma_\lambda}. \tag{128}$$

It explicitly manifests that the exponential scale develops in the broadening of the renormalized frequency-dependent vertex function in the exchange particle-hole channel.

B. Direct particle-hole channel

The flow equations for the vertex functions in this channel are split off those considered in Sec. VII A. We analogously introduce the new notations [cf. Eqs. (A15) and (A18)]

$$a_{20}(\Delta) = \frac{U + U^{\mathrm{p}}_\lambda + U^{\mathrm{x}}_\lambda}{2} + (a^{\mathrm{d}}_\lambda)_{\sigma\bar{\sigma}}(\Delta), \tag{129}$$

$$a_{2\sigma}(\Delta) = (a^{\mathrm{d}}_\lambda)_{\sigma\sigma}(\Delta) - \frac{W^{\mathrm{d}}_{\lambda\sigma}}{2}, \tag{130}$$

$$F_{2\sigma}(\Delta) = (I^{\mathrm{ph}}_\lambda)^{22|21}_{\sigma\sigma}(\Delta) + (I^{\mathrm{ph}}_\lambda)^{12|22}_{\sigma\sigma}(\Delta), \tag{131}$$

$$b_{20}(\Delta) = (b^{\mathrm{d}}_\lambda)_{\sigma\bar{\sigma}}(\Delta), \tag{132}$$

$$b_{2\sigma}(\Delta) = (b^{\mathrm{d}}_\lambda)_{\sigma\sigma}(\Delta), \tag{133}$$

$$H_{2\sigma}(\Delta) = 2i\,\mathrm{Im}\left\{(I^{\mathrm{ph}}_\lambda)^{12|21}_{\sigma\sigma}(\Delta) + \frac{1}{2}(I^{\mathrm{ph}}_\lambda)^{22|22}_{\sigma\sigma}(\Delta)\right\}, \tag{134}$$

and rewrite the corresponding Eqs. (C7) and (C9)

$$\frac{da_{20}(\Delta)}{d\lambda} = -a_{20}(\Delta)\sum_{s=\uparrow,\downarrow} a_{2s}(\Delta)F_{2s}(\Delta) + \left(\frac{\tilde{U}_\lambda}{2}\right)^2 [F_1(0) + F_3(0)], \tag{135}$$

$$\frac{da_{2\sigma}(\Delta)}{d\lambda} = -[a_{20}(\Delta)]^2 F_{2\bar{\sigma}}(\Delta) - [a_{2\sigma}(\Delta)]^2 F_{2\sigma}(\Delta) + \left(\frac{\tilde{U}_\lambda}{2}\right)^2 F_{2\bar{\sigma}}(0), \tag{136}$$

$$\begin{aligned}\frac{db_{20}(\Delta)}{d\lambda} = &-a_{20}(\Delta)a^*_{2\bar{\sigma}}(\Delta)H_{2\bar{\sigma}}(\Delta) - a^*_{20}(\Delta)a_{2\sigma}(\Delta)H_{2\sigma}(\Delta)\\ &- a_{20}(\Delta)b_{2\bar{\sigma}}(\Delta)F_{2\bar{\sigma}}(\Delta) - a^*_{20}(\Delta)b_{2\sigma}(\Delta)F^*_{2\sigma}(\Delta)\\ &- a^*_{2\bar{\sigma}}(\Delta)b_{20}(\Delta)F^*_{2\bar{\sigma}}(\Delta) - a_{2\sigma}(\Delta)b_{20}(\Delta)F_{2\sigma}(\Delta),\end{aligned} \tag{137}$$

$$\begin{aligned}\frac{db_{2\sigma}(\Delta)}{d\lambda} = &-|a_{20}(\Delta)|^2 H_{2\bar{\sigma}}(\Delta) - |a_{2\sigma}(\Delta)|^2 H_{2\sigma}(\Delta)\\ &- 2\,\mathrm{Re}\{a_{2\sigma}(\Delta)F_{2\sigma}(\Delta)\}b_{2\sigma}(\Delta)\\ &- 2i\,\mathrm{Im}\{a^*_{20}(\Delta)b_{20}(\Delta)F^*_{2\bar{\sigma}}(\Delta)\}.\end{aligned} \tag{138}$$

We note that $a_{20}(0)=\tilde{U}_\lambda/2$ and $a_{2\sigma}(0)=0$ as well as $F_{2\sigma}(\Delta)=F_3(-\Delta)$ and $H_{2\sigma}(\Delta)=H_3(-\Delta)$. One can also observe that $b_{20}(\Delta)$ contains both real $b^r_{20}(\Delta)=\mathrm{Re}\,b_{20}(\Delta)$ and imaginary $b^i_{20}(\Delta)=\mathrm{Im}\,b_{20}(\Delta)$ parts while $b_{2\sigma}(\Delta)$ is purely imaginary.

Analogously to Eq. (118) the following identity holds in equilibrium

$$H_{2\sigma}(\Delta) = \coth\left(\frac{\Delta}{2T}\right)[F_{2\sigma}(\Delta) - F^*_{2\sigma}(\Delta)]. \tag{139}$$

It allows us to express the equations for $b^r_{20}(\Delta)$ and for the combinations

$$c_{20}(\Delta) = ib^i_{20}(\Delta) - \coth\left(\frac{\Delta}{2T}\right)[a_{20}(\Delta) - a^*_{20}(\Delta)], \tag{140}$$

$$c_{2\sigma}(\Delta) = b_{2\sigma}(\Delta) - \coth\left(\frac{\Delta}{2T}\right)[a_{2\sigma}(\Delta) - a^*_{2\sigma}(\Delta)], \tag{141}$$

in the following form:

$$\begin{aligned}\frac{db^r_{20}}{d\lambda} = &-\mathrm{Re}\{F_{2\sigma}a_{2\sigma} + F_{2\bar{\sigma}}a_{2\bar{\sigma}}\}b^r_{20} - i\,\mathrm{Im}\{F_{2\sigma}a_{2\sigma} - F_{2\bar{\sigma}}a_{2\bar{\sigma}}\}c_{20}\\ &+ i\,\mathrm{Im}\{F_{2\sigma}a_{20}\}c_{2\sigma} - i\,\mathrm{Im}\{F_{2\bar{\sigma}}a_{20}\}c_{2\bar{\sigma}},\end{aligned} \tag{142}$$

$$\begin{aligned}\frac{dc_{20}}{d\lambda} = &-i\,\mathrm{Im}\{F_{2\sigma}a_{2\sigma} - F_{2\bar{\sigma}}a_{2\bar{\sigma}}\}b^r_{20} - \mathrm{Re}\{F_{2\sigma}a_{2\sigma} + F_{2\bar{\sigma}}a_{2\bar{\sigma}}\}c_{20}\\ &- \mathrm{Re}\{F_{2\sigma}a_{20}\}c_{2\sigma} - \mathrm{Re}\{F_{2\bar{\sigma}}a_{20}\}c_{2\bar{\sigma}},\end{aligned} \tag{143}$$

$$\begin{aligned}\frac{dc_{2\sigma}}{d\lambda} = &2i\,\mathrm{Im}\{F_{2\bar{\sigma}}a_{20} + F_{2\sigma}a_{2\sigma}\}b^r_{20}\\ &- 2\,\mathrm{Re}\{F_{2\bar{\sigma}}a_{20}\}c_{20} - 2\,\mathrm{Re}\{F_{2\sigma}a_{2\sigma}\}c_{2\sigma}.\end{aligned} \tag{144}$$

Since initially $b^r_{20}(\Delta)=c_{20}(\Delta)=c_{2\sigma}(\Delta)=0$, they remain zero during the flow [cf. Eq. (A16)]. This observation completes the proof of the statement that the KMS relations are preserved in the chosen approximation scheme.

C. Fermi-liquid relations for the self-energy

In the case of particle-hole symmetry it is convenient to introduce the notations

$$\bar{a}_1(\Pi) = -a_1(-\Pi), \tag{145}$$

$$\bar{a}_{2\sigma}(\Delta) = -a_{2\sigma}(-\Delta), \tag{146}$$

and rewrite an equilibrium version of the Eq. (B1) for the retarded self-energy in a simplified form

$$\begin{aligned}\frac{d}{d\lambda}\Sigma^{\mathrm{Ret}}_\sigma(\omega) = \frac{1}{\pi}\int d\tilde{\omega}\Big[&-\frac{U}{2}h_F(\tilde{\omega})\mathrm{Im}\,s^{\mathrm{Ret}}_{\bar{\sigma}}(\tilde{\omega})\\ &+ h_F(\tilde{\omega})\bar{a}_1(\tilde{\omega}-\omega)\mathrm{Im}\,s^{\mathrm{Ret}}_{\bar{\sigma}}(-\tilde{\omega})\\ &+ h_B(\tilde{\omega}-\omega)\mathrm{Im}\,\bar{a}_1(\tilde{\omega}-\omega)s^{\mathrm{Av}}_{\bar{\sigma}}(-\tilde{\omega})\\ &+ h_F(\tilde{\omega})a_3(\tilde{\omega}-\omega)\mathrm{Im}\,s^{\mathrm{Ret}}_{\bar{\sigma}}(\tilde{\omega})\\ &- h_B(\tilde{\omega}-\omega)\mathrm{Im}\,a_3(\tilde{\omega}-\omega)s^{\mathrm{Ret}}_{\bar{\sigma}}(\tilde{\omega})\end{aligned}$$

$$+ h_F(\tilde{\omega})\bar{a}_{2\sigma}(\tilde{\omega}-\omega)\mathrm{Im}\, s_\sigma^{\mathrm{Ret}}(\tilde{\omega}) - h_B(\tilde{\omega}-\omega)\mathrm{Im}\, \bar{a}_{2\sigma}(\tilde{\omega}-\omega)s_\sigma^{\mathrm{Ret}}(\tilde{\omega})\Big], \tag{147}$$

where $h_B(\omega)=\coth\frac{\omega}{2T}$. In this equation the self-energy feedback is neglected as well by replacing $S_\lambda \to s_\lambda = \frac{\partial g_\lambda}{\partial \lambda}$.

Comparing Eqs. (106) and (107) with Eqs. (135) and (136), one can observe that the relation

$$\bar{a}_{2\sigma}(\omega) = \frac{\bar{a}_1(\omega)+a_3(\omega)}{2} \tag{148}$$

holds at every λ. The identities $\mathrm{Im}\, s^{\mathrm{Ret}}(\omega)=\mathrm{Im}\, s^{\mathrm{Ret}}(-\omega)$, $s^{\mathrm{Av}}(-\omega)=-s^{\mathrm{Ret}}(\omega)$ are fulfilled as well. Therefore Eq. (147) reduces to the form

$$\frac{d}{d\lambda}\Sigma_\sigma^{\mathrm{Ret}}(\omega) = \frac{3}{2\pi}\int d\tilde{\omega}[h_F(\tilde{\omega})\bar{a}_1(\tilde{\omega}-\omega)\mathrm{Im}\, s_{\bar{\sigma}}^{\mathrm{Ret}}(\tilde{\omega}) - h_B(\tilde{\omega}-\omega)\mathrm{Im}\, \bar{a}_1(\tilde{\omega}-\omega)s_{\bar{\sigma}}^{\mathrm{Ret}}(\tilde{\omega}) + h_F(\tilde{\omega})a_3(\tilde{\omega}-\omega)\mathrm{Im}\, s_{\bar{\sigma}}^{\mathrm{Ret}}(\tilde{\omega}) - h_B(\tilde{\omega}-\omega)\mathrm{Im}\, a_3(\tilde{\omega}-\omega)s_{\bar{\sigma}}^{\mathrm{Ret}}(\tilde{\omega})]. \tag{149}$$

In particular, its imaginary part reads

$$\frac{d}{d\lambda}\mathrm{Im}\,\Sigma_\sigma^{\mathrm{Ret}}(\omega) = \frac{3}{2\pi}\int d\tilde{\omega}[h_F(\tilde{\omega})-h_B(\tilde{\omega}-\omega)] \times \mathrm{Im}[\bar{a}_1(\tilde{\omega}-\omega)+a_3(\tilde{\omega}-\omega)]\mathrm{Im}\, s_{\bar{\sigma}}^{\mathrm{Ret}}(\tilde{\omega}), \tag{150}$$

which at $T=0$ amounts to

$$\frac{d}{d\lambda}\mathrm{Im}\,\Sigma_\sigma^{\mathrm{Ret}}(\omega) = \frac{3}{\pi}\int_0^\omega d\tilde{\omega}\,\mathrm{Im}[\bar{a}_1(\tilde{\omega}-\omega) + a_3(\tilde{\omega}-\omega)]\mathrm{Im}\, s_{\bar{\sigma}}^{\mathrm{Ret}}(\tilde{\omega}). \tag{151}$$

Differentiating the latter expression with respect to ω and taking into account symmetries of integrands we obtain

$$\frac{d}{d\lambda}\mathrm{Im}\,\Sigma'' = -\frac{3}{\pi}\mathrm{Im}\left[\frac{\partial \bar{a}_1}{\partial\omega}+\frac{\partial a_3}{\partial\omega}\right]_{\omega=0}\mathrm{Im}\, s_{\bar{\sigma}}^{\mathrm{Ret}}(0),$$

where $\mathrm{Im}\,\Sigma''=\mathrm{Im}(\partial^2\Sigma_\sigma^{\mathrm{Ret}}/\partial\omega^2)|_{\omega=0}$. Note that the first derivative $\mathrm{Im}\,\Sigma'=\mathrm{Im}(\partial\Sigma_\sigma^{\mathrm{Ret}}/\partial\omega)|_{\omega=0}$ vanishes. It means that ω expansion of $\mathrm{Im}\,\Sigma^{\mathrm{Ret}}(\omega)\approx\frac{1}{2}\mathrm{Im}\,\Sigma''\omega^2$ starts from the quadratic term, in compliance with the Fermi-liquid expression (32).

In order to find an fRG estimate for $\mathrm{Im}\,\Sigma''$, we need to establish equations for $\bar{a}_1'=\mathrm{Im}(\partial\bar{a}_1/\partial\omega)|_{\omega=0}$ and $a_3'=\mathrm{Im}(\partial a_3/\partial\omega)|_{\omega=0}$. This is achieved by differentiating Eqs. (106) and (107)

$$\frac{d\bar{a}_1'}{d\lambda} = -U\bar{a}_1'F_3(0)+\frac{U^2}{4}\mathrm{Im}\, F_3'(0), \tag{152}$$

$$\frac{da_3'}{d\lambda} = Ua_3'F_3(0)+\frac{U^2}{4}\mathrm{Im}\, F_3'(0). \tag{153}$$

Using Eq. (123) and $\mathrm{Im}\, s^{\mathrm{Ret}}(0)=2/\Gamma_\lambda^2$, we obtain the following set of equations

$$\frac{d\,\mathrm{Im}\,\Sigma''}{d\lambda} = -(\bar{a}_1'+a_3')\frac{6}{\pi\Gamma_\lambda^2}, \tag{154}$$

$$\frac{d\bar{a}_1'}{d\lambda} = \bar{a}_1'\frac{4U}{\pi\Gamma_\lambda^2}+\frac{4U^2}{\pi\Gamma_\lambda^3}, \tag{155}$$

$$\frac{da_3'}{d\lambda} = -a_3'\frac{4U}{\pi\Gamma_\lambda^2}+\frac{4U^2}{\pi\Gamma_\lambda^3}. \tag{156}$$

The solution of the last equations is given by

$$\bar{a}_1' = \frac{\pi}{4}\left[1-\frac{4U}{\pi\Gamma_\lambda}-e^{-4U/\pi\Gamma_\lambda}\right], \tag{157}$$

$$a_3' = \frac{\pi}{4}\left[1+\frac{4U}{\pi\Gamma_\lambda}-e^{+4U/\pi\Gamma_\lambda}\right], \tag{158}$$

and therefore

$$\bar{a}_1'+a_3' = \frac{\pi}{2}\left[1-\cosh\frac{4U}{\pi\Gamma_\lambda}\right]. \tag{159}$$

Integrating the equation for $\mathrm{Im}\,\Sigma''$, we obtain at $\lambda=0$,

$$\mathrm{Im}\,\Sigma'' = \frac{3}{\Gamma}\left[1-\frac{\pi\Gamma}{4U}\sinh\frac{4U}{\pi\Gamma}\right]. \tag{160}$$

At large $U\gg\Gamma$ an exponentially large scale emerges in $a_3'\approx-\frac{\pi}{4}e^{4U/\pi\Gamma}$ and in $\mathrm{Im}\,\Sigma''\approx-\frac{3\pi}{8U}e^{4U/\pi\Gamma}$. We also note that a_3' determines the width $B=-U/a_3'$ given in Eq. (128).

In a similar way we can establish the Fermi-liquid coefficient corresponding to small-temperature expansion. Let us set $\omega=0$ in Eq. (150) and rescale the integration variable $\tilde{\omega}=xT$. Then

$$\frac{d}{d\lambda}\mathrm{Im}\,\Sigma_\sigma^{\mathrm{Ret}}(0) = -\frac{3}{\pi}\int\frac{d\tilde{\omega}}{\sinh\tilde{\omega}/T}\mathrm{Im}[\bar{a}_1(\tilde{\omega})+a_3(\tilde{\omega})]\mathrm{Im}\, s_{\bar{\sigma}}^{\mathrm{Ret}}(\tilde{\omega}) = -\frac{3T}{\pi}\int\frac{dx}{\sinh x}\mathrm{Im}[\bar{a}_1(xT)+a_3(xT)]\mathrm{Im}\, s_{\bar{\sigma}}^{\mathrm{Ret}}(xT). \tag{161}$$

Differentiating it twice with respect to T we obtain

$$\frac{d}{d\lambda}\mathrm{Im}\left.\frac{\partial^2\Sigma_\sigma^{\mathrm{Ret}}(0)}{\partial T^2}\right|_{T=0} = -\frac{3}{\pi}\left(\int\frac{2xdx}{\sinh x}\right)\mathrm{Im}\left[\frac{\partial\bar{a}_1}{\partial\omega}+\frac{\partial a_3}{\partial\omega}\right]_{\omega=0}\mathrm{Im}\, s_{\bar{\sigma}}^{\mathrm{Ret}}(0), \tag{162}$$

where $\int_{-\infty}^{\infty}\frac{2xdx}{\sinh x}=\pi^2$. Comparing this expression with Eq. (154) we establish [cf. Eq. (32)]

$$\mathrm{Im}\left.\frac{\partial^2\Sigma_\sigma^{\mathrm{Ret}}}{\partial T^2}\right|_{\omega,T=0} = \pi^2\,\mathrm{Im}\,\Sigma''. \tag{163}$$

Calculation of the Fermi-liquid coefficient corresponding to small-bias expansion is presented in Appendix D.

VIII. RESULTS OF THE FREQUENCY DEPENDENT FRG

In this section we discuss numerical results obtained from the frequency-dependent Keldysh fRG and compare them to those found by other methods. The underlying approximation scheme is the one described in Sec. VI; in particular, only the static part of the self-energy is fed back into the flow of Σ^λ and γ_2^λ, as explained in Sec. VI D. In the figures, results of this method are labeled by "fRG."

We start with the particle-hole symmetric model in thermal equilibrium at $B=0$. The low-energy expansion of the retarded self-energy is then given by Eq. (32). The reduced susceptibilities serving as coefficients of this expansion are known from Bethe ansatz and are[50]

$$\tilde{\chi}_{\mathrm{s}} = \exp\left(\frac{\pi}{4}\frac{U}{\Gamma}\right)\sqrt{\frac{\Gamma}{U}}\int_0^\infty dx\,\exp\left(-\frac{\pi}{4}\frac{\Gamma}{U}x^2\right)\frac{\cos(\pi x/2)}{1-x^2}, \tag{164a}$$

$$\tilde{\chi}_{\mathrm{c}} = \exp\left(-\frac{\pi}{4}\frac{U}{\Gamma}\right)\sqrt{\frac{\Gamma}{U}}\int_0^\infty dx\,\exp\left(-\frac{\pi}{4}\frac{\Gamma}{U}x^2\right)\frac{\cosh(\pi x/2)}{1+x^2}. \tag{164b}$$

For $U \gtrsim \pi\Gamma$ the reduced susceptibilities acquire their asymptotic form where[50]

$$\tilde{\chi}_{\mathrm{s}} \pm \tilde{\chi}_{\mathrm{c}} \simeq \tilde{\chi}_{\mathrm{s}} \simeq \frac{\pi}{2}\sqrt{\frac{\Gamma}{U}}\exp\left(\frac{\pi}{4}\left[\frac{U}{\Gamma}-\frac{\Gamma}{U}\right]\right), \quad U \gtrsim \pi\Gamma. \tag{165}$$

This exponential behavior governs the width of the Kondo resonance, which can be seen as follows. At $eV_{\mathrm{g}}=0(=\mu)$, $T=0$, $B=0$, $V=0$ the retarded Green's function can be approximated for ω close to 0 by

$$G_\sigma^{\mathrm{Ret}}(\omega) \simeq \frac{1}{m^*\omega + i\Gamma/2}, \tag{166}$$

compare Eqs. (3) and (32), the effective mass m^* being defined as

$$m^* = 1 - \left.\frac{\partial\Sigma^{\mathrm{Ret}}}{\partial\omega}\right|_{\omega=0}. \tag{167}$$

Hence

$$\rho_\sigma(\omega) = -\frac{1}{\pi}\mathrm{Im}\,G_\sigma^{\mathrm{Ret}}(\omega) \simeq \frac{1}{\pi}\frac{\Gamma/2}{(m^*\omega)^2+\Gamma^2/4}, \tag{168}$$

so that the full width at half maximum of the peak within this approximation is given by

$$T_{\mathrm{K}} = \frac{\Gamma}{m^*}. \tag{169}$$

From Eqs. (32) and (165) we deduce

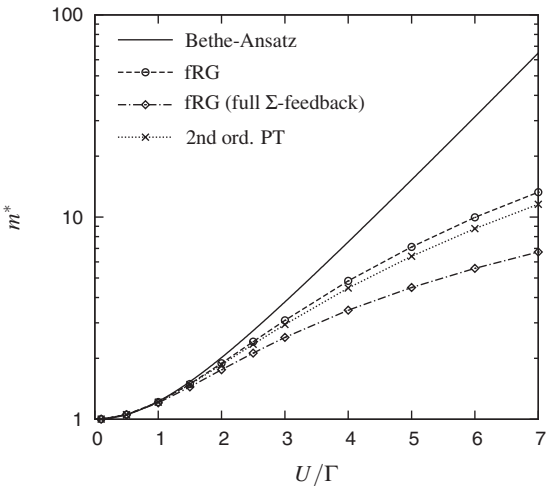

FIG. 2. The effective mass $m^* = 1 - \Sigma_\sigma^{\mathrm{Ret}\prime}|_{\omega=0}$ as function of U for $V_{\mathrm{g}}=0$, $T=0$, $B=0$, and $V=0$. The exponential behavior exhibited by the Bethe-ansatz result obtained from Eqs. (170a) and (164) at large U/Γ is neither reproduced by the fRG nor by second-order perturbation theory. While the effective mass computed from the frequency-dependent fRG with static self-energy feedback (labeled fRG and used as default throughout this section) is comparable to the one found in second-order perturbation theory, the values obtained from the fRG with full self-energy feedback are clearly worse (compare Sec. VI D).

$$m^* = \frac{\tilde{\chi}_{\mathrm{s}} + \tilde{\chi}_{\mathrm{c}}}{2} \tag{170a}$$

$$\simeq \frac{\pi}{4}\sqrt{\frac{\Gamma}{U}}\exp\left(\frac{\pi}{4}\left[\frac{U}{\Gamma}-\frac{\Gamma}{U}\right]\right), \quad U \gtrsim \pi\Gamma, \tag{170b}$$

and thus

$$T_{\mathrm{K}} = \frac{4}{\pi}\sqrt{U\Gamma}\exp\left(-\frac{\pi}{4}\left[\frac{U}{\Gamma}-\frac{\Gamma}{U}\right]\right). \tag{171}$$

Figure 2 shows a comparison of the effective mass computed by the fRG to that obtained from second-order perturbation theory and to the Bethe-ansatz result. Since second-order perturbation theory will serve us several times as a reference solution we briefly sketch how it is determined. When evaluating the frequency-dependent second-order diagram for the self-energy we use propagators dressed with the restricted self-consistent Hartree-Fock self-energy as internal propagators. The self-consistent Hartree-Fock solution is obtained from the self-consistency equation

$$\Sigma_\sigma^{\mathrm{Ret}} = U\langle n_{\bar{\sigma}}\rangle = -\frac{i}{2\pi}U\int d\omega G_{\bar{\sigma}}^<(\omega) \tag{172a}$$

$$= \frac{U}{2\pi}\int d\omega f_{\mathrm{eff}}(\omega)\frac{\Gamma}{(\omega-\varepsilon_{\bar{\sigma}}-\Sigma_{\bar{\sigma}}^{\mathrm{Ret}})^2+\Gamma^2/4}. \tag{172b}$$

This equation has a unique solution for small U but there are three solutions at larger values of U (e.g., for $U>\pi\Gamma/2$ for $T=0$, $B=0$). Two of them feature a local moment, $\Sigma_\uparrow^{\mathrm{Ret}} \neq \Sigma_\downarrow^{\mathrm{Ret}}$, even for $B=0$.[43] The notion "restricted Hartree-Fock"

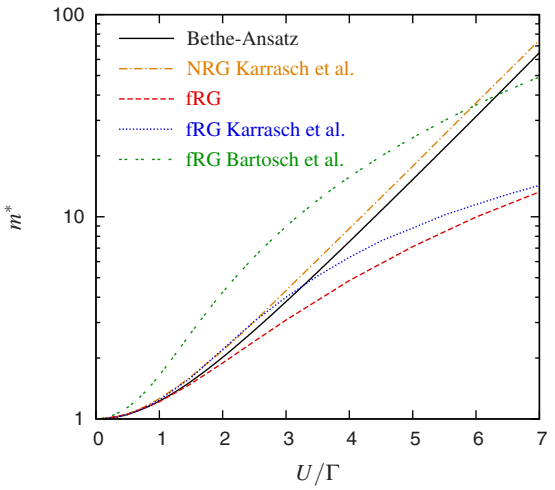

FIG. 3. (Color online) The effective mass as function of U for $V_g=0$, $T=0$, $B=0$, and $V=0$. The figure compares the Bethe-ansatz and fRG data of Fig. 2 with results of the Matsubara fRG in "approximation 1" of Ref. 57, the Matsubara fRG with partial bosonization in the spin-rotational invariant version of Ref. 53 (data extracted from the e-print arXiv:0811.2809v1), and with the NRG data used for comparison in Refs. 53 and 57.

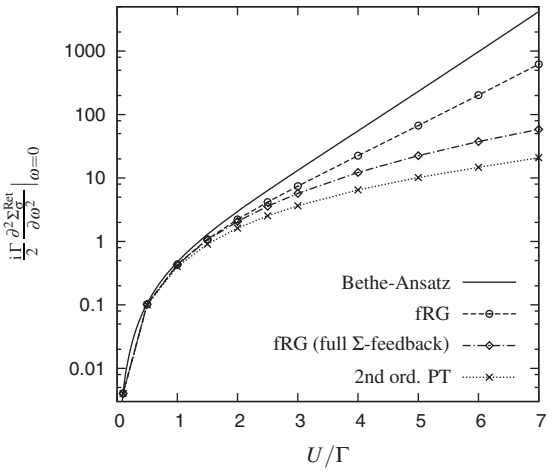

FIG. 4. The second derivative of the self-energy as function of U for $V_g=0$, $T=0$, $B=0$, and $V=0$. The fRG produces an exponential increase with the exponent $4U/\pi\Gamma$, whereas the exact exponent is $\pi U/2\Gamma$. Second-order perturbation theory and the fRG with the full frequency-dependent self-energy feedback (compare Sec. VI D) do not yield an exponential increase.

refers to the third solution which is energetically unfavorable as compared to the other two ones but is nevertheless preferable because of preserving spin symmetry, $\Sigma^{\rm Ret}_\uparrow=\Sigma^{\rm Ret}_\downarrow$. In the particle-hole symmetric case, for instance, the restricted Hartree-Fock self-energy $\Sigma^{\rm Ret}_\uparrow=\Sigma^{\rm Ret}_\downarrow=U/2$ aligns the single-particle levels with the chemical potential. We use this perturbation theory only for $B=0$. For finite magnetic field it is not clear which solution of the self-consistency equation ought to be used to dress the single-particle propagators.

In Fig. 2 we see that the effective mass computed from the fRG does not increase exponentially for large U but it is comparable to the one computed with second-order perturbation theory. As a consequence the width of the Kondo resonance of the spectral function resulting from the fRG approximation does not shrink exponentially for increasing U. Figure 2 also shows the effective mass obtained from the fRG with full frequency-dependent backcoupling of the self-energy into the flow. As mentioned in Sec. VI D this feedback leads to an artificial broadening of spectral features which becomes apparent here in the too low values for the effective mass. In Fig. 3 a comparison with the results of recent Matsubara fRG implementations is given.

From the expansion (32) and from Eqs. (165) and (170) it also follows that

$$\frac{i\Gamma}{2}\frac{\partial^2\Sigma^{\rm Ret}_\sigma}{\partial\omega^2}\bigg|_{\omega=0}=\frac{(\tilde\chi_s-\tilde\chi_c)^2}{4}\simeq m^{*2},\quad U\gtrsim\pi\Gamma, \tag{173}$$

increases exponentially with U in the Kondo regime. Figure 4 presents the respective data obtained by fRG and second-order perturbation theory in comparison to the Bethe-ansatz result. In contrast to second-order perturbation theory the fRG produces an exponential scale as has been proven already in Eq. (160). Using Eqs. (169) and (173) we can relate this exponential behavior to a Kondo scale

$$[T_K]_{\rm fRG}=4\sqrt{\frac{U\Gamma}{3\pi}}\exp\left(-\frac{2}{\pi}\frac{U}{\Gamma}\right). \tag{174}$$

The identical exponential behavior has been found to govern the pinning of the spectral weight to the chemical potential in the Matsubara fRG with frequency-independent truncation scheme.[54,55] With $2/\pi\simeq0.64$ the prefactor is slightly smaller than the correct one in Eq. (171), $\pi/4\simeq0.79$. Figure 4 also shows that the fRG with feedback of the full frequency-dependent self-energy into the flow does not produce an exponential scale in the second derivative of the self-energy. This illustrates again that the static feedback scheme which we use as standard is advantageous, compare Sec. VI D.

The fact that the fRG produces an exponential behavior in Im Σ'' but not in the effective mass constitutes an inconsistency which manifests that the method captures Kondo physics only partly. The exact result satisfies

$$m^{*2}=\frac{(\tilde\chi_s+\tilde\chi_c)^2}{4}>\frac{(\tilde\chi_s-\tilde\chi_c)^2}{4}=\frac{i\Gamma}{2}\frac{\partial^2\Sigma^{\rm Ret}_\sigma}{\partial\omega^2}\bigg|_{\omega=0}, \tag{175}$$

where both sides asymptotically approach $\tilde\chi_s^2/4$. Figure 5 illustrates that the fRG result violates this inequality for $U>4\Gamma$. Therefore we restrict the following discussions to $U\leq4\Gamma$.

Figures 6–8 show spectral functions in the particle-hole symmetric case at $B=0$, $T=0$, in equilibrium. Results of the fRG and of second-order perturbation theory are compared to essentially exact NRG data.[77] For $U\lesssim2\Gamma$ all three methods yield nearly identical results. For $U=2\Gamma$ the shape of the peak differs already significantly from the Lorentzian form produced by static approximations such as restricted Hartree-Fock. At this interaction strength the difference occurs almost exclusively due to the second-order self-energy diagrams which are also captured exactly by the fRG. For $U=3\Gamma,4\Gamma$ the resonance peaks produced by fRG and second-

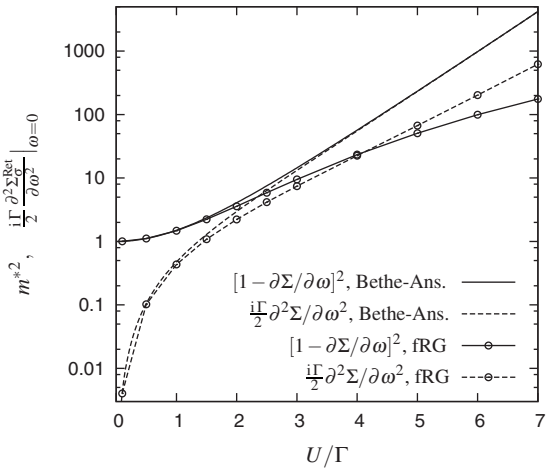

FIG. 5. Comparison of the square of the effective mass and of the second derivative of the self-energy as function of U for $V_g=0$, $T=0$, $B=0$, and $V=0$. In the exact solution both have identical large U asymptotics, m^{*2} being always the larger one of both. In the fRG data the curves cross at U slightly above 4Γ.

order perturbation theory are too broad, see insets of Figs. 7 and 8, which is a consequence of the effective mass being too small as discussed above. The overall shape of the spectral function is reproduced better by second-order perturbation theory than by fRG. The fRG has a tendency to shift spectral weight too far away from the central peak; in Fig. 8 the side peaks computed by fRG are situated at $|\omega|\simeq 3\Gamma$ whereas they are expected to be at $|\omega|\simeq U/2=2\Gamma$. For the computation of equilibrium spectra it is hence preferable to resort to the frequency-dependent Matsubara fRG which has been found to be clearly superior in this respect to second-order perturbation theory at $U=2.5\Gamma$.[57]

The linear conductance as function of gate voltage for different magnetic fields at $T=0$ and $U=4\Gamma$ is shown in Fig. 9. The fRG data agree very well with NRG results; the frequency-dependent Keldysh fRG obviously maintains the high quality in describing $G_{\mathrm{lin}}(V_g,B;T=0)$ which has already

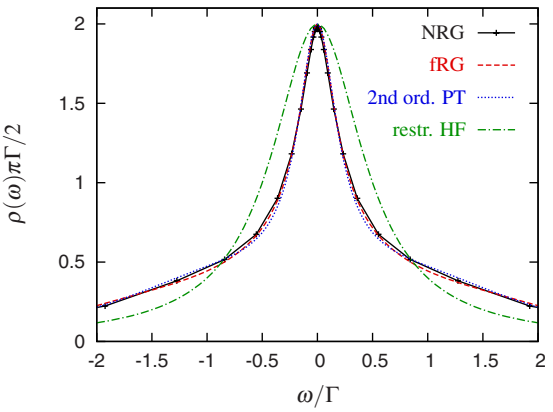

FIG. 6. (Color online) Spectral function for $V_g=0$, $T=0$, $B=0$, $V=0$, and $U=2\Gamma$. The results of fRG and second-order perturbation theory agree very well with NRG data. The peak shape differs already significantly from the Lorentzian form produced by static approximations such as restricted Hartree-Fock.

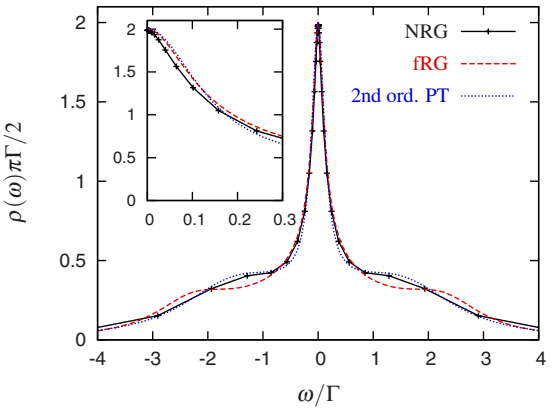

FIG. 7. (Color online) Spectral function for $V_g=0$, $T=0$, $B=0$, $V=0$, and $U=3\Gamma$.

been achieved by the fRG with frequency-independent truncation scheme.[54,55]

Figures 10 and 11 present the linear conductance as function of gate voltage for different temperatures at $B=0$ and $U=2\Gamma,3\Gamma$. In contrast to second-order perturbation theory the fRG reproduces the NRG results for the width of the plateau at $T=0$ and the position of the maxima for $T>0$ quite accurately. The decrease in the conductance at $V_g=0$ with increasing temperature is captured not completely correct by the fRG but distinctively better than by second-order perturbation theory. The fRG provides an altogether acceptable description of $G_{\mathrm{lin}}(V_g,T)$ for $U\lesssim 3$. This is an important improvement compared to previous fRG approaches. The static fRG (Refs. 54 and 55) is, in principle, unable to reproduce the minimum of G_{lin} at $V_g=0$. The reason is that the linear conductance is given by

$$G_{\mathrm{lin}}=e^2\frac{\Gamma^{\mathrm{L}}\Gamma^{\mathrm{R}}}{\Gamma}\int d\omega\left(-\frac{\partial f(\omega)}{\partial\omega}\right)\rho(\omega), \qquad (176)$$

as follows from the current formula (22). In any static approximation at $B=0$ the spectral function $\rho(\omega)$ is represented by a Lorentzian peak with fixed width and height, centered at

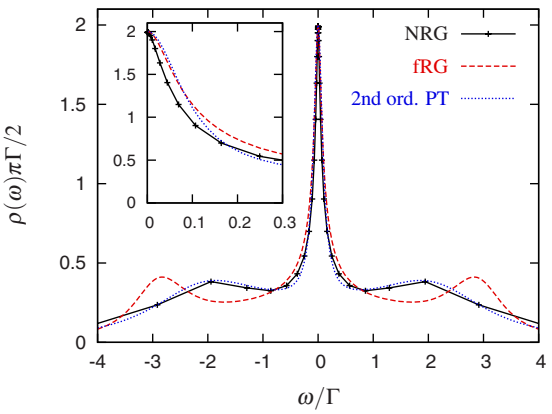

FIG. 8. (Color online) Spectral function for $V_g=0$, $T=0$, $B=0$, $V=0$, and $U=4\Gamma$. The resonance at $\omega=0$ produced by fRG and by second-order perturbation theory is too broad. The side peaks resulting from the fRG calculation are situated at too large $|\omega|$.

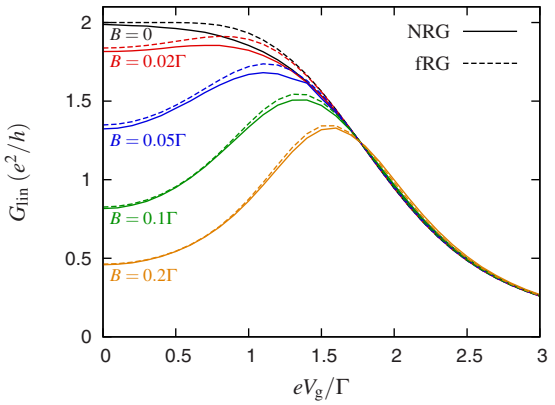

FIG. 9. (Color online) Linear conductance as function of gate voltage for $T=0$, $U=4\Gamma$, and different magnetic fields.

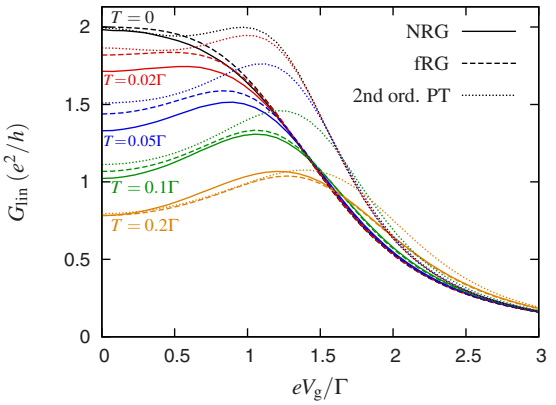

FIG. 11. (Color online) Linear conductance as function of gate voltage for $B=0$, $U=3\Gamma$, and different temperatures.

the renormalized level position. Obviously Eq. (176) can produce a single maximum of $G_{\rm lin}(V_{\rm g})$ when the renormalized level is aligned with the chemical potential but no local minimum. For the frequency-dependent Matsubara fRG, on the other hand, problems with the analytic continuation from imaginary to real frequencies obstructed the computation of the linear conductance.[57] Although it has been later found possible to circumvent this obstacle, the results for $G_{\rm lin}(V_{\rm g})$ are less accurate than those obtained from the Keldysh fRG.[78] A static fRG scheme based on a real-frequency cutoff in Keldysh formalism has also been found to reproduce qualitatively the shape of $G_{\rm lin}(V_{\rm g},T)$.[39] In view of the argument presented after Eq. (176) this has to be the consequence of a renormalization of the level broadening. The latter however can be achieved only in a dynamic approximation as can be seen from the fluctuation dissipation theorem, Eq. (94), that manifestly requires a frequency-dependent Keldysh component of the self-energy if $\Sigma^{\rm Ret}$ has nonvanishing imaginary part. Therefore we suspect that the corresponding result of the static flow scheme used in Ref. 39 is an artifact connected to the violation of causality as consequence of the real-frequency cutoff.

The results of our Keldysh fRG for the current as function of bias voltage at $V_{\rm g}=0$, $B=0$, $T=0$ have been compared in Ref. 13 to data obtained by a TD-DMRG treatment. Excellent agreement between both methods has been found for $U\leq 4\Gamma$. A more sensitive quantity for comparisons is however the differential conductance. Unfortunately, the TD-DMRG conductance data existing by now are not enough for a meaningful comparison. In Fig. 12 we compare the differential conductance as computed by fRG to the fourth-order perturbation theory results of Ref. 59. The agreement for small and large voltages is rather good. A discrepancy is found at intermediate V where the fRG does not reproduce the anomalous peak found by Ref. 59 for sufficiently large U. Probably the anomalous peak is an artifact of fourth-order perturbation theory; this conclusion is supported by recent nonequilibrium QMC results for the SIAM.[20]

The data for $G_{\rm diff}(V)$ at different magnetic fields presented in Figs. 13 and 14 could, in principle, be compared to results of the recently introduced scattering states NRG.[12] The data of the latter approach is however is still too noisy to allow for definite conclusions. Finally, Figs. 15 and 16 present the differential conductance for different temperatures in comparison to second-order perturbation theory.

A detailed comparison of nonequilibrium results of the fRG with that of recent numerical methods is given in Ref. 61.

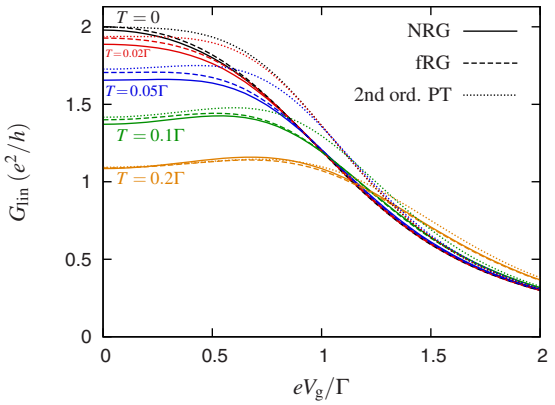

FIG. 10. (Color online) Linear conductance as function of gate voltage for $B=0$, $U=2\Gamma$, and different temperatures.

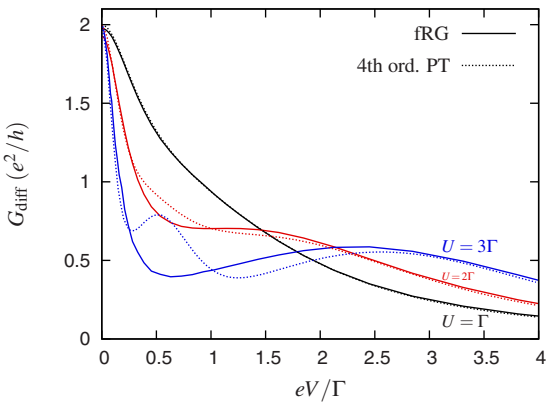

FIG. 12. (Color online) Differential conductance as function of bias voltage for $V_{\rm g}=0$, $B=0$, and different values of U. The temperature is zero except for the two fRG curves with $U=\Gamma$, 2Γ, where $T=0.02\Gamma$; the corresponding two data sets for the current at $T=0$ have not been sufficiently smooth to allow for numerical differentiation. The fourth-order perturbation theory results have been extracted from the e-print arXiv:cond-mat/0211616v1 to Ref. 59.

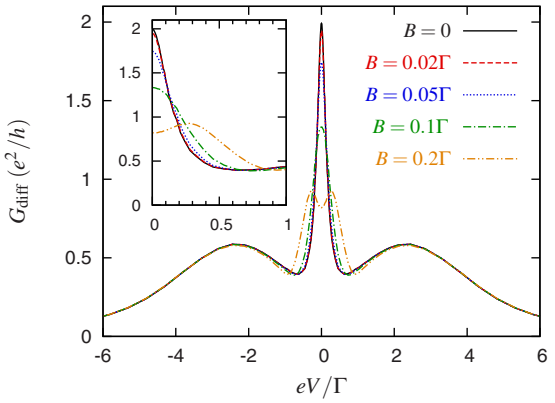

FIG. 13. (Color online) FRG results for the differential conductance as function of bias voltage for V_g=0, T=0, U=3Γ and different values of the magnetic field.

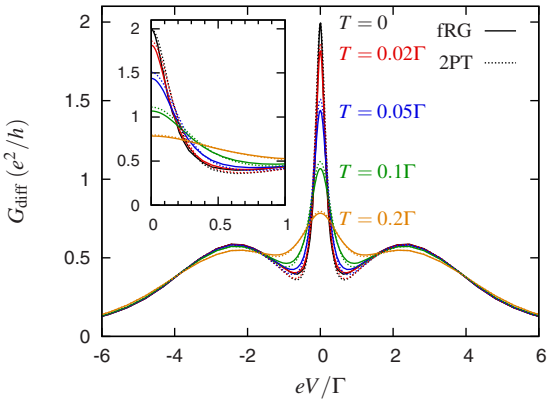

FIG. 15. (Color online) FRG results for the differential conductance as function of bias voltage for V_g=0, B=0, U=3Γ, and different values of temperature, in comparison with second-order perturbation theory.

IX. CONCLUSION

In this paper we studied a frequency-dependent fRG approximation for the Anderson impurity model. In equilibrium this model provides the possibility to compare our results to reliable data from Bethe ansatz or the NRG. Existing studies of the model within Matsubara fRG give indication on how to approach the problem within Keldysh formalism. The nonequilibrium properties of the model are subject of numerous investigations in recent time; however, a consistent picture did not yet emerge.

In order to preserve the Fermi-liquid properties of the model we have chosen as flow parameter the level broadening $\Gamma/2=\Delta$. In Sec. V we studied the basic approximation scheme with static vertex renormalization and reproduced the results of the static Matsubara fRG. For the more advanced dynamic second-order truncation scheme it was necessary to parametrize the frequency dependence of the vertex in order to obtain tractable equations. The self-energy which we feed back into the flow is static and does not contain interaction induced quasiparticle decay rates. Nevertheless, it turned out that the results can be trusted up to values of the Coulomb interaction $U\lesssim 3\Gamma=6\Delta$, which are typical parameter regimes also used in diverse recent numerical studies of the model; see, e.g., Ref. 61. Furthermore, for technical reasons we restricted our study to $T_L=T_R$ and $\Gamma_L=\Gamma_R$.

At the particle-hole symmetric point the description of the spectral function obtained by our fRG is comparable to second-order perturbation theory at weak interactions while getting worse for increasing values of U. But in contrast to perturbation theory the fRG generates exponential behavior in certain quantities. The exponent of the Kondo temperature extracted from the second-order derivative of the self-energy is identical to that found from the pinning mechanism in the static fRG, which is not far from the exact value. The fact that the effective mass derived from the fRG does not exhibit an exponential scale is related to the missing renormalization of the static part of the two-particle vertex in the present second-order truncation scheme. An extension which takes into account contributions from the flow of the three-particle vertex could probably cure this deficiency. In that case we expect that also the feedback of the full frequency-dependent self-energy into the flow will be favorable compared to the static feedback used here.

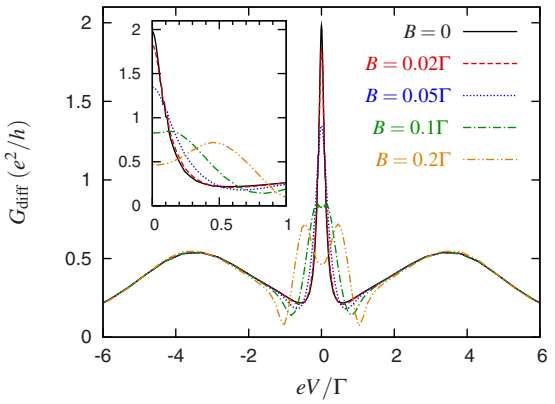

FIG. 14. (Color online) FRG results for the differential conductance as function of bias voltage for V_g=0, T=0, U=4Γ, and different values of the magnetic field.

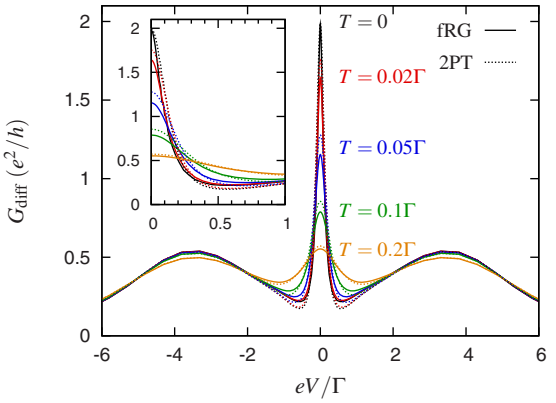

FIG. 16. (Color online) FRG results for the differential conductance as function of bias voltage for V_g=0, B=0, U=4Γ, and different values of temperature, in comparison with second-order perturbation theory.

A big success of the method is the very good description of the linear conductance as function of gate voltage, temperature, and magnetic field. At zero temperature excellent conductance data are obtained even for $U=4\Gamma$ while for finite T acceptable quality is achieved for $U\lesssim 3\Gamma$ with much better results than in perturbation theory. In this respect the method is a utile complement to existing fRG approaches: the static fRG is applicable only at $T=0$, and the frequency-dependent Matsubara fRG does not produce conductance data of comparable quality.

Concerning nonequilibrium properties the results of the fRG compare rather good to those of other methods for $U\lesssim 3\Gamma$ as far as comparisons are possible. In particular, we obtained very good agreement for the nonlinear current $I(V)$ with TD-DMRG data at the most critical point $V_g=T=B=0$. Together with the fact that our equilibrium results agree well with NRG at finite magnetic field and finite temperature, we expect our results for the nonlinear conductance $G(V)$ to be reliable at finite T and B, although no firm benchmark has yet been obtained by other techniques.

An issue to be addressed for future research is the problem of current conservation by the fRG. For the finite bias data which we presented in Sec. VIII current conservation is given as a consequence of the complete symmetry established by $eV_g=(\mu_L+\mu_R)/2$, $T_L=T_R$, $\Gamma_L=\Gamma_R$. In more general cases the fRG is not expected to be a current conserving method. Similar problems are known for other methods, for example, perturbation theory.[58] Only when reliable benchmarks become available, it can be concluded, whether the violation of current conservation generates serious errors in the nonlinear conductance $G(V)$, and whether more elaborate parametrizations within nonequilibrium fRG are necessary.

The comparison of the frequency-dependent Keldysh and Matsubara fRG reveals that in spite of being closely related, the two methods are not equivalent in equilibrium. The choice of an imaginary frequency cutoff as used in Matsubara fRG is not possible in the Keldysh fRG without destroying the Fermi-liquid property at the particle-hole symmetric point. For the Keldysh fRG the static self-energy feedback into the flow is preferable to the feedback of the full one, as opposed to the Matsubara fRG. And while the Matsubara fRG yields better results for the form of the spectral function at the particle-hole symmetric point, the Keldysh fRG produces better data for the linear conductance as function of gate voltage, making accessible finite temperatures where the Matsubara fRG is handicapped by the problem of analytic continuation.

In total our investigation gave insight on how a frequency-dependent approximation to the Keldysh fRG can be constructed and produced a flexible method to compute properties of the Anderson impurity model for moderate interactions. A fundamental problem of applying the fRG in the considered truncation scheme to this model is that the justification for the performed approximations can only be given by perturbative arguments. This difficulty is rooted in the regular perturbative expansion of the model. This contrasts with the situation in models with low-energy divergencies which typically allow to distinguish relevant and irrelevant contributions to the RG flow by power counting. It would be interesting to figure out whether perturbative RG techniques are still capable to capture the exponentially small scale of the Kondo temperature in the effective mass for large Coulomb interactions. Within our proposed approximation scheme, this scale already appeared in the second-order derivative of the self-energy, showing that our perturbative RG scheme has the potential to extract such scales. Therefore, it might appear possible that certain contributions from the three-particle vertex can help to reveal the same scale for the effective mass as well. We expect that the approximation can be systematically improved by including the influence of higher-order vertices on the flow, if care is taken to formulate the approximation scheme in accordance with Ward identities. It might be also interesting to access the Kondo limit of the Anderson model using an approach based on Hubbard-Stratonovich fields decomposition as proposed in Ref. 53 in combination with nonequilibrium fRG.

In summary, the method proposed in the present paper seems to be sufficient to describe Coulomb interactions up to the order of the bandwidth D of the local system. For a single-level quantum dot, the band width is given by $D\sim\Gamma$, whereas in quantum wires it is given by $D\sim t$, where t is the hopping matrix element. In both cases, the nonequilibrium fRG schemes of this paper and of Ref. 25 seem to be reliable for $U\lesssim D$, providing the hope for a unified approach describing the whole crossover from local to extended quantum systems.

ACKNOWLEDGMENTS

We are especially grateful to Theo Costi for providing us with a program to produce NRG data for comparison with the results of the fRG. We thank Christoph Karrasch and Volker Meden for numerous valuable discussion on applying the fRG to the SIAM and for providing data for comparison. We thank Sabine Andergassen, Frithjof Anders, Johannes Bauer, Fabian Heidrich-Meisner, and Frank Reininghaus for helpful discussions. This work was supported by the DFG-Forschergruppe 723.

APPENDIX A: IDENTIFICATION OF INDEPENDENT COMPONENTS OF $\varphi_\lambda^{p,x,d}$

The numerous Keldysh and spin components of the functions $\varphi_\lambda^{p,x,d}$ are not independent of each other. In this section we identify a set of independent components from which all the others can be determined. For that purpose we make extensive use of the relations for the vertex functions which originate from permutation of particles, complex conjugation, causality, and the KMS conditions and are described in Ref. 42. As explained in that reference, the hybridization flow parameter preserves these relations during the truncated RG flow. This is as well the case under the additional approximation induced by the replacement, Eq. (77), since the static renormalized vertices appearing in the flow Eq. (81) have the same spin and Keldysh structure as the original bare vertex. The relations can be even used for the three individual functions $\varphi_\lambda^{p,x,d}$ since the diagrammatic structure of the three corresponding flow equations is invariant under the

manipulations done in the proof of those relations, cf. Ref. 42. The only exception is that permutation of either the incoming or the outgoing indices maps φ^{x} onto φ^{d} and vice versa.

1. Analysis of the spin structure

Due to the spin structure of $\bar{v}$, $(\Phi_\lambda^{\mathrm{p,x,d}})$, and $(I_\lambda^{\mathrm{pp,xph}})$ certain spin components of $\varphi_\lambda^{\mathrm{p,x,d}}$ vanish: knowing that

$$\left.\begin{aligned} \bar{v}_{\sigma_1'\sigma_2'|\sigma_1\sigma_2} &= 0 \\ (\Phi_\lambda^{\mathrm{p}})_{\sigma_1'\sigma_2'|\sigma_1\sigma_2} &= 0 \\ (\Phi_\lambda^{\mathrm{x}})_{\sigma_1'\sigma_2'|\sigma_1\sigma_2} + (\Phi_\lambda^{\mathrm{d}})_{\sigma_1'\sigma_2'|\sigma_1\sigma_2} &= 0 \end{aligned}\right\} \text{ if } \sigma_1 \neq \bar{\sigma}_2 \text{ or } \sigma_1' \neq \bar{\sigma}_2', \tag{A1a}$$

$$(\Phi_\lambda^{\mathrm{x,d}})_{\sigma_1'\sigma_2'|\sigma_1\sigma_2} = 0 \quad \text{if } \sigma_1' + \sigma_2' \neq \sigma_1 + \sigma_2, \tag{A1b}$$

we conclude from the flow Eq. (81) that

$$(\varphi_\lambda^{\mathrm{p}})_{\sigma_1'\sigma_2'|\sigma_1\sigma_2} = 0, \quad \text{if } \sigma_1 \neq \bar{\sigma}_2 \text{ or } \sigma_1' \neq \bar{\sigma}_2', \tag{A2a}$$

$$(\varphi_\lambda^{\mathrm{x}})_{\sigma_1'\sigma_2'|\sigma_1\sigma_2} = 0, \quad \text{if } \sigma_1 + \sigma_2 \neq \sigma_1' + \sigma_2', \tag{A2b}$$

$$(\varphi_\lambda^{\mathrm{d}})_{\sigma_1'\sigma_2'|\sigma_1\sigma_2} = 0, \quad \text{if } \sigma_1 + \sigma_2 \neq \sigma_1' + \sigma_2'. \tag{A2c}$$

Concerning the remaining spin components, we can restrict our study to

$$(\varphi_\lambda^{\mathrm{p}})_{\sigma\bar{\sigma}|\sigma\bar{\sigma}},\ (\varphi_\lambda^{\mathrm{x}})_{\sigma\bar{\sigma}|\sigma\bar{\sigma}},\ (\varphi_\lambda^{\mathrm{d}})_{\sigma\bar{\sigma}|\sigma\bar{\sigma}},\ (\varphi_\lambda^{\mathrm{d}})_{\sigma\sigma|\sigma\sigma}, \tag{A3}$$

because the other ones can be derived from these by permutations of particle indices,

$$(\varphi_\lambda^{\mathrm{p}})_{\sigma\bar{\sigma}|\bar{\sigma}\sigma}^{\alpha_1'\alpha_2'|\alpha_1\alpha_2}(\Pi) = -(\varphi_\lambda^{\mathrm{p}})_{\sigma\bar{\sigma}|\sigma\bar{\sigma}}^{\alpha_1'\alpha_2'|\alpha_2\alpha_1}(\Pi), \tag{A4a}$$

$$(\varphi_\lambda^{\mathrm{x}})_{\sigma\bar{\sigma}|\bar{\sigma}\sigma}^{\alpha_1'\alpha_2'|\alpha_1\alpha_2}(X) = -(\varphi_\lambda^{\mathrm{d}})_{\sigma\bar{\sigma}|\sigma\bar{\sigma}}^{\alpha_1'\alpha_2'|\alpha_2\alpha_1}(-X), \tag{A4b}$$

$$(\varphi_\lambda^{\mathrm{d}})_{\sigma\bar{\sigma}|\bar{\sigma}\sigma}^{\alpha_1'\alpha_2'|\alpha_1\alpha_2}(\Delta) = -(\varphi_\lambda^{\mathrm{x}})_{\sigma\bar{\sigma}|\sigma\bar{\sigma}}^{\alpha_1'\alpha_2'|\alpha_2\alpha_1}(-\Delta), \tag{A4c}$$

$$(\varphi_\lambda^{\mathrm{x}})_{\sigma\sigma|\bar{\sigma}\sigma}^{\alpha_1'\alpha_2'|\alpha_1\alpha_2}(X) = -(\varphi_\lambda^{\mathrm{d}})_{\sigma\sigma|\sigma\sigma}^{\alpha_1'\alpha_2'|\alpha_2\alpha_1}(-X). \tag{A4d}$$

2. Analysis of the Keldysh structure

In the following it is convenient to describe the Keldysh components of two-particle functions in terms of block matrices, in which they are arranged according to the table

$$\begin{pmatrix} (11|11) & (11|21) & (11|12) & (11|22) \\ (21|11) & (21|21) & (21|12) & (21|22) \\ (12|11) & (12|21) & (12|12) & (12|22) \\ (22|11) & (22|21) & (22|12) & (22|22) \end{pmatrix}. \tag{A5}$$

The indices α_2', α_2 of an index tuple $(\alpha_1'\alpha_2'|\alpha_1\alpha_2)$ indicate which 2×2-submatrix is to be chosen, while α_1', α_1 defines the position inside a submatrix. The bare interaction vertex, Eq. (40), for example, is described by the matrix

$$\bar{v}_{\sigma_1'\sigma_2'|\sigma_1\sigma_2}^{\alpha_1'\alpha_2'|\alpha_1\alpha_2} = \frac{1}{2}\bar{v}_{\sigma_1'\sigma_2'|\sigma_1\sigma_2}\begin{pmatrix} 0 & 1 & 1 & 0 \\ 1 & 0 & 0 & 1 \\ 1 & 0 & 0 & 1 \\ 0 & 1 & 1 & 0 \end{pmatrix}_{\alpha_1'\alpha_2'|\alpha_1\alpha_2}. \tag{A6}$$

From the flow Eq. (81a) it follows that $\varphi_\lambda^{\mathrm{p}}(\Pi)$ has the Keldysh structure

$$\varphi_\lambda^{\mathrm{p}} = \begin{pmatrix} c & d & d & c \\ a & b & b & a \\ a & b & b & a \\ c & d & d & c \end{pmatrix}_\lambda, \tag{A7}$$

which can be seen as follows: the initial value $\varphi_{\lambda=\infty}^{\mathrm{p}} \equiv 0$ is consistent with the structure, Eq. (A7). Since $\varphi_\lambda^{\mathrm{p}}(\Pi)$ has this structure so does $[\bar{v}+\varphi_\lambda^{\mathrm{p}}(\Pi)+\Phi_\lambda^{\mathrm{x}}+\Phi_\lambda^{\mathrm{d}}]$. From Eq. (81a) it can then be derived that $d\varphi_\lambda^{\mathrm{p}}/d\lambda$ has the structure, Eq. (A7), as well. Therefore this structure is conserved during the flow.

Exploiting the causality relation $(\varphi_\lambda^{\mathrm{p}})^{22|22} \equiv 0$ and the transformation properties with respect to complex conjugation we find

$$(\varphi_\lambda^{\mathrm{p}})_{\sigma\bar{\sigma}|\sigma\bar{\sigma}}(\Pi) = \begin{pmatrix} 0 & a_\lambda^{\mathrm{p}*} & a_\lambda^{\mathrm{p}*} & 0 \\ a_\lambda^{\mathrm{p}} & b_\lambda^{\mathrm{p}} & b_\lambda^{\mathrm{p}} & a_\lambda^{\mathrm{p}} \\ a_\lambda^{\mathrm{p}} & b_\lambda^{\mathrm{p}} & b_\lambda^{\mathrm{p}} & a_\lambda^{\mathrm{p}} \\ 0 & a_\lambda^{\mathrm{p}*} & a_\lambda^{\mathrm{p}*} & 0 \end{pmatrix}_{\sigma\bar{\sigma}}(\Pi), \tag{A8}$$

where $(a_\lambda^{\mathrm{p}})_{\sigma\bar{\sigma}}(\Pi)$ is a complex valued function while $(b_\lambda^{\mathrm{p}})_{\sigma\bar{\sigma}}(\Pi)$ is purely imaginary. As a consequence of causality, $(a_\lambda^{\mathrm{p}})_{\sigma\bar{\sigma}}(\Pi)$ is analytic in the upper half plane of Π. The relations for exchange of particle indices yield

$$(a_\lambda^{\mathrm{p}})_{\sigma\bar{\sigma}}(\Pi) = (a_\lambda^{\mathrm{p}})_{\bar{\sigma}\sigma}(\Pi), \tag{A9a}$$

$$(b_\lambda^{\mathrm{p}})_{\sigma\bar{\sigma}}(\Pi) = (b_\lambda^{\mathrm{p}})_{\bar{\sigma}\sigma}(\Pi). \tag{A9b}$$

In case of thermal equilibrium at temperature T and chemical potential $\mu=0$ the only nontrivial component of the generalized fluctuation dissipation theorem of Ref. 42 reads

$$(b_\lambda^{\mathrm{p}})_{\sigma\bar{\sigma}}(\Pi) = i2\coth\left(\frac{\Pi}{2T}\right)\mathrm{Im}(a_\lambda^{\mathrm{p}})_{\sigma\bar{\sigma}}(\Pi). \tag{A10}$$

The same reasoning as used for $(\varphi_\lambda^{\mathrm{p}})_{\sigma\bar{\sigma}|\sigma\bar{\sigma}}(\Pi)$ shows that the Keldysh structure of $(\varphi_\lambda^{\mathrm{x}})_{\sigma\bar{\sigma}|\sigma\bar{\sigma}}(X)$ is

$$(\varphi_\lambda^{\mathrm{x}})_{\sigma\bar{\sigma}|\sigma\bar{\sigma}}(X) = \begin{pmatrix} 0 & a_\lambda^{\mathrm{x}*} & a_\lambda^{\mathrm{x}} & b_\lambda^{\mathrm{x}} \\ a_\lambda^{\mathrm{x}} & b_\lambda^{\mathrm{x}} & 0 & a_\lambda^{\mathrm{x}*} \\ a_\lambda^{\mathrm{x}*} & 0 & b_\lambda^{\mathrm{x}} & a_\lambda^{\mathrm{x}} \\ b_\lambda^{\mathrm{x}} & a_\lambda^{\mathrm{x}} & a_\lambda^{\mathrm{x}*} & 0 \end{pmatrix}_{\sigma\bar{\sigma}}(X) \tag{A11}$$

with a complex valued function $(a^{\mathrm{x}}_{\lambda})_{\sigma\bar{\sigma}}(X)$ and a purely imaginary function $(b^{\mathrm{x}}_{\lambda})_{\sigma\bar{\sigma}}(X)$. $(a^{\mathrm{x}}_{\lambda})_{\sigma\bar{\sigma}}(X)$ is analytic in the lower half plane of X. The behavior of a^{x}_{λ} and b^{x}_{λ} under exchange of particle indices is

$$(a^{\mathrm{x}}_{\lambda})_{\sigma\bar{\sigma}}(X) = (a^{\mathrm{x}}_{\lambda})_{\bar{\sigma}\sigma}(-X)^*, \tag{A12a}$$

$$(b^{\mathrm{x}}_{\lambda})_{\sigma\bar{\sigma}}(X) = (b^{\mathrm{x}}_{\lambda})_{\bar{\sigma}\sigma}(-X). \tag{A12b}$$

In case of thermal equilibrium the KMS conditions are

$$(b^{\mathrm{x}}_{\lambda})_{\sigma\bar{\sigma}}(X) = -i2\coth\left(\frac{X}{2T}\right)\mathrm{Im}(a^{\mathrm{x}}_{\lambda})_{\sigma\bar{\sigma}}(X). \tag{A13}$$

The Keldysh structure of $(\varphi^{\mathrm{d}}_{\lambda})_{\sigma\bar{\sigma}|\sigma\bar{\sigma}}(\Delta)$ has the form

$$(\varphi^{\mathrm{d}}_{\lambda})_{\sigma\bar{\sigma}|\sigma\bar{\sigma}}(\Delta) = \begin{pmatrix} 0 & (a^{\mathrm{d}}_{\lambda})_{\sigma\bar{\sigma}} & (a^{\mathrm{d}}_{\lambda})^*_{\bar{\sigma}\sigma} & (b^{\mathrm{d}}_{\lambda})_{\sigma\bar{\sigma}} \\ (a^{\mathrm{d}}_{\lambda})_{\sigma\bar{\sigma}} & 0 & (b^{\mathrm{d}}_{\lambda})_{\sigma\bar{\sigma}} & (a^{\mathrm{d}}_{\lambda})^*_{\bar{\sigma}\sigma} \\ (a^{\mathrm{d}}_{\lambda})^*_{\bar{\sigma}\sigma} & (b^{\mathrm{d}}_{\lambda})_{\sigma\bar{\sigma}} & 0 & (a^{\mathrm{d}}_{\lambda})_{\sigma\bar{\sigma}} \\ (b^{\mathrm{d}}_{\lambda})_{\sigma\bar{\sigma}} & (a^{\mathrm{d}}_{\lambda})^*_{\bar{\sigma}\sigma} & (a^{\mathrm{d}}_{\lambda})_{\sigma\bar{\sigma}} & 0 \end{pmatrix}(\Delta), \tag{A14}$$

where $(a^{\mathrm{d}}_{\lambda})_{\sigma\bar{\sigma}}(\Delta)$ and $(b^{\mathrm{d}}_{\lambda})_{\sigma\bar{\sigma}}(\Delta)$ are complex valued functions which satisfy

$$(a^{\mathrm{d}}_{\lambda})_{\sigma\bar{\sigma}}(\Delta) = (a^{\mathrm{d}}_{\lambda})_{\sigma\bar{\sigma}}(-\Delta)^*, \tag{A15a}$$

$$(b^{\mathrm{d}}_{\lambda})_{\sigma\bar{\sigma}}(\Delta) = -(b^{\mathrm{d}}_{\lambda})_{\sigma\bar{\sigma}}(-\Delta)^*, \tag{A15b}$$

$$(b^{\mathrm{d}}_{\lambda})_{\sigma\bar{\sigma}}(\Delta) = (b^{\mathrm{d}}_{\lambda})_{\bar{\sigma}\sigma}(-\Delta). \tag{A15c}$$

The function $(a^{\mathrm{d}}_{\lambda})_{\sigma\bar{\sigma}}(\Delta)$ is analytic in the upper half plane of Δ. In case of thermal equilibrium the KMS conditions demand

$$\mathrm{Re}(b^{\mathrm{d}}_{\lambda})_{\sigma\bar{\sigma}}(\Delta) = \tanh\left(\frac{\Delta}{2T}\right)\mathrm{Re}[(a^{\mathrm{d}}_{\lambda})_{\sigma\bar{\sigma}}(\Delta) - (a^{\mathrm{d}}_{\lambda})_{\bar{\sigma}\sigma}(\Delta)], \tag{A16a}$$

$$\mathrm{Im}(b^{\mathrm{d}}_{\lambda})_{\sigma\bar{\sigma}}(\Delta) = \coth\left(\frac{\Delta}{2T}\right)\mathrm{Im}[(a^{\mathrm{d}}_{\lambda})_{\sigma\bar{\sigma}}(\Delta) + (a^{\mathrm{d}}_{\lambda})_{\bar{\sigma}\sigma}(\Delta)]. \tag{A16b}$$

Finally the Keldysh structure of $(\varphi^{\mathrm{d}}_{\lambda})_{\sigma\sigma|\sigma\sigma}(\Delta)$ is

$$(\varphi^{\mathrm{d}}_{\lambda})_{\sigma\sigma|\sigma\sigma}(\Delta) = \begin{pmatrix} 0 & a^{\mathrm{d}}_{\lambda} & a^{\mathrm{d}*}_{\lambda} & b^{\mathrm{d}}_{\lambda} \\ a^{\mathrm{d}}_{\lambda} & 0 & b^{\mathrm{d}}_{\lambda} & a^{\mathrm{d}*}_{\lambda} \\ a^{\mathrm{d}*}_{\lambda} & b^{\mathrm{d}}_{\lambda} & 0 & a^{\mathrm{d}}_{\lambda} \\ b^{\mathrm{d}}_{\lambda} & a^{\mathrm{d}*}_{\lambda} & a^{\mathrm{d}}_{\lambda} & 0 \end{pmatrix}_{\sigma\sigma}(\Delta), \tag{A17}$$

where $(a^{\mathrm{d}}_{\lambda})_{\sigma\sigma}(\Delta)$ is a complex valued and $(b^{\mathrm{d}}_{\lambda})_{\sigma\sigma}(\Delta)$ a purely imaginary function; they satisfy

$$(a^{\mathrm{d}}_{\lambda})_{\sigma\sigma}(\Delta) = (a^{\mathrm{d}}_{\lambda})_{\sigma\sigma}(-\Delta)^*, \tag{A18a}$$

$$(b^{\mathrm{d}}_{\lambda})_{\sigma\sigma}(\Delta) = (b^{\mathrm{d}}_{\lambda})_{\sigma\sigma}(-\Delta). \tag{A18b}$$

$(a^{\mathrm{d}}_{\lambda})_{\sigma\sigma}(\Delta)$ is analytic in the upper half plane of Δ. In case of thermal equilibrium the KMS conditions are

$$(b^{\mathrm{d}}_{\lambda})_{\sigma\sigma}(\Delta) = i2\coth\left(\frac{\Delta}{2T}\right)\mathrm{Im}(a^{\mathrm{d}}_{\lambda})_{\sigma\sigma}(\Delta). \tag{A19}$$

In summary we conclude that all spin and Keldysh components of the functions $\varphi^{\mathrm{p,x,d}}$ can be determined from the selection

$$(a^{\mathrm{p,x,d}}_{\lambda})_{\uparrow\downarrow},\ (b^{\mathrm{p,x,d}}_{\lambda})_{\uparrow\downarrow},\ (a^{\mathrm{d}}_{\lambda})_{\downarrow\uparrow},\ (a^{\mathrm{d}}_{\lambda})_{\sigma\sigma},\ (b^{\mathrm{d}}_{\lambda})_{\sigma\sigma},\quad \sigma = \uparrow,\downarrow. \tag{A20}$$

The precise form of the flow equations shows, that $(a^{\mathrm{d}}_{\lambda})_{\downarrow\uparrow}$ can be expressed through $(a^{\mathrm{d}}_{\lambda})_{\uparrow\downarrow}$, see Eq. (C8) below.

APPENDIX B: FLOW EQUATION FOR THE SELF-ENERGY

In our approximation the two-particle vertex acquires a special structure described in Sec. VI B and Appendix A. When we insert this structure into Eq. (27) we obtain as flow equation for the retarded component of the self-energy

$$\begin{aligned}\frac{d\Sigma^{\mathrm{Ret}\,\lambda}_{\sigma}(\omega)}{d\lambda} = -\frac{i}{2\pi}\int d\omega' \Big\{ & [(b^{\mathrm{x}}_{\lambda})_{\sigma\bar{\sigma}}(\omega'-\omega) + (b^{\mathrm{d}}_{\lambda})_{\sigma\bar{\sigma}}(0)]S^{\mathrm{Ret}\,\lambda}_{\bar{\sigma}}(\omega') - [(b^{\mathrm{d}}_{\lambda})_{\sigma\sigma}(\omega-\omega') \\ & - (b^{\mathrm{d}}_{\lambda})_{\sigma\sigma}(0)]S^{\mathrm{Ret}\,\lambda}_{\sigma}(\omega') + [(b^{\mathrm{p}}_{\lambda})_{\sigma\bar{\sigma}}(\omega'+\omega) \\ & + (b^{\mathrm{d}}_{\lambda})_{\sigma\bar{\sigma}}(0)]S^{\mathrm{Av}\,\lambda}_{\bar{\sigma}}(\omega') + (b^{\mathrm{d}}_{\lambda})_{\sigma\sigma}(0)S^{\mathrm{Av}\,\lambda}_{\sigma}(\omega') \\ & + \left[\frac{U}{2} + (a^{\mathrm{p}}_{\lambda})_{\sigma\bar{\sigma}}(\omega'+\omega) + (a^{\mathrm{x}}_{\lambda})_{\sigma\bar{\sigma}}(\omega'-\omega) \right. \\ & \left. + (a^{\mathrm{d}}_{\lambda})_{\sigma\bar{\sigma}}(0)\right]S^{\mathrm{K}\lambda}_{\bar{\sigma}}(\omega') - [(a^{\mathrm{d}}_{\lambda})_{\sigma\sigma}(\omega-\omega') \\ & - (a^{\mathrm{d}}_{\lambda})_{\sigma\sigma}(0)]S^{\mathrm{K}\lambda}_{\sigma}(\omega')\Big\}. \end{aligned} \tag{B1}$$

As a consequence of Eq. (36) $S^{\mathrm{Ret}}(\omega')$ $[S^{\mathrm{Av}}(\omega')]$ is analytic in the upper [lower] half plane of ω' and vanishes as ω'^{-2} for $|\omega'|\to\infty$. Hence,

$$\int d\omega' S^{\mathrm{Ret,Av}}(\omega') = 0, \tag{B2}$$

and Eq. (B1) is reduced to

$$\frac{d\Sigma_\sigma^{\mathrm{Ret}\,\lambda}(\omega)}{d\lambda} = -\frac{i}{2\pi}\int d\omega' \Bigg\{ (b_\lambda^{\mathrm{x}})_{\sigma\bar{\sigma}}(\omega'-\omega) S_{\bar{\sigma}}^{\mathrm{Ret}\,\lambda}(\omega') - (b_\lambda^{\mathrm{d}})_{\sigma\sigma}(\omega-\omega') S_\sigma^{\mathrm{Ret}\,\lambda}(\omega') + (b_\lambda^{\mathrm{p}})_{\sigma\bar{\sigma}}(\omega'+\omega) S_{\bar{\sigma}}^{\mathrm{Av}\,\lambda}(\omega') + \left[\frac{U}{2} + (a_\lambda^{\mathrm{p}})_{\sigma\bar{\sigma}}(\omega'+\omega) + (a_\lambda^{\mathrm{x}})_{\sigma\bar{\sigma}}(\omega'-\omega) + (a_\lambda^{\mathrm{d}})_{\sigma\bar{\sigma}}(0)\right] S_{\bar{\sigma}}^{\mathrm{K}\lambda}(\omega') - [(a_\lambda^{\mathrm{d}})_{\sigma\sigma}(\omega-\omega') - (a_\lambda^{\mathrm{d}})_{\sigma\sigma}(0)] S_\sigma^{\mathrm{K}\lambda}(\omega') \Bigg\}. \tag{B3}$$

Since the relation $\Sigma_\sigma^{\mathrm{Av}\,\lambda}(\omega)=\Sigma_\sigma^{\mathrm{Ret}\,\lambda}(\omega)^*$ is maintained during the flow, it is not necessary to compute the flow of $\Sigma_\sigma^{\mathrm{Av}\,\lambda}(\omega)$ separately. Following similar steps as for Σ^{Ret} we acquire the flow equation for Σ^{K},

$$\frac{d\Sigma_\sigma^{\mathrm{K}\lambda}(\omega)}{d\lambda} = -\frac{i}{2\pi}\int d\omega' \Bigg(2\,\mathrm{Re}\left\{\left[\frac{\mathrm{U}}{2} + (a_\lambda^{\mathrm{p}})_{\sigma\bar{\sigma}}(\omega'+\omega)^* + (a_\lambda^{\mathrm{x}})_{\sigma\bar{\sigma}}(\omega'-\omega)\right] S_{\bar{\sigma}}^{\mathrm{Ret}\,\lambda}(\omega')\right\} - 2\,\mathrm{Re}[(a_\lambda^{\mathrm{d}})_{\sigma\sigma}(\omega-\omega') S_\sigma^{\mathrm{Ret}\,\lambda}(\omega')] + [(b_\lambda^{\mathrm{p}})_{\sigma\bar{\sigma}}(\omega'+\omega) + (b_\lambda^{\mathrm{x}})_{\sigma\bar{\sigma}}(\omega'-\omega)] S_{\bar{\sigma}}^{\mathrm{K}\lambda}(\omega') - (b_\lambda^{\mathrm{d}})_{\sigma\sigma}(\omega-\omega') S_\sigma^{\mathrm{K}\lambda}(\omega') \Bigg). \tag{B4}$$

APPENDIX C: FLOW EQUATION FOR THE TWO-PARTICLE VERTEX

Due to the structure of the two-particle vertex function described in Sec. VI B and Appendix A, its flow is determined completely by the flow of the components, Eq. (A20). The flow equations of these components can be formulated as a closed set if the other components are eliminated by use of the relations found in Appendix A. Setting up these flow equations is cumbersome but straightforward. This section is devoted to a brief sketch of some simplifications which can be made during the calculation and indicating the result.

The flow equations for $(a_\lambda^{\mathrm{p}})_{\sigma\bar{\sigma}}=(\varphi_\lambda^{\mathrm{p}})_{\sigma\bar{\sigma}|\sigma\bar{\sigma}}^{12|22}$ and $(b_\lambda^{\mathrm{p}})_{\sigma\bar{\sigma}}=(\varphi_\lambda^{\mathrm{p}})_{\sigma\bar{\sigma}|\sigma\bar{\sigma}}^{12|21}$ follow from Eq. (81a). Due to Eqs. (79), (82), and (A2a) the implicit summation over spin indices in Eq. (81a) is reduced to the two contributions $(\sigma_3\sigma_4|\sigma_3'\sigma_4')=(\sigma\bar{\sigma}|\sigma\bar{\sigma}),(\bar{\sigma}\sigma|\bar{\sigma}\sigma)$. The summation over Keldysh indices is also largely reduced: first, because of the vanishing components in Eq. (A8), and, second, because of

$$(I_\lambda^{\mathrm{pp}})^{\alpha_1\alpha_2|\alpha_1'\alpha_2'} = 0, \quad \text{if} \quad \alpha_1=\alpha_1'=1 \quad \text{or} \quad \alpha_2=\alpha_2'=1, \tag{C1a}$$

$$(I_\lambda^{\mathrm{pp}})^{12|21} = (I_\lambda^{\mathrm{pp}})^{21|12} = 0. \tag{C1b}$$

Equation (C1a) is a consequence of $G^{1|1}=0$, $S^{1|1}=0$, while Eq. (C1b) follows from $G^{\mathrm{Ret}}(\omega)$, $S^{\mathrm{Ret}}(\omega)$ [$G^{\mathrm{Av}}(\omega)$, $S^{\mathrm{Av}}(\omega)$] being analytic in the upper [lower] half plane of ω. Making further use of

$$(I_\lambda^{\mathrm{pp}})^{\alpha_1'\alpha_2'|\alpha_1\alpha_2}(\omega) = -(-1)^{\alpha_1'+\alpha_2'+\alpha_1+\alpha_2}(I_\lambda^{\mathrm{pp}})^{\alpha_1\alpha_2|\alpha_1'\alpha_2'}(\omega)^* \tag{C2}$$

for the remaining components, which follows form $G_\sigma^{\mathrm{Ret}}(\omega)^*=G_\sigma^{\mathrm{Av}}(\omega)$, $S_\sigma^{\mathrm{Ret}}(\omega)^*=S_\sigma^{\mathrm{Av}}(\omega)$ and $G_\sigma^{\mathrm{K}}(\omega)^*=-G_\sigma^{\mathrm{K}}(\omega)$, $S_\sigma^{\mathrm{K}}(\omega)^*=-S_\sigma^{\mathrm{K}}(\omega)$, we find

$$\frac{d(a_\lambda^{\mathrm{p}})_{\sigma\bar{\sigma}}(\Pi)}{d\lambda} = \left[\frac{U+U_\lambda^{\mathrm{x}}+U_\lambda^{\mathrm{d}}}{2} + (a_\lambda^{\mathrm{p}})_{\sigma\bar{\sigma}}(\Pi)\right]^2 [(I_\lambda^{\mathrm{pp}})_{\sigma\bar{\sigma}}^{22|12}(\Pi) + (I_\lambda^{\mathrm{pp}})_{\sigma\bar{\sigma}}^{22|21}(\Pi)], \tag{C3a}$$

$$\frac{d(b_\lambda^{\mathrm{p}})_{\sigma\bar{\sigma}}(\Pi)}{d\lambda} = 2i\,\mathrm{Im}\Bigg\{ \left|\frac{U+U_\lambda^{\mathrm{x}}+U_\lambda^{\mathrm{d}}}{2} + (a_\lambda^{\mathrm{p}})_{\sigma\bar{\sigma}}(\Pi)\right|^2 \times \left[(I_\lambda^{\mathrm{pp}})_{\sigma\bar{\sigma}}^{22|11}(\Pi) + \frac{1}{2}(I_\lambda^{\mathrm{pp}})_{\sigma\bar{\sigma}}^{22|22}(\Pi)\right] + \left[\frac{U+U_\lambda^{\mathrm{x}}+U_\lambda^{\mathrm{d}}}{2} + (a_\lambda^{\mathrm{p}})_{\sigma\bar{\sigma}}(\Pi)\right](b_\lambda^{\mathrm{p}})_{\sigma\bar{\sigma}}(\Pi) \times [(I_\lambda^{\mathrm{pp}})_{\sigma\bar{\sigma}}^{22|12}(\Pi) + (I_\lambda^{\mathrm{pp}})_{\sigma\bar{\sigma}}^{22|21}(\Pi)]\Bigg\}. \tag{C3b}$$

The flow equations for $(a_\lambda^{\mathrm{x}})_{\sigma\bar{\sigma}}(X)$ and $(b_\lambda^{\mathrm{x}})_{\sigma\bar{\sigma}}(X)$ can be derived in an analogous way. Instead of Eqs. (C2) we use

$$(I_\lambda^{\mathrm{ph}})^{\alpha_1\alpha_2|\alpha_1'\alpha_2'} = 0, \quad \text{if} \quad \alpha_1=\alpha_1'=1 \quad \text{or} \quad \alpha_2=\alpha_2'=1, \tag{C4a}$$

$$(I_\lambda^{\mathrm{ph}})^{11|22} = (I_\lambda^{\mathrm{ph}})^{22|11} = 0, \tag{C4b}$$

and

$$(I_\lambda^{\mathrm{ph}})^{\alpha_1'\alpha_2'|\alpha_1\alpha_2}(\omega) = -(-1)^{\alpha_1'+\alpha_2'+\alpha_1+\alpha_2}(I_\lambda^{\mathrm{ph}})^{\alpha_1\alpha_2|\alpha_1'\alpha_2'}(\omega)^*, \tag{C5}$$

and find

$$\frac{d(a^{\mathrm{x}}_{\lambda})_{\sigma\bar{\sigma}}(X)}{d\lambda} = \left[\frac{U+U^{\mathrm{p}}_{\lambda}+U^{\mathrm{d}}_{\lambda}}{2} + (a^{\mathrm{x}}_{\lambda})_{\sigma\bar{\sigma}}(X)\right]^2 [(I^{\mathrm{ph}}_{\lambda})^{21|22}_{\sigma\bar{\sigma}}(X) + (I^{\mathrm{ph}}_{\lambda})^{22|12}_{\sigma\bar{\sigma}}(X)], \tag{C6a}$$

$$\frac{d(b^{\mathrm{x}}_{\lambda})_{\sigma\bar{\sigma}}(X)}{d\lambda} = 2i\,\mathrm{Im}\left\{\left|\frac{U+U^{\mathrm{p}}_{\lambda}+U^{\mathrm{d}}_{\lambda}}{2} + (a^{\mathrm{x}}_{\lambda})_{\sigma\bar{\sigma}}(X)\right|^2\left[(I^{\mathrm{ph}}_{\lambda})^{12|21}_{\sigma\bar{\sigma}}(X) + \frac{1}{2}(I^{\mathrm{ph}}_{\lambda})^{22|22}_{\sigma\bar{\sigma}}(X)\right]\right.$$
$$\left. + \left[\frac{U+U^{\mathrm{p}}_{\lambda}+U^{\mathrm{d}}_{\lambda}}{2} + (a^{\mathrm{x}}_{\lambda})_{\sigma\bar{\sigma}}(X)\right](b^{\mathrm{p}}_{\lambda})_{\sigma\bar{\sigma}}(X)[(I^{\mathrm{ph}}_{\lambda})^{21|22}_{\sigma\bar{\sigma}}(X) + (I^{\mathrm{ph}}_{\lambda})^{22|12}_{\sigma\bar{\sigma}}(X)]\right\}. \tag{C6b}$$

The flow equations for $(a^{\mathrm{d}}_{\lambda})_{\sigma\bar{\sigma}}(\Delta)$ and $(b^{\mathrm{d}}_{\lambda})_{\sigma\bar{\sigma}}(\Delta)$ are

$$\frac{d(a^{\mathrm{d}}_{\lambda})_{\sigma\bar{\sigma}}(\Delta)}{d\lambda} = -\left[\frac{U+U^{\mathrm{p}}_{\lambda}+U^{\mathrm{x}}_{\lambda}}{2} + (a^{\mathrm{d}}_{\lambda})_{\sigma\bar{\sigma}}(\Delta)\right]\sum_{s=\uparrow,\downarrow}\left[(a^{\mathrm{d}}_{\lambda})_{ss}(\Delta) - \frac{W^{\mathrm{d}}_{\lambda s}}{2}\right][(I^{\mathrm{ph}}_{\lambda})^{22|21}_{ss}(\Delta) + (I^{\mathrm{ph}}_{\lambda})^{12|22}_{ss}(\Delta)], \tag{C7a}$$

$$\begin{aligned}\frac{d(b^{\mathrm{d}}_{\lambda})_{\sigma\bar{\sigma}}(\Delta)}{d\lambda} = &-\left[\frac{U+U^{\mathrm{p}}_{\lambda}+U^{\mathrm{x}}_{\lambda}}{2} + (a^{\mathrm{d}}_{\lambda})_{\sigma\bar{\sigma}}(\Delta)\right]\left[(a^{\mathrm{d}}_{\lambda})_{\bar{\sigma}\bar{\sigma}}(\Delta)^* - \frac{W^{\mathrm{d}}_{\lambda\bar{\sigma}}}{2}\right][(I^{\mathrm{ph}}_{\lambda})^{12|21}_{\bar{\sigma}\bar{\sigma}}(\Delta) + (I^{\mathrm{ph}}_{\lambda})^{21|12}_{\bar{\sigma}\bar{\sigma}}(\Delta) + (I^{\mathrm{ph}}_{\lambda})^{22|22}_{\bar{\sigma}\bar{\sigma}}(\Delta)]\\
&-\left[\frac{U+U^{\mathrm{p}}_{\lambda}+U^{\mathrm{x}}_{\lambda}}{2} + (a^{\mathrm{d}}_{\lambda})_{\bar{\sigma}\sigma}(\Delta)^*\right]\left[(a^{\mathrm{d}}_{\lambda})_{\sigma\sigma}(\Delta) - \frac{W^{\mathrm{d}}_{\lambda\sigma}}{2}\right][(I^{\mathrm{ph}}_{\lambda})^{12|21}_{\sigma\sigma}(\Delta) + (I^{\mathrm{ph}}_{\lambda})^{21|12}_{\sigma\sigma}(\Delta) + (I^{\mathrm{ph}}_{\lambda})^{22|22}_{\sigma\sigma}(\Delta)]\\
&-\left[\frac{U+U^{\mathrm{p}}_{\lambda}+U^{\mathrm{x}}_{\lambda}}{2} + (a^{\mathrm{d}}_{\lambda})_{\sigma\bar{\sigma}}(\Delta)\right](b^{\mathrm{d}}_{\lambda})_{\bar{\sigma}\bar{\sigma}}(\Delta)[(I^{\mathrm{ph}}_{\lambda})^{22|21}_{\bar{\sigma}\bar{\sigma}}(\Delta) + (I^{\mathrm{ph}}_{\lambda})^{12|22}_{\bar{\sigma}\bar{\sigma}}(\Delta)]\\
&-\left[\frac{U+U^{\mathrm{p}}_{\lambda}+U^{\mathrm{x}}_{\lambda}}{2} + (a^{\mathrm{d}}_{\lambda})_{\bar{\sigma}\sigma}(\Delta)^*\right](b^{\mathrm{d}}_{\lambda})_{\sigma\sigma}(\Delta)[(I^{\mathrm{ph}}_{\lambda})^{21|22}_{\sigma\sigma}(\Delta) + (I^{\mathrm{ph}}_{\lambda})^{22|12}_{\sigma\sigma}(\Delta)]\\
&-\left[(a^{\mathrm{d}}_{\lambda})_{\bar{\sigma}\bar{\sigma}}(\Delta)^* - \frac{W^{\mathrm{d}}_{\lambda\bar{\sigma}}}{2}\right](b^{\mathrm{d}}_{\lambda})_{\sigma\bar{\sigma}}(\Delta)[(I^{\mathrm{ph}}_{\lambda})^{21|22}_{\bar{\sigma}\bar{\sigma}}(\Delta) + (I^{\mathrm{ph}}_{\lambda})^{22|12}_{\bar{\sigma}\bar{\sigma}}(\Delta)]\\
&-\left[(a^{\mathrm{d}}_{\lambda})_{\sigma\sigma}(\Delta) - \frac{W^{\mathrm{d}}_{\lambda\sigma}}{2}\right](b^{\mathrm{d}}_{\lambda})_{\sigma\bar{\sigma}}(\Delta)[(I^{\mathrm{ph}}_{\lambda})^{22|21}_{\sigma\sigma}(\Delta) + (I^{\mathrm{ph}}_{\lambda})^{12|22}_{\sigma\sigma}(\Delta)].\end{aligned} \tag{C7b}$$

Since $(a^{\mathrm{d}}_{\lambda})_{\sigma\bar{\sigma}}$ and $(a^{\mathrm{d}}_{\lambda})_{\bar{\sigma}\sigma}$ have the same (zero) initial value at $\lambda=\infty$ we conclude from Eq. (C7a) that

$$(a^{\mathrm{d}}_{\lambda})_{\sigma\bar{\sigma}}(\Delta) = (a^{\mathrm{d}}_{\lambda})_{\bar{\sigma}\sigma}(\Delta). \tag{C8}$$

Finally, the flow equations for $(a^{\mathrm{d}}_{\lambda})_{\sigma\sigma}(\Delta)$ and $(b^{\mathrm{d}}_{\lambda})_{\sigma\sigma}(\Delta)$ turn out to be

$$\frac{d(a^{\mathrm{d}}_{\lambda})_{\sigma\sigma}(\Delta)}{d\lambda} = -\left[\frac{U+U^{\mathrm{p}}_{\lambda}+U^{\mathrm{x}}_{\lambda}}{2} + (a^{\mathrm{d}}_{\lambda})_{\sigma\bar{\sigma}}(\Delta)\right]^2[(I^{\mathrm{ph}}_{\lambda})^{22|21}_{\bar{\sigma}\bar{\sigma}}(\Delta) + (I^{\mathrm{ph}}_{\lambda})^{12|22}_{\bar{\sigma}\bar{\sigma}}(\Delta)] - \left[(a^{\mathrm{d}}_{\lambda})_{\sigma\sigma}(\Delta) - \frac{W^{\mathrm{d}}_{\lambda\sigma}}{2}\right]^2[(I^{\mathrm{ph}}_{\lambda})^{22|21}_{\sigma\sigma}(\Delta) + (I^{\mathrm{ph}}_{\lambda})^{12|22}_{\sigma\sigma}(\Delta)], \tag{C9a}$$

$$\begin{aligned}\frac{d(b^{\mathrm{d}}_{\lambda})_{\sigma\sigma}(\Delta)}{d\lambda} = &-2i\,\mathrm{Im}\left\{\left|\frac{U+U^{\mathrm{p}}_{\lambda}+U^{\mathrm{x}}_{\lambda}}{2} + (a^{\mathrm{d}}_{\lambda})_{\sigma\bar{\sigma}}(\Delta)\right|^2\left[(I^{\mathrm{ph}}_{\lambda})^{12|21}_{\bar{\sigma}\bar{\sigma}}(\Delta) + \frac{1}{2}(I^{\mathrm{ph}}_{\lambda})^{22|22}_{\bar{\sigma}\bar{\sigma}}(\Delta)\right]\right.\\
&+\left|(a^{\mathrm{d}}_{\lambda})_{\sigma\sigma}(\Delta) - \frac{W^{\mathrm{d}}_{\lambda\sigma}}{2}\right|^2\left[(I^{\mathrm{ph}}_{\lambda})^{12|21}_{\sigma\sigma}(\Delta) + \frac{1}{2}(I^{\mathrm{ph}}_{\lambda})^{22|22}_{\sigma\sigma}(\Delta)\right]\\
&+\left[\frac{U+U^{\mathrm{p}}_{\lambda}+U^{\mathrm{x}}_{\lambda}}{2} + (a^{\mathrm{d}}_{\lambda})_{\sigma\bar{\sigma}}(\Delta)^*\right](b^{\mathrm{d}}_{\lambda})_{\sigma\bar{\sigma}}(\Delta)[(I^{\mathrm{ph}}_{\lambda})^{21|22}_{\bar{\sigma}\bar{\sigma}}(\Delta) + (I^{\mathrm{ph}}_{\lambda})^{22|12}_{\bar{\sigma}\bar{\sigma}}(\Delta)]\\
&+\left.\left[(a^{\mathrm{d}}_{\lambda})_{\sigma\sigma}(\Delta)^* - \frac{W^{\mathrm{d}}_{\lambda\sigma}}{2}\right](b^{\mathrm{d}}_{\lambda})_{\sigma\sigma}(\Delta)[(I^{\mathrm{ph}}_{\lambda})^{21|22}_{\sigma\sigma}(\Delta) + (I^{\mathrm{ph}}_{\lambda})^{22|12}_{\sigma\sigma}(\Delta)]\right\}.\end{aligned} \tag{C9b}$$

APPENDIX D: NONEQUILIBRIUM FERMI-LIQUID COEFFICIENT

In this evaluation we make the same assumptions as in the Sec. VII, i.e., $\Gamma_{\mathrm{L}}=\Gamma_{\mathrm{R}}$ and $\mu_{\mathrm{L}}=-\mu_{\mathrm{R}}=\frac{eV}{2}$, $B=eV_g=0$. We remind that these conditions are important to ensure the real value of the static component of the vertex as well as the current conservation.

Let us define a nonequilibrium distribution function

$$h_F^{neq}(\omega) = \alpha_L h_{F,L}(\omega) + \alpha_R h_{F,R}(\omega) = \frac{1}{2} h_F\left(\omega - \frac{eV}{2}\right) + \frac{1}{2} h_F\left(\omega + \frac{eV}{2}\right), \tag{D1}$$

where $\alpha_L + \alpha_R = 1$.

The nonequilibrium equation for the self-energy Eq. (B1) in the particle-hole symmetric case reads

$$\begin{aligned}\frac{d}{d\lambda}\Sigma_\sigma^{\mathrm{Ret}}(\omega) = \frac{1}{\pi}\int d\tilde{\omega}[&- \gamma_0 h_F^{neq}(\tilde{\omega})\mathrm{Im}\, s_{\bar{\sigma}}^{\mathrm{Ret}}(\tilde{\omega}) \\ &+ h_F^{neq}(\tilde{\omega}) a_1(\tilde{\omega}+\omega)\mathrm{Im}\, s_{\bar{\sigma}}^{\mathrm{Ret}}(\tilde{\omega}) \\ &+ b_1(\tilde{\omega}+\omega) s_{\bar{\sigma}}^{\mathrm{Av}}(\tilde{\omega}) \\ &+ h_F^{neq}(\tilde{\omega}) a_3(\tilde{\omega}-\omega)\mathrm{Im}\, s_{\bar{\sigma}}^{\mathrm{Ret}}(\tilde{\omega}) \\ &+ b_3(\tilde{\omega}-\omega) s_{\bar{\sigma}}^{\mathrm{Ret}}(\tilde{\omega}) \\ &+ h_F^{neq}(\tilde{\omega}) \bar{a}_{2\sigma}(\tilde{\omega}-\omega)\mathrm{Im}\, s_{\sigma}^{\mathrm{Ret}}(\tilde{\omega}) \\ &+ \bar{b}_{2\sigma}(\tilde{\omega}-\omega) s_{\sigma}^{\mathrm{Ret}}(\tilde{\omega})],\end{aligned} \tag{D2}$$

where the vertex functions a and b components are no longer related to each other by the KMS equalities, and where $\bar{b}_{2\sigma}$ is defined on the analogy of Eq. (146).

In the following we will need an expression for a product of the two distribution functions, Eq. (D1), evaluated at different frequency arguments ω_1 and ω_2. At small eV such a product can be represented as

$$\begin{aligned}&[\alpha_L h_{F,L}(\omega_1) + \alpha_R h_{F,R}(\omega_1)][\alpha_L h_{F,L}(\omega_2) + \alpha_R h_{F,R}(\omega_2)] \\ &= \alpha_L h_{F,L}(\omega_1) h_{F,L}(\omega_2) + \alpha_R h_{F,R}(\omega_1) h_{F,R}(\omega_2) \\ &\quad - \alpha_L \alpha_R [h_{F,L}(\omega_1) - h_{F,R}(\omega_1)][h_{F,L}(\omega_2) - h_{F,R}(\omega_2)] \\ &\approx \alpha_L h_{F,L}(\omega_1) h_{F,L}(\omega_2) + \alpha_R h_{F,R}(\omega_1) h_{F,R}(\omega_2) \\ &\quad - 4\alpha_L \alpha_R (eV)^2 \delta(\omega_1)\delta(\omega_2).\end{aligned} \tag{D3}$$

Let us consequently analyze voltage-induced corrections to the KMS relations occurring in each channel.

1. Particle-particle channel

In order to evaluate Eq. (115) we set $\omega_1 = \frac{\Pi}{2} + \omega'$, $\omega_2 = \frac{\Pi}{2} - \omega'$ and use for the PP channel the identity

$$h_{F,\eta}(\omega_1) h_{F,\eta}(\omega_2) = -1 + h_{B,\eta}(\omega_1+\omega_2)[h_{F,\eta}(\omega_1) + h_{F,\eta}(\omega_2)], \tag{D4}$$

where $h_{B,\eta}(\Pi) \underset{T\to 0}{=} h_B(\Pi - \eta eV)$, $\eta = \pm$ for $\eta = \mathrm{L/R}$, and $h_B(\omega) = \coth\frac{\omega}{2T} = \mathrm{sign}(\omega)$. It leads to

$$\begin{aligned}\sum_{\eta=\pm} &\alpha_\eta h_{F,\eta}(\omega_1) h_{F,\eta}(\omega_2) \\ &= -1 + \frac{1}{2}\sum_{\eta=\pm} h_{B,\eta}(\Pi)[h_F^{neq}(\omega_1) + h_F^{neq}(\omega_2)] \\ &\quad + \frac{1}{2}\sum_{\eta=\pm} \eta h_{B,\eta}(\Pi)\{\alpha_L[h_{F,L}(\omega_1) + h_{F,L}(\omega_2)] \\ &\quad - \alpha_R[h_{F,R}(\omega_1) + h_{F,R}(\omega_2)]\},\end{aligned} \tag{D5}$$

where

$$\sum_{\eta=\pm} \frac{\eta h_{B,\eta}(\Pi)}{2} \approx -2eV\delta(\Pi), \tag{D6}$$

as well as

$$\begin{aligned}&\alpha_L[h_{F,L}(\omega_1) + h_{F,L}(\omega_2)] - \alpha_R[h_{F,R}(\omega_1) + h_{F,R}(\omega_2)] \\ &\approx -eV[\delta(\omega_1) + \delta(\omega_2)]\end{aligned} \tag{D7}$$

for $\alpha_L = \alpha_R = \frac{1}{2}$. Therefore, the second sum in Eq. (D5) approximately equals $\approx 4(eV)^2\delta(\omega')\delta(\Pi)$.

We can represent

$$H_1(\Pi) = H_1^{\mathrm{I}}(\Pi) + H_1^{\mathrm{II}}(\Pi), \tag{D8}$$

where

$$H_1^{\mathrm{I}}(\Pi) = \frac{1}{2}\left[\sum_{\eta=\pm} h_{B,\eta}(\Pi)\right][F_1(\Pi) - F_1^*(\Pi)], \tag{D9}$$

$$H_1^{\mathrm{II}}(\Pi) \approx i(s_1^a + s_1^b)\delta(\Pi), \tag{D10}$$

and

$$s_1^a = \frac{8}{\pi}\alpha_L\alpha_R(eV)^2\frac{d}{d\lambda}[\mathrm{Im}\, g_\sigma^{\mathrm{Ret}}(0)]^2, \tag{D11}$$

$$s_1^b = -4s_1^a. \tag{D12}$$

Therefore the solution of Eq. (111) has the form

$$b_1(\Pi) = b_1^{\mathrm{I}}(\Pi) + i(b_1^{\mathrm{II}a} + b_1^{\mathrm{II}b})\delta(\Pi), \tag{D13}$$

where

$$b_1(\Pi) = \frac{1}{2}\left[\sum_{\eta=\pm} h_{B,\eta}(\Pi)\right][a_1(\Pi) - a_1^*(\Pi)], \tag{D14}$$

and $b_1^{\mathrm{II}a}$ and $b_1^{\mathrm{II}b}$ correspond to the inhomogeneity terms $\propto (eV)^2$ in Eqs. (D3) and (D5), respectively. They can be found from the equation

$$\frac{db_1^{\mathrm{II},a/b}}{d\lambda} = |a_1(0)|^2 s_1^{a/b} + 2a_1(0)F_1(0)b_1^{\mathrm{II},a/b}. \tag{D15}$$

2. Particle-hole channel

In order to evaluate Eq. (116) we set $\omega_1 = \omega' - \frac{X}{2}$, $\omega_2 = \omega' + \frac{X}{2}$ and use for the PH channel the identity

$$h_{F,\eta}(\omega_1) h_{F,\eta}(\omega_2) = 1 - h_B(\omega_1 - \omega_2)[h_{F,\eta}(\omega_1) - h_{F,\eta}(\omega_2)]. \tag{D16}$$

Then

$$H_3(X) = H_3^{\mathrm{I}}(X) + H_3^{\mathrm{II}}(X), \tag{D17}$$

where

$$H_3^{\mathrm{I}}(X) = -h_B(X)\{F_3(X) - F_3^*(X)\}, \tag{D18}$$

$$H_3^{\mathrm{II}}(X) = is_3\delta(X), \tag{D19}$$

and

$$s_3 = \frac{8}{\pi}\alpha_{\mathrm{L}}\alpha_{\mathrm{R}}(eV)^2\frac{d}{d\lambda}[\mathrm{Im}\, g_\sigma^{\mathrm{Ret}}(0)]^2. \tag{D20}$$

The solution of Eq. (112) has the form

$$b_3(X) = b_3^{\mathrm{I}}(X) + ib_3^{\mathrm{II}}\delta(X), \tag{D21}$$

where

$$b_3^{\mathrm{I}}(X) = -h_B(X)\{a_3(X) - a_3^*(X)\}, \tag{D22}$$

and $b_3^{\mathrm{II}}(X)$ obeys the equation

$$\frac{db_3^{\mathrm{II}}}{d\lambda} = |a_3(0)|^2 s_3 + 2a_3(0)F_3(0)b_3^{\mathrm{II}}. \tag{D23}$$

Analogously, the function $H_{2\sigma}(\Delta)$ occurring in the Eqs. (137) and (138) can be represented as

$$H_{2\sigma}(\Delta) = H_{2\sigma}^{\mathrm{I}}(\Delta) + H_{2\sigma}^{\mathrm{II}}(\Delta), \tag{D24}$$

where

$$H_{2\sigma}^{\mathrm{I}}(\Delta) = h_B(\Delta)\{F_{2\sigma}(\Delta) - F_{2\sigma}^*(\Delta)\}, \tag{D25}$$

$$H_{2\sigma}^{\mathrm{II}}(\Delta) = is_{2\sigma}\delta(\Delta), \tag{D26}$$

and

$$s_{2\sigma} = \frac{8}{\pi}\alpha_{\mathrm{L}}\alpha_{\mathrm{R}}(eV)^2\frac{d}{d\lambda}[\mathrm{Im}\, g_\sigma^{\mathrm{Ret}}(0)]^2. \tag{D27}$$

Note that from Eq. (124) it follows

$$s_1^a = s_3 = s_{2\sigma} = -(eV)^2\mathrm{Im}\, F_3'(0). \tag{D28}$$

The solution of Eqs. (137) and (138) then takes the form

$$b_{20/2\sigma}(\Delta) = b_{20/2\sigma}^{\mathrm{I}}(\Delta) + ib_{20/2\sigma}^{\mathrm{II}}\delta(\Delta), \tag{D29}$$

where

$$b_{20/2\sigma}^{\mathrm{I}}(\Delta) = h_B(\Delta)\{F_{20/2\sigma}(\Delta) - F_{20/2\sigma}^*(\Delta)\}, \tag{D30}$$

and

$$\frac{db_{20}^{\mathrm{II}}}{d\lambda} = -2a_{20}(0)F_{2\sigma}(0)b_{2\sigma}^{\mathrm{II}}, \tag{D31}$$

$$\frac{db_{2\sigma}^{\mathrm{II}}}{d\lambda} = -|a_{20}(0)|^2 s_{2\sigma} - 2a_{20}(0)F_{2\sigma}(0)b_{20}^{\mathrm{II}}. \tag{D32}$$

Comparing the latter relations with Eqs. (D15) and (D23) and using Eq. (D28) we establish that

$$b_{2\sigma}^{\mathrm{II}} = -\frac{b_1^{\mathrm{II}a} + b_3^{\mathrm{II}}}{2}, \quad b_{20}^{\mathrm{II}} = \frac{b_3^{\mathrm{II}} - b_1^{\mathrm{II}a}}{2}. \tag{D33}$$

3. Self-energy

An equation for the imaginary part of the self-energy in nonequilibrium reads

$$\frac{d}{d\lambda}\mathrm{Im}\,\Sigma_\sigma^{\mathrm{Ret}}(0) = \frac{1}{\pi}\int d\tilde{\omega}\Bigg[h_F^{neq}(\tilde{\omega})\mathrm{Im}\, a_1(\tilde{\omega})\mathrm{Im}\, s_{\bar{\sigma}}^{\mathrm{Ret}}(\tilde{\omega}) - \frac{i}{2}b_1^{\mathrm{I}}(\tilde{\omega})\mathrm{Im}\, s_{\bar{\sigma}}^{\mathrm{Av}}(\tilde{\omega}) + h_F^{neq}(\tilde{\omega})\mathrm{Im}\, a_3(\tilde{\omega})\mathrm{Im}\, s_{\bar{\sigma}}^{\mathrm{Ret}}(\tilde{\omega}) - \frac{i}{2}b_3^{\mathrm{I}}(\tilde{\omega})\mathrm{Im}\, s_{\bar{\sigma}}^{\mathrm{Ret}}(\tilde{\omega})$$
$$+ h_F^{neq}(\tilde{\omega})\mathrm{Im}\,\bar{a}_{2\sigma}(\tilde{\omega})\mathrm{Im}\, s_\sigma^{\mathrm{Ret}}(\tilde{\omega}) - \frac{i}{2}\bar{b}_{2\sigma}^{\mathrm{I}}(\tilde{\omega})\mathrm{Im}\, s_\sigma^{\mathrm{Ret}}(\tilde{\omega})\Bigg] + \frac{1}{2\pi}[(b_1^{\mathrm{II}a} + b_1^{\mathrm{II}b})\mathrm{Im}\, s^{\mathrm{Av}}(0) + (b_3^{\mathrm{II}} - b_{2\sigma}^{\mathrm{II}})\mathrm{Im}\, s^{\mathrm{Ret}}(0)], \tag{D34}$$

which simplifies due to the particle-hole symmetry to the form

$$\frac{d}{d\lambda}\mathrm{Im}\,\Sigma_\sigma^{\mathrm{Ret}}(0) = \frac{1}{\pi}\int d\tilde{\omega}\Bigg\{\Bigg[h_F^{neq}(\tilde{\omega}) - \frac{1}{2}\sum_{\eta=\pm}h_{B,\eta}(\tilde{\omega})\Bigg]\mathrm{Im}\,\bar{a}_1(\tilde{\omega})\mathrm{Im}\, s_{\bar{\sigma}}^{\mathrm{Ret}}(\tilde{\omega}) + [h_F^{neq}(\tilde{\omega}) - h_B(\tilde{\omega})]\mathrm{Im}[a_3(\tilde{\omega}) + \bar{a}_{2\sigma}(\tilde{\omega})]\mathrm{Im}\, s_{\bar{\sigma}}^{\mathrm{Ret}}(\tilde{\omega})\Bigg\}$$
$$+ \frac{1}{2\pi}\Bigg[-2b_1^{\mathrm{II}a} - b_1^{\mathrm{II}b} + \frac{3}{2}(b_1^{\mathrm{II}a} + b_3^{\mathrm{II}})\Bigg]\mathrm{Im}\, s^{\mathrm{Ret}}(0). \tag{D35}$$

Expanding it in eV, we obtain

$$\frac{d}{d\lambda}\mathrm{Im}\,\Sigma_\sigma^{\mathrm{Ret}}(0) = \frac{3}{2\pi}\left(\frac{eV}{2}\right)^2\int d\tilde{\omega}\delta'(\tilde{\omega})\mathrm{Im}[\bar{a}_1(\tilde{\omega}) + a_3(\tilde{\omega})]\mathrm{Im}\, s^{\mathrm{Ret}}(\tilde{\omega}) - \frac{1}{\pi}(eV)^2\int d\tilde{\omega}\delta'(\tilde{\omega})\mathrm{Im}\,\bar{a}_1(\tilde{\omega})\mathrm{Im}\, s^{\mathrm{Ret}}(\tilde{\omega})$$
$$+ \frac{1}{2\pi}\Bigg[-2b_1^{\mathrm{II}a} - b_1^{\mathrm{II}b} + \frac{3}{2}(b_1^{\mathrm{II}a} + b_3^{\mathrm{II}})\Bigg]\mathrm{Im}\, s^{\mathrm{Ret}}(0) = -\frac{3}{2\pi}\left(\frac{eV}{2}\right)^2\mathrm{Im}\left[\frac{\partial\bar{a}_1}{\partial\omega} + \frac{\partial a_3}{\partial\omega}\right]_{\omega=0}\mathrm{Im}\, s^{\mathrm{Ret}}(0)$$
$$+ \frac{1}{\pi}(eV)^2\mathrm{Im}\left[\frac{\partial\bar{a}_1}{\partial\omega}\right]_{\omega=0}\mathrm{Im}\, s^{\mathrm{Ret}}(0) + \frac{1}{2\pi}\Bigg[-2b_1^{\mathrm{II}a} - b_1^{\mathrm{II}b} + \frac{3}{2}(b_1^{\mathrm{II}a} + b_3^{\mathrm{II}})\Bigg]\mathrm{Im}\, s^{\mathrm{Ret}}(0). \tag{D36}$$

Comparing Eqs. (D15) and (D23) with Eqs. (152) and (153) we establish that

$$b_1^{\mathrm{II}a} = -(eV)^2 \mathrm{Im}\left[\frac{\partial \bar{a}_1}{\partial \omega}\right]_{\omega=0}, \tag{D37}$$

$$b_1^{\mathrm{II}b} = -4b_1^{\mathrm{II}a}, \tag{D38}$$

$$b_3^{\mathrm{II}} = -(eV)^2 \mathrm{Im}\left[\frac{\partial a_3}{\partial \omega}\right]_{\omega=0}. \tag{D39}$$

These relations allow us to express Eq. (D36) as

$$\frac{d}{d\lambda}\mathrm{Im}\,\Sigma_\sigma^{\mathrm{Ret}}(0) = -\frac{3}{2\pi}\frac{3(eV)^2}{4}\mathrm{Im}\left[\frac{\partial \bar{a}_1}{\partial \omega} + \frac{\partial a_3}{\partial \omega}\right]_{\omega=0} \mathrm{Im}\, s^{\mathrm{Ret}}(0). \tag{D40}$$

After comparison with Eq. (154) it becomes clear that

$$\mathrm{Im}\left.\frac{\partial^2 \Sigma_\sigma^{\mathrm{Ret}}}{\partial V^2}\right|_{\omega,V=0} = \frac{3}{4}\mathrm{Im}\,\Sigma'', \tag{D41}$$

which agrees with Eq. (32) and Ref. 62.

[1] U. Weiss, *Quantum Dissipative Systems* (World Scientific, Singapore, 2000); A. J. Leggett, S. Chakravarty, A. T. Dorsey, M. P. A. Fisher, A. Garg, and W. Zwerger, Rev. Mod. Phys. **59**, 1 (1987).

[2] *Single Charge Tunneling: Coulomb Blockade Phenomena in Nanostructures*, edited by H. Grabert and M. H. Devoret (Plenum, New York, 1992).

[3] *Mesoscopic Electron Transport*, edited by L. L. Sohn, L. P. Kouwenhoven, and G. Schön (Kluwer, Dordrecht, 1997).

[4] M. Mayor, H. B. Weber, and R. Waser, in *Nanoelectronics and Information Technology*, edited by R. Waser (Wiley-VCH, Weinheim, 2003), pp. 503–525.

[5] K. Hiruma, M. Yazawa, T. Katsuyama, K. Ogawa, K. Haraguchi, M. Koguchi, and H. Kakibayashi, J. Appl. Phys. **77**, 447 (1995).

[6] S. Huang, X. Cai, and J. Liu, J. Am. Chem. Soc. **125**, 5636 (2003).

[7] F. Lesage and H. Saleur, Phys. Rev. Lett. **80**, 4370 (1998); A. Schiller and S. Hershfield, Phys. Rev. B **62**, R16271 (2000); A. Komnik, *ibid.* **79**, 245102 (2009).

[8] E. Boulat, H. Saleur, and P. Schmitteckert, Phys. Rev. Lett. **101**, 140601 (2008).

[9] E. Boulat and H. Saleur, Phys. Rev. B **77**, 033409 (2008).

[10] P. Mehta and N. Andrei, Phys. Rev. Lett. **96**, 216802 (2006); P. Mehta, S. p. Chao, and N. Andrei, arXiv:cond-mat/0703426 (unpublished).

[11] N. Andrei (private communication); S.-P. Chao and G. Palacios, arXiv:1003.5395 (unpublished).

[12] F. B. Anders, Phys. Rev. Lett. **101**, 066804 (2008).

[13] F. Heidrich-Meisner, A. E. Feiguin, and E. Dagotto, Phys. Rev. B **79**, 235336 (2009).

[14] J. E. Han and R. J. Heary, Phys. Rev. Lett. **99**, 236808 (2007).

[15] S. Weiss, J. Eckel, M. Thorwart, and R. Egger, Phys. Rev. B **77**, 195316 (2008).

[16] F. B. Anders and A. Schiller, Phys. Rev. Lett. **95**, 196801 (2005); Phys. Rev. B **74**, 245113 (2006); F. B. Anders, R. Bulla, and M. Vojta, Phys. Rev. Lett. **98**, 210402 (2007).

[17] D. Roosen, M. R. Wegewijs, and W. Hofstetter, Phys. Rev. Lett. **100**, 087201 (2008).

[18] A. J. Daley, C. Kollath, U. Schollwöck, and G. Vidal, J. Stat. Mech.: Theory Exp. **2004**, P04005; S. R. White and A. E. Feiguin, Phys. Rev. Lett. **93**, 076401 (2004); P. Schmitteckert, Phys. Rev. B **70**, 121302(R) (2004).

[19] T. L. Schmidt, P. Werner, L. Mühlbacher, and A. Komnik, Phys. Rev. B **78**, 235110 (2008).

[20] P. Werner, T. Oka, and A. J. Millis, Phys. Rev. B **79**, 035320 (2009); P. Werner, T. Oka, M. Eckstein, and A. J. Millis, *ibid.* **81**, 035108 (2010).

[21] H. Wang and M. Thoss, J. Chem. Phys. **131**, 024114 (2009).

[22] H. Schoeller and J. König, Phys. Rev. Lett. **84**, 3686 (2000).

[23] H. Schoeller, in *Low-Dimensional Systems*, edited by T. Brandes, Lecture Notes in Physics (Springer, New York, 2000), p. 137.

[24] M. Keil and H. Schoeller, Phys. Rev. B **63**, 180302(R) (2001).

[25] S. G. Jakobs, V. Meden, and H. Schoeller, Phys. Rev. Lett. **99**, 150603 (2007).

[26] H. Schoeller, Eur. Phys. J. Spec. Top. **168**, 179 (2009).

[27] H. Schoeller and F. Reininghaus, Phys. Rev. B **80**, 045117 (2009).

[28] D. Schuricht and H. Schoeller, Phys. Rev. B **80**, 075120 (2009).

[29] M. Pletyukhov, D. Schuricht, and H. Schoeller, Phys. Rev. Lett. **104**, 106801 (2010).

[30] C. Karrasch, S. Andergassen, M. Pletyukhov, D. Schuricht, L. Borda, V. Meden, and H. Schoeller, arXiv:0911.5496, Europhys. Lett. (to be published).

[31] A. Rosch, J. Kroha, and P. Wölfle, Phys. Rev. Lett. **87**, 156802 (2001).

[32] A. Rosch, J. Paaske, J. Kroha, and P. Wölfle, Phys. Rev. Lett. **90**, 076804 (2003); J. Phys. Soc. Jpn. **74**, 118 (2005).

[33] H. Schmidt and P. Wölfle, Ann. Phys. (Berlin) **19**, 60 (2010).

[34] S. Kehrein, Phys. Rev. Lett. **95**, 056602 (2005).

[35] F. Wegner, Ann. Phys. **506**, 77 (1994); S. D. Glazek and K. G. Wilson, Phys. Rev. D **48**, 5863 (1993); **49**, 4214 (1994).

[36] Ch. Wetterich, Phys. Lett. B **301**, 90 (1993); T. R. Morris, Int. J. Mod. Phys. A **9**, 2411 (1994).

[37] S. Jakobs, Diploma thesis, Rheinisch-Westfälische Technische Hochschule Aachen, 2003.

[38] R. Gezzi, Th. Pruschke, and V. Meden, Phys. Rev. B **75**, 045324 (2007).

[39] R. Gezzi, Ph.D. thesis, Georg-August-Universität zu Göttingen, 2007.

[40] A. Mitra, S. Takei, Y. B. Kim, and A. J. Millis, Phys. Rev. Lett. **97**, 236808 (2006).

[41] T. Gasenzer and J. M. Pawlowski, Phys. Lett. B **670**, 135 (2008).

[42] S. G. Jakobs, M. Pletyukhov, and H. Schoeller, J. Phys. A: Math. Theor. **43**, 103001 (2010).

[43] P. W. Anderson, Phys. Rev. **124**, 41 (1961).

[44] A. C. Hewson, *The Kondo Problem to Heavy Fermions* (Cambridge University Press, Cambridge, 1993).
[45] L. I. Glazman and M. E. Raikh, Pis'ma Zh. Eksp. Teor. Fiz. **47**, 378 (1988) [JETP Lett. **47**, 452 (1988)]; T. K. Ng and P. A. Lee, Phys. Rev. Lett. **61**, 1768 (1988).
[46] D. Goldhaber-Gordon, H. Shtrikman, D. Mahalu, D. Abusch-Magder, U. Meirav, and M. A. Kastner, Nature (London) **391**, 156 (1998); S. M. Cronenwett, T. H. Oosterkamp, and L. P. Kouwenhoven, Science **281**, 540 (1998); F. Simmel, R. H. Blick, J. P. Kotthaus, W. Wegscheider, and M. Bichler, Phys. Rev. Lett. **83**, 804 (1999); J. Schmid, J. Weis, K. Eberl, and K. v. Klitzing, *ibid.* **84**, 5824 (2000); W. G. van der Wiel, S. De Franceschi, T. Fujisawa, J. M. Elzerman, S. Tarucha, and L. P. Kouwenhoven, Science **289**, 2105 (2000).
[47] K. Yamada, Prog. Theor. Phys. **53**, 970 (1975).
[48] K. Yosida and K. Yamada, Prog. Theor. Phys. **53**, 1286 (1975).
[49] K. Yamada, Prog. Theor. Phys. **54**, 316 (1975).
[50] V. Zlatić and B. Horvatić, Phys. Rev. B **28**, 6904 (1983).
[51] T. A. Costi, A. C. Hewson, and V. Zlatic, J. Phys.: Condens. Matter **6**, 2519 (1994); R. Bulla, T. A. Costi, and T. Pruschke, Rev. Mod. Phys. **80**, 395 (2008).
[52] A. M. Tsvelick and P. B. Wiegmann, Adv. Phys. **32**, 453 (1983).
[53] L. Bartosch, H. Freire, J. J. R. Cardenas, and P. Kopietz, J. Phys.: Condens. Matter **21**, 305602 (2009); A. Isidori, D. Roosen, L. Bartosch, W. Hofstetter, and P. Kopietz, arXiv:1003.3188 (unpublished).
[54] C. Karrasch, T. Enss, and V. Meden, Phys. Rev. B **73**, 235337 (2006).
[55] S. Andergassen, T. Enss, C. Karrasch, and V. Meden, in *Quantum Magnetism*, edited by B. Barbara, Y. Imry, G. Sawatzky, and P. C. E. Stamp (Springer, New York, 2008).
[56] R. Hedden, V. Meden, Th. Pruschke, and K. Schönhammer, J. Phys.: Condens. Matter **16**, 5279 (2004).
[57] C. Karrasch, R. Hedden, R. Peters, Th. Pruschke, K. Schönhammer, and V. Meden, J. Phys.: Condens. Matter **20**, 345205 (2008).
[58] S. Hershfield, J. H. Davies, and J. W. Wilkins, Phys. Rev. Lett. **67**, 3720 (1991); Phys. Rev. B **46**, 7046 (1992).
[59] T. Fujii and K. Ueda, Phys. Rev. B **68**, 155310 (2003).
[60] C. D. Spataru, M. S. Hybertsen, S. G. Louie, and A. J. Millis, Phys. Rev. B **79**, 155110 (2009).
[61] J. Eckel, F. Heidrich-Meisner, S. G. Jakobs, M. Thorwart, M. Pletyukhov, and R. Egger, New J. Phys. **12**, 043042 (2010).
[62] A. Oguri, Phys. Rev. B **64**, 153305 (2001).
[63] D. C. Langreth, in *Linear and Nonlinear Response Theory with Applications*, NATO Advanced Study Institutes Series B: Physics, Vol. 17, edited by J. T. Devreese and V. E. van Doren (Plenum, New York, 1976).
[64] E. M. Lifshitz and L. P. Pitaevskii, *Physical Kinetics* (Pergamon, New York, 1981).
[65] J. Rammer and H. Smith, Rev. Mod. Phys. **58**, 323 (1986).
[66] H. Haug and A.-P. Jauho, *Quantum Kinetics in Transport and Optics of Semiconductors* (Springer, Berlin, 1996).
[67] L. V. Keldysh, Zh. Eksp. Teor. Fiz. **47**, 1515 (1964) [Sov. Phys. JETP **20**, 1018 (1965)].
[68] J. R. Schrieffer and D. C. Mattis, Phys. Rev. **140**, A1412 (1965).
[69] Y. Meir and N. S. Wingreen, Phys. Rev. Lett. **68**, 2512 (1992).
[70] M. Salmhofer, *Renormalization: An Introduction* (Springer, Heidelberg, 1998).
[71] M. Salmhofer and C. Honerkamp, Prog. Theor. Phys. **105**, 1 (2001).
[72] W. Metzner, Prog. Theor. Phys. Suppl. **160**, 58 (2005).
[73] V. Meden, in *Advances in Solid State Physics*, edited by R. Haug (Springer, New York, 2008), Vol. 46.
[74] J. W. Negele and H. Orland, *Quantum Many-Particle Systems* (Addison-Wesley, Reading, MA, 1988).
[75] V. Janiš and P. Augustinský, Phys. Rev. B **75**, 165108 (2007); **77**, 085106 (2008).
[76] D. E. Logan, M. P. Eastwood, and M. A. Tusch, J. Phys.: Condens. Matter **10**, 2673 (1998).
[77] The NRG data presented here and in the following figures have been created with a ready-to-use program by courtesy of Dr. Theo Costi, Institute of Solid State Research, Forschungszentrum Jülich.
[78] C. Karrasch and V. Meden (private communication).